

SOURCE ROCK QUALITY, DEPOSITIONAL AND GEOCHEMICAL
CHARACTERIZATION OF THE KHOOT BASIN IN MONGOLIA

by
Kherlen Batbayar

A thesis submitted to the Faculty and the Board of Trustees of the Colorado School of Mines in partial fulfillment of the requirements for the degree of Master of Science (Geology).

Golden, Colorado

Date _____

Signed: _____
Kherlen Batbayar

Signed: _____
Alexei V. Milkov
Thesis Advisor

Signed: _____
Lesli J. Wood
Thesis Advisor

Golden, Colorado

Date _____

Signed: _____
Dr. M. Stephen Enders
Professor and Head
Department of Geology and Geological Engineering

ABSTRACT

The Khoot Basin is located in the Eastern Mongolian Basinal Province. The basin has long been of interest to international and domestic petroleum and mining companies as the most prolific oil shale (Eedemt deposits) in the country outcrop at the basin surface.

The Khoot Basin is located near the margin of two larger Early Cretaceous sedimentary basins: Choir-Nyalga and Middle Gobi. Like many Mongolian sedimentary basins, the Khoot Basin is relatively less studied. Therefore, for the first time, this study is providing an integrated source rock evaluation, subsurface correlation and geochemical analysis (XRD, XRF, and WOGC) of the Khoot Basin. Additionally, based on the depositional trends and well-log correlation, the sequence stratigraphic framework of the basin was established.

Historically, the Khoot oil shales were regarded, based on outcrop samples, as the best quality oil shale in Mongolia. However, the results from this study suggests that the shale in the subsurface is not rich enough in organic matter to be classified as oil shale. The Khoot outcrop oil shales contain 10-25 % organic matter and are a Type I lacustrine oil shale with higher algal input. The Khoot subsurface samples, on the other hand, are a Type I and mixed Type II lacustrine source rock with greater higher-plant input. The terrestrial contents peak near the maximum flooding surfaces and the bottom sequence. The total organic content of the subsurface oil shales is 2-11 %. Based on these results, the Khoot outcrop and subsurface samples are likely different temporal deposits and possibly deposited in different lakes.

From the analytical data and subsurface data correlation, the gross rock volume was calculated for the Khoot Basin and the ultimate expellable potential (UEP) was estimated. The KinEx calculation yielded a total UEP of 4.94 bnboe, in which the oil content is 4.07 bnboe and the gas content is 0.87 bnboe. Although the Khoot oil shale is similar to world-class source rocks based on the yield per unit meter (0.66-0.87 mmboe/m²), it is not a world-class play, because of the relatively small size and thickness of the basin. The ultimate expellable potentials were also estimated for the neighboring Choir-

Nyalga and Middle Gobi basins, which ranged from a low of 2,023 (3,515) bnboe to a high of 18,041 (31,352) bnboe depending on assumptions regarding source rock thickness and type.

TABLE OF CONTENTS

ABSTRACT	iii
LIST OF FIGURES.....	viii
LIST OF TABLES.....	xvi
ACKNOWLEDGMENTS.....	xviii
CHAPTER ONE	1
INTRODUCTION.....	1
1.1 Overview of the Study Area.....	1
1.2 Dataset from Genie Oil and Gas	3
1.3 Core and Outcrop Samples from Khoot Basin	4
1.4 Geochemical Analytical Methods	6
1.4.1 XRF Analysis Method	6
1.4.1 XRD Analysis Method.....	6
1.4.2 Biomarker Analysis Method	8
CHAPTER 2	9
PREVIOUS RESEARCH AND GEOLOGIC BACKGROUND.....	9
2.1 Geologic Background.....	9
2.2 Previous Studies on Khoot Area Deposits	13
CHAPTER 3	17
SUBSURFACE ARCHITECTURE OF THE KHOOT BASIN	17
3.1 Tectonic and Depositional Architecture from Seismic Data.....	17
3.2 Stratigraphic Successions of the Jurassic and Cretaceous Strata....	21
3.3 Sequence Stratigraphic Correlation in the Khoot Basin	23
3.3.1 Identification of Systems Tracts and Surfaces	23
3.3.2 Interpretation and Correlation of the Khoot Basin Sequences	24
CHAPTER 4	28
ROCK-EVAL 6 PERFORMANCE AND DATA VERACITY	28
4.1 Veracity of Drill Hole 1 (DH 1) Samples and Data Calibration.....	30
4.1.1 Quality of Drill Hole 1 (DH 1) Samples.....	30
4.1.2 Data Calibration and Selection	30
4.2 Veracity of Drill Hole 2 (DH 2) Samples	32
4.3 Veracity of Drill Hole 3 (DH 3) Samples	34
4.4 Veracity of Drill Hole 4 (DH 4) Samples	36

4.5 Veracity of Drill Hole 5 (DH 5) Samples	36
4.6 Veracity of the Shallow Depth Samples	38
4.7 Data Veracity of the Outcrop Samples	40
CHAPTER 5	47
SOURCE ROCK POTENTIAL BASED ON ROCK-EVAL DATA	47
5.1 Organic Matter Richness.....	47
5.1.1 Total Organic Content (TOC) of the Non-Calibrated Samples	47
5.1.2 True Organic Richness from the Calibrated Samples	48
5.1.3 Potential for Oil Shale Development	51
5.2 Kerogen Type	52
5.3 Thermal Maturation	56
5.3.1 Thermal Maturation of Mongolian Samples	56
5.3.2 Thermal Maturation from Calculated Vitrinite Reflectance	57
5.3.3 Thermal Maturation Map of the Surface Samples.....	62
5.4 Influence of Mineral Matter on Thermal Maturation and Organic Richness.....	63
5.5 Hydrocarbon Generating Capacity	69
5.5.1 Production Index.....	71
5.5.2 Genetic Potential	73
5.5.3 Pyrolyzable Carbon Index.....	75
5.5.4 Oil Saturation and Migration	76
CHAPTER 6	80
6.1 Elemental Analysis Results.....	80
6.2 Mineralogical Analysis Results.....	88
6.3 Weathering and Depositional Environment.....	95
6.4 Whole Oil Gas Chromatograph (WOGC) Analysis Results	97
CHAPTER 7	103
THE ULTIMATE EXPELLABLE POTENTIAL OF THE	103
KHOOT SOURCE ROCKS	103
7.1 KinEx Basics	103
7.2 Modeling the Khoot Basin	105
7.2 The Khoot Basin's Potential for Hydrocarbon Exploration.....	112
7.3 Potentials of the Middle Gobi Basin and the Choir-Nyalga Basin.....	115

CHAPTER 8	117
DISCUSSION AND CONCLUSION.....	117
8.1 Integration of Rock-Eval Data and Sequence Stratigraphic Interpretation	117
8.2 Depositional Environment Inferred from Geochemical Data	123
8.3 Conclusion	125
REFERENCES.....	127

LIST OF FIGURES

Figure 1.1	Locations of the 28 exploration blocks in Mongolia. Block XXV is circled in yellow.	1
Figure 1.2	Enlarged map of the Eastern Mongolian Basinal Province (EMBP). Sub-basins (Choir, Khoot, Khashaat Khudag, and Olongiin Uhaa) within Block XXV are displayed on the map. The smallest of the four sub-basins is the Khoot Basin located at the northern edge of the Middle Gobi Basin.	2
Figure 1.3	Bouguer gravity map of the Khoot basin that has the locations of the five deep drill holes, two shallow depth drill holes and the surface samples. The locations of the two cores extracted during Li et al's 2014 study are also provided.	4
Figure 1.4	Photographic image of the studied outcrop sample from the Khoot basin.	5
Figure 1.5	Photographic images of the selected subsurface samples from Khoot basin.	5
Figure 1.6	Handheld XRF Analyzing Device (Niton XL3t - Thermo Scientific).	6
Figure 1.7	Photographic image of crushed Khoot samples suspended in diluted hydrogen peroxide.	7
Figure 2.1	NE-SW trending Late Jurassic to Early Cretaceous basins in the EMBP: Choir-Nyalga Basin, Middle Gobi Basin, East Gobi Basin, Onon Basin, Choibalsan Basin, and the Sukhbaatar Basin. The Har Horin and the South Gobi basins are located outside of the EMBP (Redrawn from Yamamoto et al., 1993; Traynor and Sladen, 2000; Genyao et al., 2013). Illustrated in circles are the oil shale sediments possibly deposited in these basins: HH-Har Horin; BE-Bayan Erkhiti; EM-Eedemt; SO-Shawart Obo; SH-Shinekhudag; TH-Tavan Har.	10
Figure 2.2	The paleo-tectonic map of northeastern Asia from the Late Permian to the Present (From Li et al., 2016).	11
Figure 2.3	Early-Middle Jurassic basins relative to the location of Block XXV. The Western and the Eastern North belt Molasse basins are the westward extension of the Hailar Basin. The Eastern Middle Belt Molasse Basin is the westward extension of the Erlia Basin. The South Belt Molasse Basin is the northward extension of the Yingen Basin (Redrawn from Genyao et al., 2013). Illustrated in circles are the oil shale sediments possibly deposited in these basins: SB-Sayan Obo; TO-Tsagan Obo; NU-Noyon Uul; EM-Eedemt; SO-Shawart Obo.	12

Figure 2.4 Illustration of the subducting Mongol – Okhotsk Oceanic (MOO) plate under the Siberian Craton (SBC), which eventually led to the collision of the SBC and the China-SE Asia subcontinent (CAC). OSB: Orkhon-Selenge Basin; NMB: North Belt Molasse Basin; MMB: Middle Belt Molasse Basin; SMB: South Belt Molasse Basin (Adapted from Genyao et al., 2013).	13
Figure 2.5 An SEM image of a Khoot oil shale sample (Avid and Purevsuren, 2001).	14
Figure 2.6 The X-ray diffraction analysis result of a Khoot oil shale sample under CuK α radiation on a Siemens D-5000 diffractometer (Avid and Purevsuren, 2001). The minerals identified by Avid and Purevsuren (2001) are calcite (d=3.03, 2.08, 1.87 Å, e.g.), dolomite (d=2.89, 1.78, 2.19 Å), quartz (d=3.34, 1.81, 1.54, 1.37, 2.45, 2.12 Å), illite (d=2.57, 1.49 Å), smectite (d=1.495, 4.45 Å), getite (d=2.45 Å), halloysite, feldspar (3.21, 3.18, 3.95 Å) and hydromica (d=2.54, 4.41, 1.48 Å). This study showed no kaolinite.	15
Figure 2.7 A) Shallow depth core sampling from the Eedemt (Khoot) locality has proven that the Eedemt Formation is abundant in <i>Triglypta eedemtensis</i> Li sp. nov. (Left) and B) <i>Dundgobiestheria mandalgobiensis</i> Li gen. et sp. nov. (Right), which are typical of Middle Jurassic lacustrine deposits of northern Hebei, and the Junggar and Turpan basins of northwestern China (Li et al., 2014).	16
Figure 3.1 Position of the seismic line in the Khoot basin. The seismic line was shot through DH 1, DH 2, DH 3, and DH 4.	17
Figure 3.2 A) The interpreted seismic line of the Khoot Basin. The seismic line was shot along the line of DH 1, DH 2, DH 3 and DH 4 B) Enlarged image of the selected area in Figure 3.2 A C) Southwestern slope of the Khoot basin depo-center D) Northeastern side of the Khoot basin (See Figure 3.2B for legend.) E) Identified stratigraphic sequences and sequence boundaries in the Khoot basin.	19
Figure 3.3 The general stratigraphic successions of the Early-Middle Jurassic Bakhar Formation and the Early Cretaceous And Khudag Formation in the Ongi River basin (From Erdenetsogt et al., 2009). The stratigraphic succession of the Early Cretaceous Shine Khudag Formation is similar to the And Khudag Formation.	21
Figure 3.4 Cross section view of the Jurassic tectonic events and deposits in Mongolia. A) Early Jurassic or the pre-coal stage, B) coal-bearing stage, C) Latest Middle Jurassic or the post-coal stage (Modified from Genyao et al., 2014). See Chapter 2 for the detailed Early-Middle Jurassic basins in Mongolia.	22

Figure 3.5 The interpreted well log correlation of Khoot subsurface intervals. 25

Figure 4.1 Rock-Eval 2 programmed pyrolysis sample results from the Niobrara Formation, Denver Basin. Measured parameters stabilize at 40 mg (Thul, 2012).....28

Figure 4.2 Programmed pyrolysis analysis results from Peters (1986). Measured parameters start to show consistency at 60 mg (Peters, 1986; Thul, 2000).....29

Figure 4.3 Cross-plots of the measured and calculated Rock-Eval 6 programmed pyrolysis parameters vs. sample weight for DH 1 samples. The threshold weight is the minimum recommended weight (60 mg) by Peters (1986). 31

Figure 4.4 Cross-plots of the measured and calculated Rock-Eval 6 programmed pyrolysis parameters vs. sample weight for DH 2 samples. The threshold weight is the minimum recommend weight (40 mg) by Thul (2000). 33

Figure 4.5 Cross-plots of the measured and calculated Rock-Eval 6 programmed pyrolysis parameters vs. sample weight for DH 3 samples. The threshold weight was chosen as 33 mg. 35

Figure 4.6 Cross-plots of the measured and calculated Rock-Eval 6 programmed pyrolysis parameters vs. sample weight for DH 4 samples. The threshold weight is 34.5 mg. 37

Figure 4.7 Cross-plots of the measured and calculated Rock-Eval 6 programmed pyrolysis parameters vs. sample weight for DH 5 samples. The threshold weight is 38 mg. 39

Figure 4.8 Cross-plots of the measured and calculated Rock-Eval 6 programmed pyrolysis parameters vs. sample weight for the two-shallow depth SD1 and SD2 samples..... 41

Figure 4.9 Cross-plots of the measured and calculated Rock-Eval 6 programmed pyrolysis parameters vs. sample weight for Campaign 1 samples. The threshold weight was chosen as 35 mg. 43

Figure 4.10 Cross-plots of the measured and calculated Rock-Eval 6 programmed pyrolysis parameters vs. sample weight for Campaign 2 outcrop samples. The threshold weight was chosen as 34 mg. 44

Figure 4.11 Cross-plots of the measured and calculated Rock-Eval 6 programmed pyrolysis parameters vs. sample weight for surface samples collected during Campaign 3. The threshold weight is 35 mg 46

Figure 5.1 TOC frequencies in the non-calibrated subsurface samples.	47
Figure 5.2 TOC levels in the non-calibrated Khoot near surface and outcrop samples as well as the Eideimt (Eedemt) samples from Yamamoto et al (1993).	48
Figure 5.3 A) Interpolated (IDW) TOC map of the Khoot basin from the non-calibrated samples B) Interpolated (IDW) TOC map of the Khoot from the calibrated samples.	50
Figure 5.4 HI plotted against TOC for weight calibrated Khoot samples (core and outcrop). Additionally, nine different shale and oil shale samples from various locations in Mongolia are plotted for comparison. This plot indicates the kerogen type and oil shale quality of the studied samples. Non-Khoot sample locations are available in Chapter 2 (Figures 2.1, 2.3). .	51
Figure 5.5 S2/S3 plotted against TOC shows the overall quality of the source rocks and kerogen type. Plotted on the graph are the weight calibrated subsurface and outcrop samples from the Khoot Basin and additional samples from literature. See Figure 4.4 for legend.	53
Figure 5.6 Modified Van-Krevlen diagram shows the organic matter type of the studied samples. All Mongolian samples have exclusively oil-prone Type I/Type II kerogen.	54
Figure 5.7 A) Interpolated (IDW) HI distribution map of the Khoot basin from the non-calibrated outcrop samples B) Interpolated (IDW) HI distribution map of the Khoot basin from the calibrated outcrop samples.	55
Figure 5.8 HI plotted against Tmax shows the maturity of each sample. The subsurface Khoot samples are immature to early mature while the outcrop samples are early mature to mature.	58
Figure 5.9 Tmax vs Vitrinite Reflectance (%) plot of subsurface Khoot oil shale samples. VOZ stands for volatile oil zone.	59
Figure 5.10 Tmax vs Vitrinite Reflectance (%) plot of outcrop Khoot oil shale samples compared to Eedemt samples. VOZ stands for volatile oil zone.	60
Figure 5.11 Tmax vs Vitrinite Reflectance (%) plot of Mongolian oil shale and shale deposits. VOZ stands for volatile oil zone.	61

Figure 5.12 A) Interpolated (IDW) Tmax map of the Khoot Basin from the non-calibrated outcrop samples B) Interpolated (IDW) Tmax map of the Khoot basin from the calibrated outcrop samples..	62
Figure 5.13 A) Plot S3 vs Tmax serves to show the relationship between thermal maturity and CO ₂ created from organic content. Displayed on the graph are core and outcrop samples from the Khoot Basin and Mongolian samples from seven different locations B) Plot S3' vs Tmax serves to show the relationship between thermal maturity and CO ₂ created from mineral contents in the samples. Displayed on the graph are core and outcrop samples from the Khoot Basin.....	64
Figure 5.14 S3' vs TOC plot shows the relationship between organic richness and CO ₂ created from mineral matter. Higher mineral content is associated with lower level of organic richness.....	67
Figure 5.15 S3' vs HI plot shows the relationship between hydrogen index and CO ₂ created from mineral matter in the Khoot samples.....	67
Figure 5.16 S3' vs Tmax plot shows the relationship between source rock maturation and CO ₂ created from mineral matter in the Khoot samples.	68
Figure 5.17 Plot S2 vs TOC shows the source rock quality and the kerogen type. All samples plotted in this graph are the Khoot Basin samples. Levels of HI indicates the kerogen type.....	70
Figure 5.18 Plot S2 vs TOC shows the source quality and the kerogen type. All samples plotted in this graph are from previous studies. Levels of HI indicates the kerogen type.	70
Figure 5.19 A) The Production Index vs Tmax plot shows whether a source rock is in the oil window or immature. Production Index is calculated as S1/(S1+S2). The plot indicates that almost all Mongolian source rocks have very low production index B) Enlarged PI vs Tmax plot shows that samples from literature have higher PI values than the Khoot samples.....	71
Figure 5.20 A) The total oil generating capacity of the Khoot samples is indicated by the Genetic Potential vs TOC plot. The plot shows that most Khoot samples have very good to excellent potential B) This plot shows the total oil generating potential of samples published in previous studies. Tavan Har samples have the lowest quality in this group.	74
Figure 5.21 The Pyrolyzable Carbon Index (PCI) vs TOC plot indicates the kerogen types of the source rocks.	75

Figure 5.22 The Hydrogen Index vs Oil Saturation Index plot shows that most Mongolian source rocks have very low oil saturation index. The oil saturation index must be over 80-100 to be considered producible.	77
Figure 5.23 S1 vs TOC plot of potentially producible oil from selected Mongolian oil shales and Khoot samples.....	78
Figure 5.24 The S1 vs TOC plot showing hydrocarbon saturation and migration qualities of selected Mongolian oil shales and Khoot samples.....	79
Figure 6.1 Percentages of the major elements in the Khoot samples. The percentages of the minor and trace elements are too little to be displayed here.....	80
Figure 6.2 Comparison of elements associated with terrigenous minerals, including clay minerals, feldspars and quartz.....	81
Figure 6.3 A) Si/Al ratio vs. Ca/K ratio B) Plot of element K vs. element Al.....	82
Figure 6.4 Ba/Sr and Rb/Sr analysis indicates the presence of detrital materials vs carbonate minerals and smectite.	83
Figure 6.5 A) Analysis of pyrite presence. B) Si vs. Al trends indicate origins of the silica present in studied samples.....	84
Figure 6.6 Percentage of minor elements in the Khoot samples. Some of the elements present in the subsurface samples are absent in the outcrop sample.	85
Figure 6.7 X-Ray Diffraction patterns of Khoot samples. The samples were scanned under CuK α radiation from 5° to 65° 2 θ at a continuous scan rate of 3°/minute.....	89
Figure 6.8 Heat-treated Sample-4 compared against the untreated sample. The sample was heated for 1 hour at 550°C.....	90
Figure 6.9 Heat-treated Sample-1 compared against the untreated sample. The sample was heated for 1 hour at 550°C.....	91
Figure 6.10 Heat-treated Sample-2 compared against the untreated sample. The sample was heated for 1 hour at 550°C.....	92
Figure 6.11 Heat-treated outcrop sample compared against the untreated sample. The sample was heated for 1 hour at 550°C.....	93

Figure 6.12 X-ray diffraction analysis of the EG-treated outcrop sample compared to the non-treated sample. The sample was left under EG-treatment for 2 days.	94
Figure 6.13 Clay mineral ratios of the five studied samples. S/K stands for Smectite 001 /Kaolinite 001. K/I means Kaolinite 001/Illite 001. And S/I and I/S stand for Smectite 001 /Illite 001 and Illite 001/Smectite 001, respectively. The smectite peaks were measured from air-dried samples.	96
Figure 6.14 The WOGC result of the outcrop sample. The <i>N</i> -alkanes peak at <i>n</i> -C ₂₃	98
Figure 6.15 The WOGC result of Sample-4. The <i>N</i> -alkanes peak at <i>n</i> -C ₂₃	99
Figure 6.16 The WOGC result of Sample-2. The <i>N</i> -alkanes peak at <i>n</i> -C ₂₅	100
Figure 6.17 Ternary plots of C ₂₇ , C ₂₈ and C ₂₉ steranes. The background image is modified from Johnson et al (2003). ZB stands for Zuunbayan and TE stands for Tsagan Els. Both oil samples and core sample were from the Zuunbayan sub-basin in the East Gobi Basin. In this diagram, the Khoot samples are showing broad similarities to the East Gobi Basin oil samples and core.	101
Figure 6.18 Graph of pristane/ <i>n</i> -C ₁₇ versus phytane/ <i>n</i> -C ₁₈ for the Khoot samples. ...	102
Figure 7.1 Illustrated depositional environments of the five types of organofacies KinEx recognizes (from Roller and Pepper, 2018).	103
Figure 7.2 Calculated UEP from the most common depositional environments (from Zetaware software).	105
Figure 7.3 Location of the Khoot Basin in the Eastern Mongolian Basinal Province. This small basin is located between two large sedimentary basins: Middle Gobi and Choir-Nyalga.	106
Figure 7.4 Map of the Khoot basin. The basin depo-center is relatively low. The remaining parts of the basin is relatively flat.	107
Figure 7.5 A) HC yield fractions of aquatic non-marine (lacustrine) deposits and aquatic marine clay-rich samples B) Kinetic curves of the cumulative hydrocarbons expelled from DH 1 source rock interval. The red curve shows the HC1-5 expelled. The green curve shows the HC6+ expelled....	111
Figure 7.6 The calculated UEP from each source rock interval in DH 1.	112
Figure 8.1 TOC and HI correlation across DH 1, DH 2, DH 3 and DH 4. For the log correlation, see Chapter 3.	118

Figure 8.2 Interpreted well-log and selected Rock-Eval parameter trends from DH 1.....	119
Figure 8.3 Three different basin types: Overfilled, Balanced-fill and Underfilled (Bohacs et al., 2000).....	120
Figure 8.4 Interpolated (IDW) maps of the Khoot basin that were created from calibrated Rock-Eval data. Each map was created using different parameters. Black line on maps is the seismic line.....	122

LIST OF TABLES

Table 4. 1	Tabulated sample weight range and number of collected samples from each drill hole and outcrop sampling campaigns.	30
Table 4. 2	Data range and standard deviations of DH 2 samples. The threshold weight is 40 mg.	32
Table 4. 3	Data range and standard deviations of DH 3 samples. The threshold weight is 33 mg. SD stands for Standard Deviation.	34
Table 4. 4	Data range and standard deviations of DH 4 samples. The threshold weight is 34.5 mg.	36
Table 4. 5	Data range and standard deviations of DH 5 samples. The threshold weight is 38 mg.	38
Table 4. 6	Data range and standard deviations of the two shallow depth drill hole samples (SD1 and SD2). The threshold weight is 40 mg.	40
Table 4. 7	Data range and standard deviations of Campaign 1 outcrop samples. The threshold weight is 35 mg.	42
Table 4. 8	Data range and standard deviations of Campaign 2 outcrop samples.	42
Table 4. 9	Data range and standard deviations of Campaign 3 outcrop samples. The threshold weight is 35 mg.	45
Table 5. 1	TOC range of the calibrated Khoot oil shale samples as well as Mongolian oil shale and shale samples from various basins in Mongolia. See Chapter 2 for Mongolian Basin locations. *These three are considered the same deposition, thus will be referred to as the Shinekhudag Type Samples. **This is the age that was assigned by Li et al (2014) to the cores which were drilled nearby SD1 and SD2 of this study. Before this study, Khoot oil shales were considered to the same age as the Shinekhudag Type Samples. ***These three samples will be referred to as the Central Mongolian Shales. Sladen and Traynor (2000) considered them to be of oil shale quality.	49
Table 6. 1	Major and minor elements (ppm) detected in the Khoot subsurface and outcrop samples. The results displayed below are calculated average values of 2-3 scans from each sample.	86
Table 6. 2	Trace elements (ppm) detected in the Khoot subsurface and outcrop samples. The results displayed below are calculated average values of 2-3 scans from each sample.	87

Table 7. 1 Description of the depositional environments and basic characteristics of the organofacies types (from Roller and Pepper, 2018).....	104
Table 7. 2 Calculated original TOC and HI values from the present-day Rock-Eval measurements of DH 1 samples.....	108
Table 7. 3 Calculated original TOC and HI values from the present-day Rock-Eval readings of DH 4 and Campaign 2 outcrop samples.....	109
Table 7. 4 Input values used for the DH 1 UEP calculations.....	110
Table 7. 5 Calculated UEP of the three different types of Khoot basin.....	113
Table 7. 6 Volumetric qualities and expulsion potentials of the Khoot basin and compared world-class basins.....	114
Table 7. 7 Hydrocarbon potentials of the Middle Gobi and Choir-Nyalga basins.	116
Table 8. 1 Summary of geochemical, geological and organic matter characteristics of the source rocks distributed across the Khoot basin.....	124

ACKNOWLEDGMENTS

I would like to express my sincere gratitude to my advisor Dr. Alexei Milkov and co-advisor Dr. Lesli Wood for their support and faith in me. Without their guidance and support, I would not have gone this far in my studies. I am most grateful to my advisors for their patience and for helping me with scholarship applications. Moreover, thank you, Dr. Alexei Milkov, for continuously pushing me towards my goals and for always being available for discussions.

This study would not have been possible without Genie Oil and Gas's Chief Geologist Dr. Yuval Bartov's support and data donation. I would also like to take a moment to devote special thanks to Dr. Rick Wendlandt for helping me improve my understanding of X-Ray Diffraction Analysis and allowing me to use the laboratory. Dr. Rick Sarg and Dr. Jeremy Boak for sharing their knowledge and expertise about oil shales.

Thank you, Dr. Stephen M. Enders, Cheryl Medford, Dorie Chen, Roxane Aungst and Suzanne Beach, for your dedication to the Mines students' wellbeing and success.

A very special thanks to the wonderful researchers at the U.S. Geological Survey, Dr. Paul Lillis, Dr. Justin Birdwell and, especially, the lovely Katherine French for helping me with advanced organic geochemical tests and reports.

I would also like to thank my undergraduate advisor Dr. Paul Mann at the University of Houston for leading me in the right direction and encouraging me to pursue my graduate degree.

Finally, I would like to take time to thank my sister, Ankh-Enerel Batbayar, my fiancé Khuslentugs Mendbayar, and my dear friends Dulguun Tumurbat, Gantuya Yanjindulam as well as Moath Al Qaod for sharing this journey with me and for encouraging me at times of doubt and troubles.

Thank you, God, for the many blessings and opportunities.

CHAPTER ONE
INTRODUCTION

1.1 Overview of the Study Area

Kerogen-rich lacustrine oil shale formations serve as an excellent source rock for conventional oil and gas plays and has potential for unconventional shale oil production. In recent years, Mongolian government opened exploration and project development blocks throughout the country, with the hopes of improving the country's economy. In this study, we will focus on the richest oil shale-bearing Khootiin Khotgor area or the Khoot Basin and explore its potentials for hydrocarbon production.

The study area is located in Block XXV, one of the 28 commercially licensed exploration blocks leased by Mongolian government (Figure 1.1). Block XXV was explored by several domestic and international companies in the past three to five years.



Figure 1. 1 Locations of the 28 exploration blocks in Mongolia. Block XXV is circled in yellow.

One of the main exploration companies was Genie Oil and Gas, from whom data for this study was obtained. The total exploration area of the block is 2800 km². Aside from the Khoot basin, the block contains the following basins, all of which have oil shale deposits: Choir, Khashaat Khudag and Olongiin Uhaa (Figure 1.2).

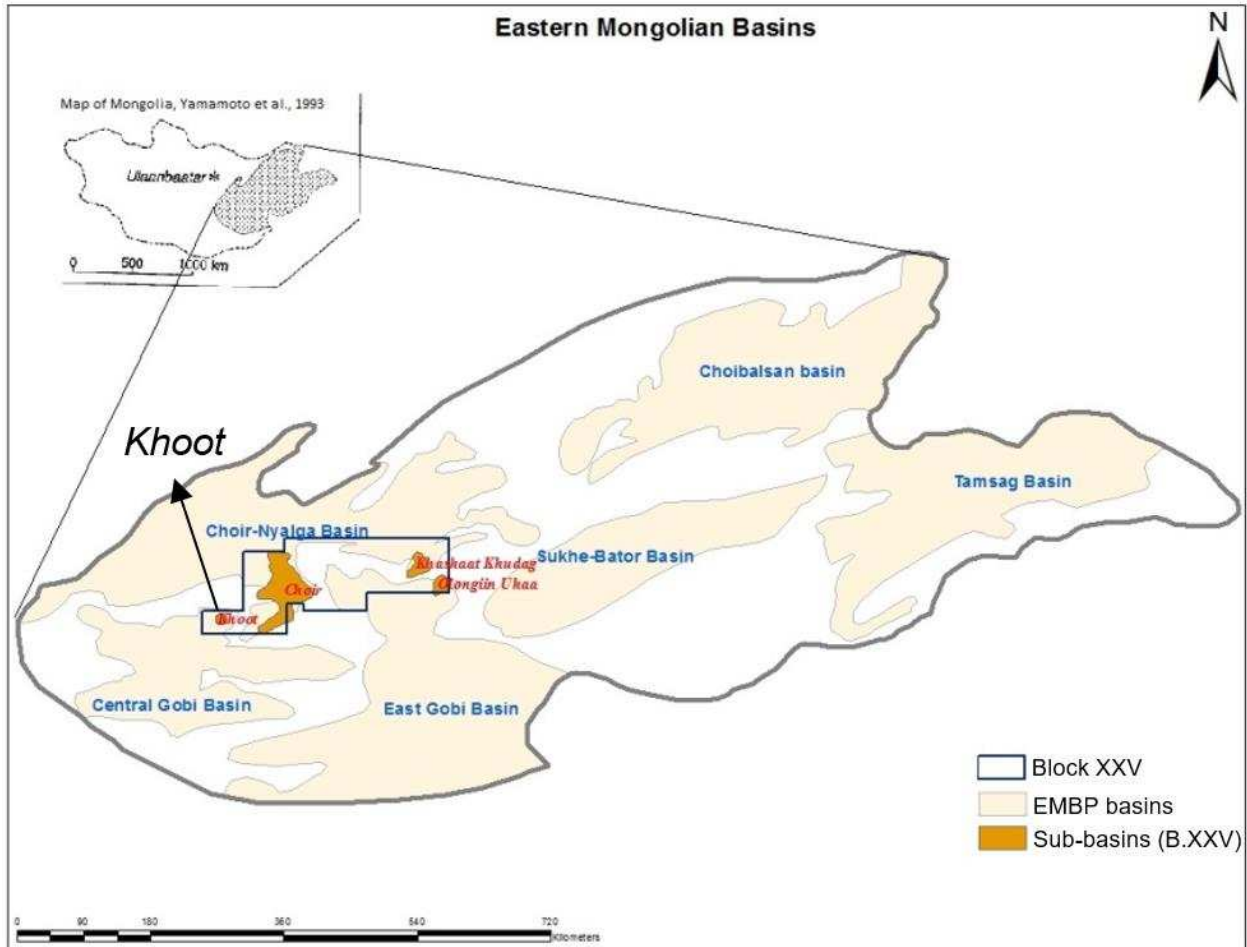


Figure 1. 2 Enlarged map of the Eastern Mongolian Basinal Province (EMBP). Sub-basins (Choir, Khoot, Khashaat Khudag, and Olongiin Uhaa) within Block XXV are displayed on the map. The smallest of the four sub-basins is the Khoot Basin located at the northern edge of the Central (Middle) Gobi Basin.

Among these four sub-basins, the Khoot Basin received major attention due to outcrops in this area containing highly organic rich oil shales, as previously mentioned. The Khoot oil shale has a total TOC of 14.5 wt% - 28.8 wt % (Avid et al., 2000). Despite this, after three years of exploration in the Khoot basin, Genie Oil and Gas considered

the Khoot oil shale to be of mediocre quality for shale oil production because of two key issues (Personal communication with Yuval Bartov, December 2015). For one, Khoot subsurface samples, by large, had lower TOC values compared to the outcrop samples. For two, the thickness of the oil shale subsurface intervals was not enough to be economically viable. Hence, the purpose of this research is to identify the source rock potential of the Khoot Basin and to explore the underlying geologic reasons for the difference between the organic-rich outcrop oil shale samples and the organic-lean subsurface deposits in the Khoot basin.

1.2 Dataset from Genie Oil and Gas

Data for this study was provided by Genie Oil and Gas (Courtesy of Yuval Bartov, the Chief Geologist of Genie Oil and Gas). The dataset consisted of complete well logs of five uninterpreted wells sections and two basic core descriptions from Drill Hole 2 and Drill Hole 4.

Raw Rock-Eval data was available from the afore-mentioned five drill holes as well as two shallow-depth drill holes and outcrop samples from three different sampling campaigns. In addition to that, two 2D seismic lines were given. One of the two seismic lines was interpreted in this study. The selected seismic line was shot along Drill Hole 1 (DH 1), Drill Hole 2 (DH 2), Drill Hole 3 (DH 3), and Drill Hole 4 (DH 4). The location is provided in Figure 1.3.

Drill holes 1 and 2 are located at the center of the Khoot Basin, DH 3 is in the midzone, and drill holes 4 and 5 are located at the margin of the basin (Figure 1.3). The shallow depth drill holes (SD1 and SD2) are 20 m deep each and located near DH 4 at the margin of the basin (Figure 1.3). Two additional locations are provided on the gravity map as Eedemt-A and Eedemt-B, where shallow depth cores were extracted to study the age of the Eedemt (Khoot) oil shales by Li et al (2014).

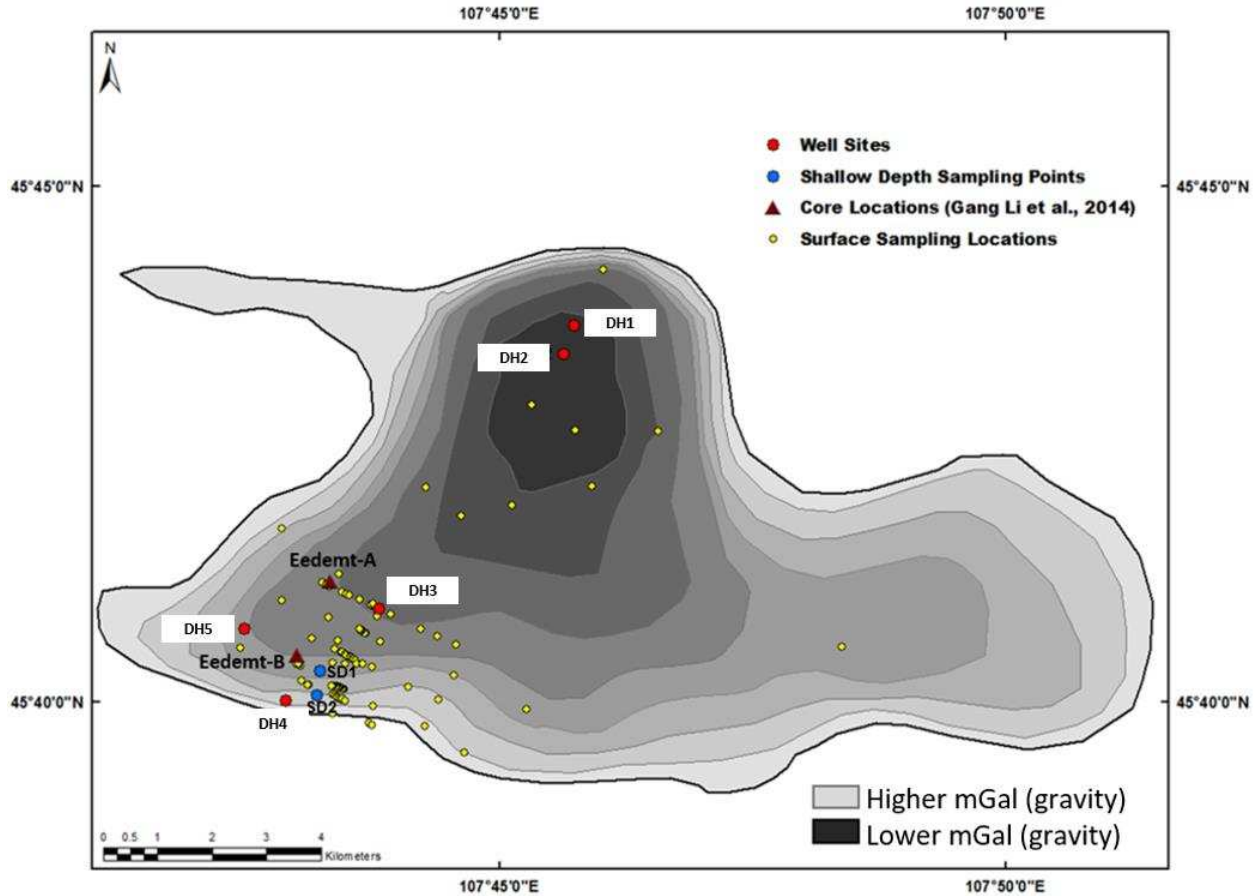


Figure 1. 3 Bouguer gravity map of the Khoot basin that has the locations of the five deep drill holes, two shallow depth drill holes and the surface samples. The locations of the two cores extracted during Li et al’s 2014 study are also provided.

1.3 Core and Outcrop Samples from Khoot Basin

Five samples were shipped to the Colorado School of Mines campus in Golden, CO from Genie Oil and Gas in Israel for advanced geochemical analysis. Additional samples were not available. Four of the five samples are subsurface samples from different depths and stratigraphic sequences in Drill Hole 1. The fifth sample is an outcrop sample. These five samples are described below.

The surface sample is a laminated light brown to copper-brown colored oil shale. The sample is brittle, fissile and easily breaks apart. Particle sizes were not visible through hand lens. Compared to the subsurface samples, this sample does not react with HCl.



Figure 1. 4 Photographic image of the studied outcrop sample from the Khoot basin.

By comparison, all four of the subsurface samples reacted with HCl. Samples 2 and 3 are the hardest. Sample-1 and Sample-2 are non-laminated light grey to greenish grey colored oil shales. However, Sample-1 is easily breakable. It is harder than Sample-4, but softer than the two middle samples. Sample-3 is a laminated grey colored oil shale that is as hard as Sample-2 sample. Sample-4 is a dark colored, laminated oil shale. This sample is the softest among all studied samples and easily breaks apart. Grain size is not visible through hand lens.

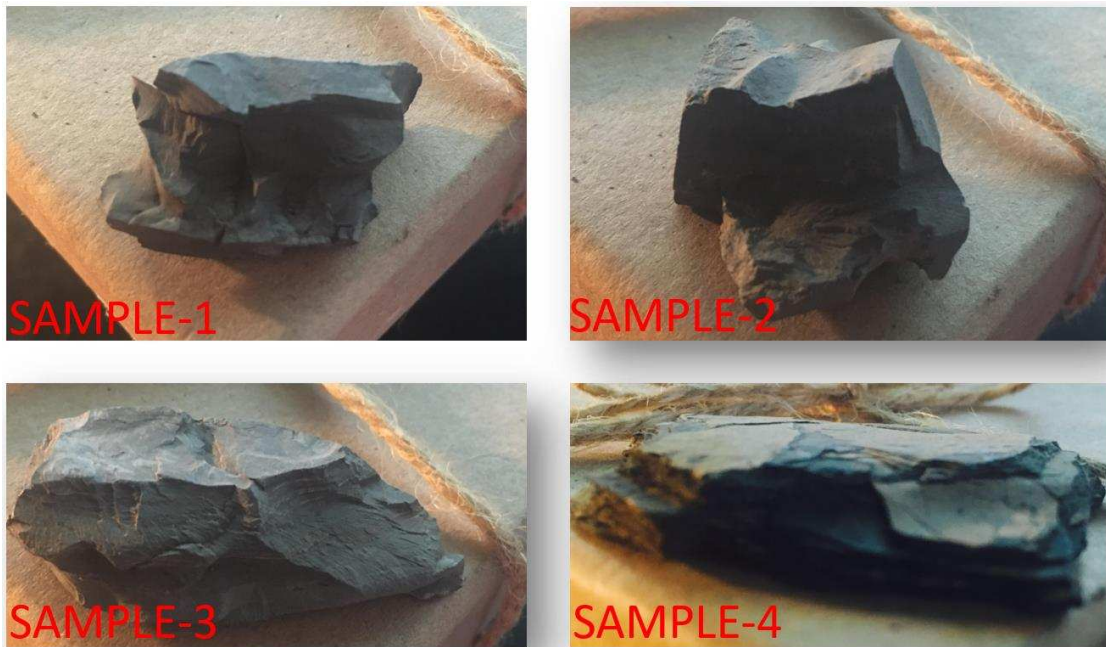


Figure 1. 5 Photographic images of the selected subsurface samples from Khoot basin.

1.4 Geochemical Analytical Methods

1.4.1 XRF Analysis Method

The samples were initially analyzed by a handheld Niton XL3t Thermo Scientific XRF analyzer. Standard safety procedures were observed in this experiment according to the Colorado School of Mines X-Ray safety training regulations. Sample-4 was analyzed three times. All the other samples (Sample-3, Sample-2, Sample-1 and the outcrop sample) were analyzed twice.



Figure 1. 6 Handheld XRF Analyzing Device (Niton XL3t - Thermo Scientific).

1.4.1 XRD Analysis Method

X-ray diffraction analysis was conducted in the Colorado School of Mines X-Ray Diffraction Laboratory. To run X-ray diffraction analysis on organic-rich samples, the organic matter (OM) needs to be removed first. Several different OM removal methods were explored before deciding on using diluted hydrogen peroxide (H_2O_2). This method

was slower than the method involving NaOCl - Sodium Hypochlorite (found in commercial bleaches), in which the mixture is heated in boiling water (Moore and Reynolds, 1989).

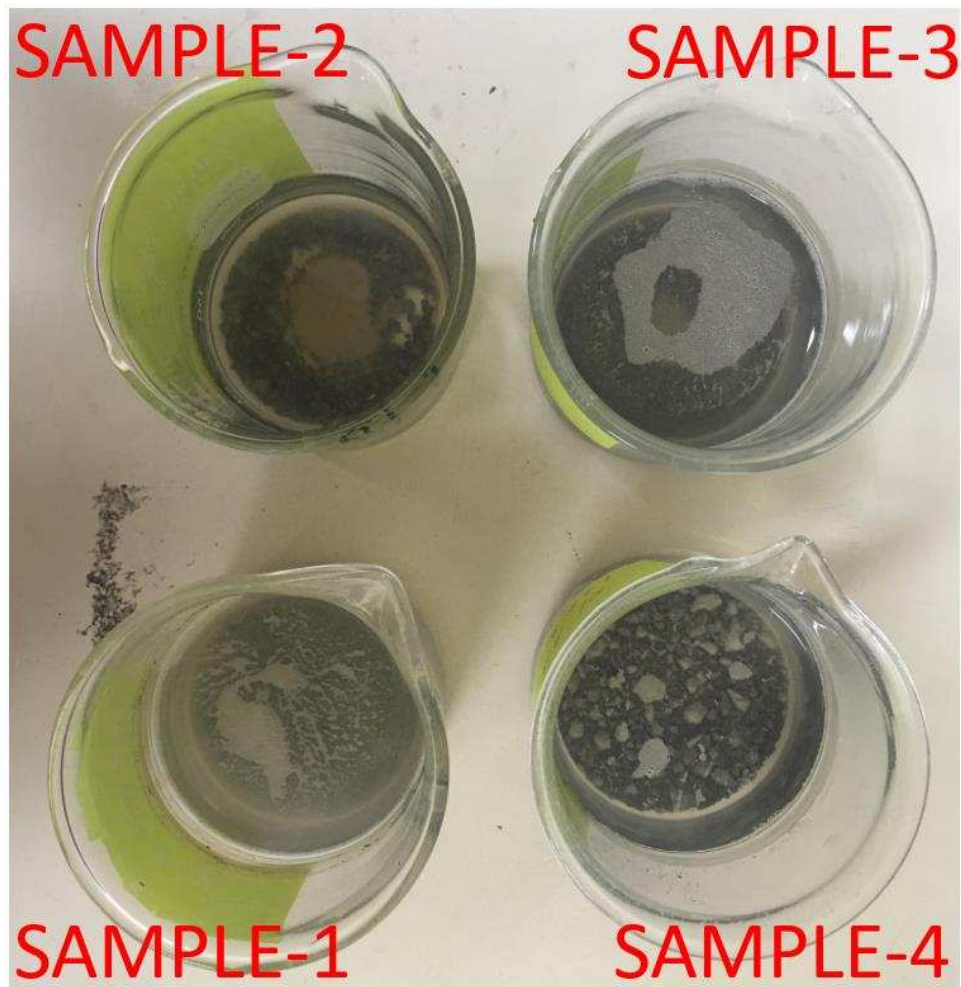


Figure 1. 7 Photographic image of crushed Khoot samples suspended in diluted hydrogen peroxide.

The samples were crushed and ground to smaller size (< 3 mm diameter) by mortar and pestle before adding the diluted H_2O_2 . In terms of reaction with hydrogen peroxide, samples 1 and 3 fizzed more than samples 2 and 4. Sample-4 fizzed in the hydrogen peroxide solution for just 3-5 days while samples 1 and 3 continuously fizzed about three weeks in the hydrogen peroxide solution. After several days of soaking the samples in hydrogen peroxide. This procedure was repeated until the samples stopped fizzing.

To create oriented clay mineral aggregate with 3-micron size fractions, the samples were centrifuged for 60 seconds at 1000 RPM. The supernatant was then microfiltered to extract the thin film layer of oriented sample mount using the Millipore filter transfer method (Moore and Reynolds, 1989). All samples were analyzed from 5° to 65° at 3°/min under CuK α radiation. Further investigation techniques involved reanalysis of the samples following EG-treatment and heat treatment up to 550°C.

1.4.2 Biomarker Analysis Method

Three powdered (mortar/pestle) rock samples (the outcrop sample, Sample-4, and Sample-2) from Khoot, Mongolia were extracted using sonication with chloroform (Courtesy of Katherine French, USGS in Lakewood). 15-30 mL of chloroform was added to each powdered sample and sonicated at 30°C for 30 minutes to an hour. The resulting extract was decanted and filtered through a combusted glass fiber filter loaded into a Pasteur pipette. The sonication procedure was repeated for a total of 10 times, where extracts were combined and concentrated under a stream on N₂ gas.

Then, in order to remove the asphatenes, the chloroform was evaporated under a N₂ stream and was replaced with isooctane before being refrigerated at ~ 2-4°C for two days. Next, the samples were filtered through a solvent-rinsed glass fiber filter attached to a solvent-rinsed glass syringe to remove any precipitated asphaltenes. The resulting maltenes were brought up in 1.5 mL of isooctane. An aliquot of each maltene sample was analyzed on an Agilent GC-MSD in full scan mode (50-570 m/z) on a DB-1 column with a flow rate of 1.2mL/min. The GC oven was held at 60°C for 2 minutes, ramped at 20°C /min to 150°C, then ramped at 3°C/min to 315°C, and finally held for 28.5 minutes at 315°C.

CHAPTER 2

PREVIOUS RESEARCH AND GEOLOGIC BACKGROUND

2.1 Geologic Background

Lacustrine oil shale deposits are abundant in the Early Cretaceous sedimentary rift successions of eastern Mongolia and northeast China. The Khoot area is located in one of these resource rich provinces, the Eastern Mongolian Basinal Province (EMBP). The total area of the EMBP is 450,000 km² and each basin bears an abundance of oil shale and coal deposits, with many active coal mines operating in the basins (Erdenetsogt et al., 2009). The majority of the EMBP basins are coeval with the Early Cretaceous Yingen, Hailar, Erlian, and Songliao basins which developed during the Late Jurassic-Early Cretaceous extensive NE-SW rift and transtensional tectonic phases in northeast Asia (Yamamoto et al., 1993; Sladen and Traynor, 2000; Graham et al., 2012).

Mongolian rift basins are not as deep and as large as the basins in China (Graham et al., 2012). The mechanisms by which these rift basins had formed are still poorly understood. Researchers generally agree that the Cretaceous rifts are caused by orogenic collapses following inter-cratonic collisions along the Mongol – Okhotsk suture zone (Figure 2.2) (Yamamoto et al., 1993; Sladen and Traynor., 2000; Graham et al., 2012; Li et al., 2016).

This suture zone was formed as a result of the Mongol – Okhotsk Sea's rapid closure in the latest Jurassic – earliest Cretaceous (Yang et al., 2006). What is remaining from this ancient ocean is the Okhotsk Sea in Russia. To the east, the Mongol – Okhotsk suture zone runs all the way to the Okhotsk Sea (Figure 2.1 and Figure 2.2), but to the west, it abruptly ends in central Mongolian territory (Fritzell et al., 2016).

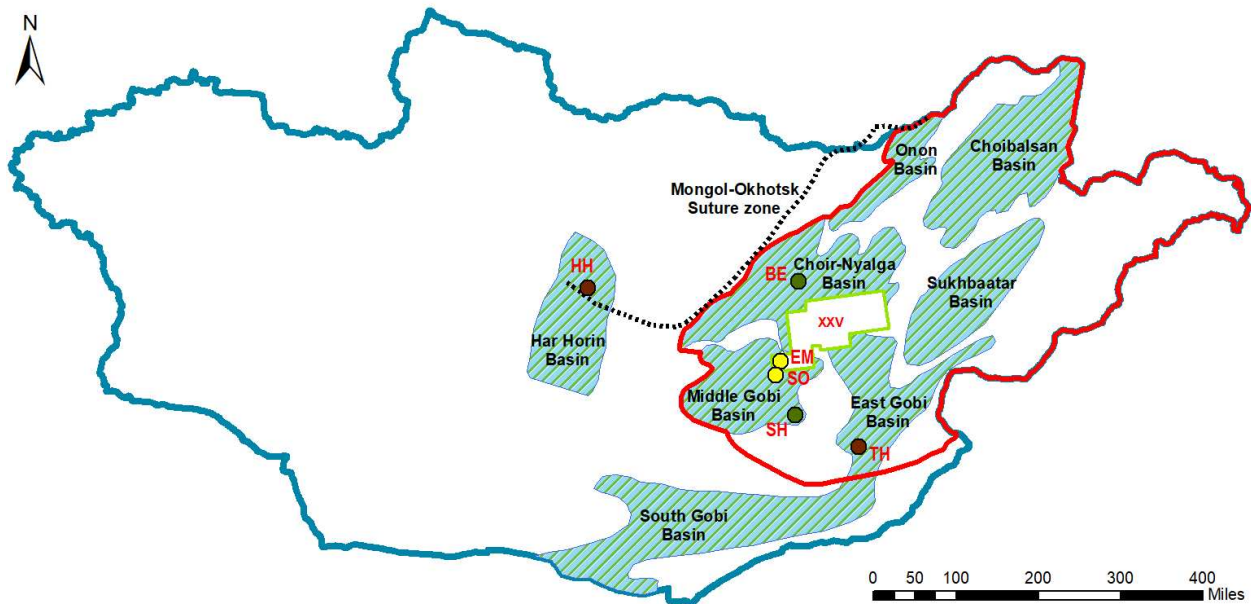


Figure 2. 1 NE-SW trending Late Jurassic to Early Cretaceous basins in the EMBP: Choir-Nyalga Basin, Middle Gobi Basin, East Gobi Basin, Onon Basin, Choibalsan Basin, and the Sukhbaatar Basin. The Har Horin and the South Gobi basins are located outside of the EMBP (Redrawn from Yamamoto et al., 1993; Traynor and Sladen, 2000; Genyao et al., 2013). Illustrated in circles are the oil shale sediments possibly deposited in these basins: HH-Har Horin; BE-Bayan Erkhiti; EM-Eedemti; SO-Shawart Obo; SH-Shinekhudag; TH-Tavan Har

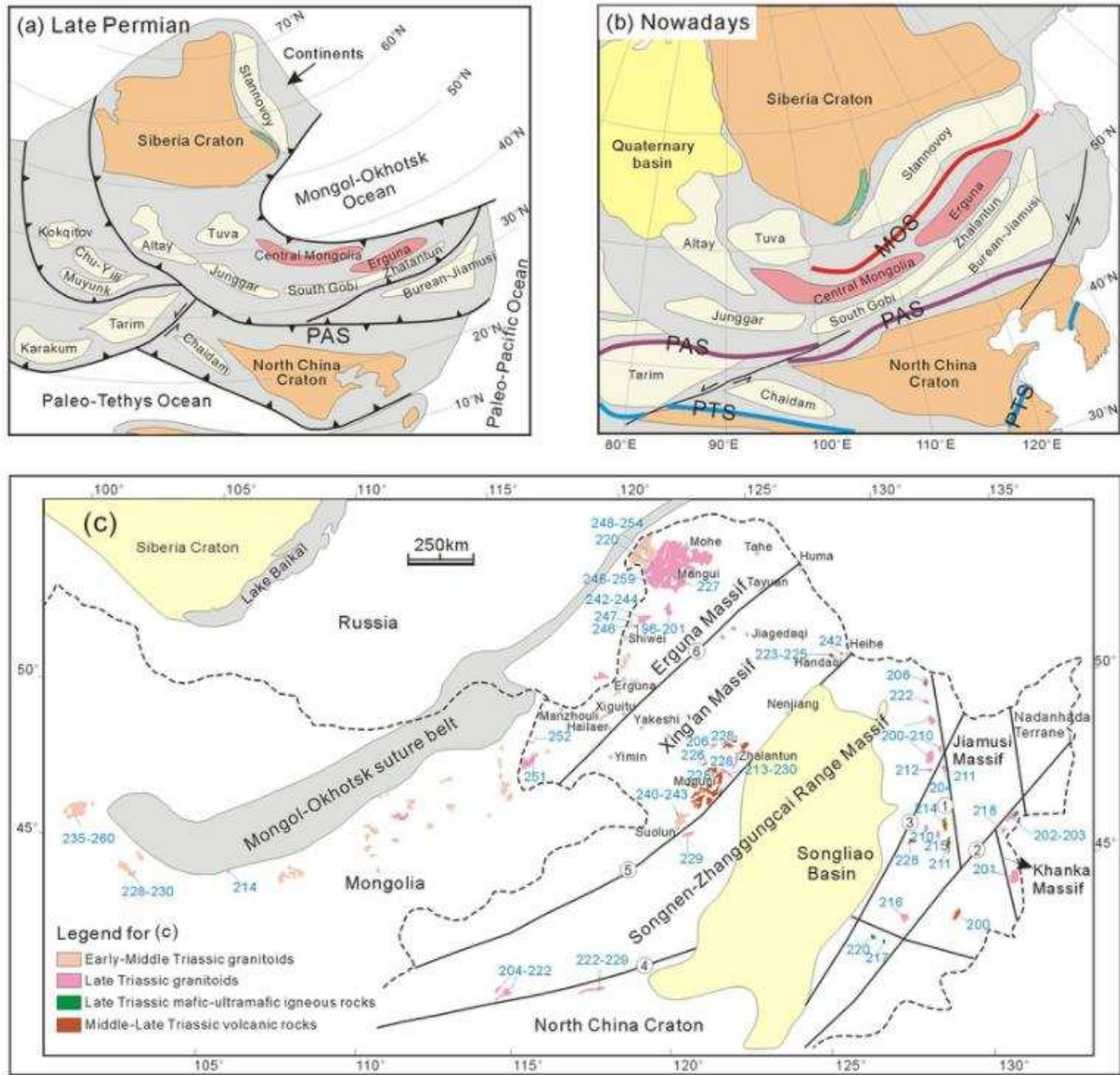


Figure 2. 2 The paleo-tectonic map of northeastern Asia from the Late Permian to the Present (From Li et al., 2016).

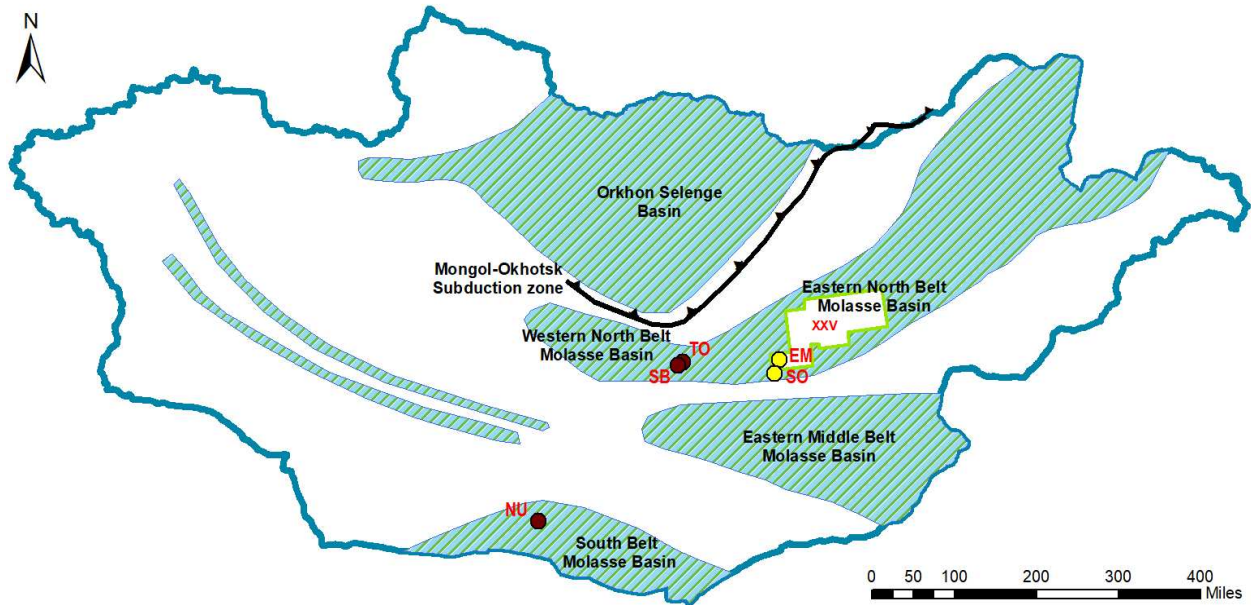


Figure 2. 3 Early-Middle Jurassic basins relative to the location of Block XXV. The Western and the Eastern North belt Molasse basins are the westward extension of the Hailar Basin. The Eastern Middle Belt Molasse Basin is the westward extension of the Erlian Basin. The South Belt Molasse Basin is the northward extension of the Yingen Basin (Redrawn from Genyao et al., 2013). Illustrated in circles are the oil shale sediments possibly deposited in these basins: SB-Sayan Obo; TO-Tsagan Obo; NU-Noyon Uul; EM-Eedemt; SO-Shawart Obo.

Superimposed underneath these Late Jurassic-Early Cretaceous rift basins are the Triassic-Jurassic basins (Figure 2.3), which were considered not as economically significant and viable as the Cretaceous basins (Sladen and Traynor, 2000; Genyao et al., 2013). Formerly, these Triassic-Jurassic basins in Mongolia were classified as small-scale intermountain foreland basins that developed in front of a major mountain chain that had already existed across Mongolia by the Triassic (Sladen and Traynor, 2000). These few tens of square kilometers long intermountain basins were neither large nor long-lived enough to have had extensively distributed geologic formations (Sladen and Traynor, 2000).

An alternative and comprehensive picture of the Jurassic tectonic events was given by Genyao et al (2013) (Figure 2.4). By their estimate, the Yingen, Erlian and

Hailar basins are of Early-Middle Jurassic age, and their westward extensions exist on eastern and central parts of Mongolian territory.

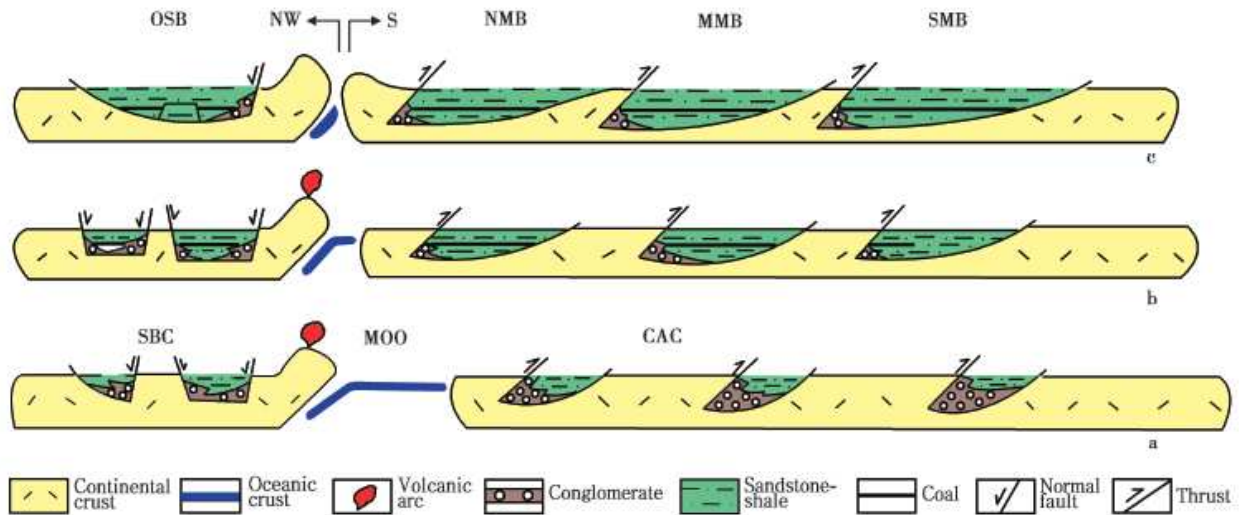


Figure 2. 4 Illustration of the subducting Mongol – Okhotsk Oceanic (MOO) plate under the Siberian Craton (SBC), which eventually led to the collision of the SBC and the China-SE Asia subcontinent (CAC). OSB: Orkhon-Selenge Basin; NMB: North Belt Molasse Basin; MMB: Middle Belt Molasse Basin; SMB: South Belt Molasse Basin (Adapted from Genyao et al., 2013).

By the Early Jurassic, the Mongol – Okhotsk oceanic crust had been subducting underneath the Siberian Craton (Yang et al., 2015). The back-arc basin that formed due to the subduction of the Mongol – Okhotsk oceanic crust is called the Orkhon-Selenge Basin (Figure 2.3). Basins to the south of the suture zone are a series of molasse (synorogenic foreland) basins (Genyao et al., 2013). Block XXV is located in the Eastern North Belt Molasse basin, which is the extension of Hailar Basin in China (Figure 2.3).

2.2 Previous Studies on Khoot Area Deposits

Mongolian sedimentary basins are relatively less studied, except for a few producing basins such as the East Gobi Basin and the Tamsag Basin. The majority of the geologic surveys conducted on Mongolian territory were published in Russian and

are difficult to obtain. However, in recent years, Khoot area surface deposits were mainly studied by Avid et al (2000), Avid and Purevsuren (2001) and by Purevsuren and Ochirbat (2016). These authors have extensively studied the thermal behavior, pyrolysis characteristics and geochemical compositions of the Khoot area coal and oil shale deposits.



Figure 2. 5 An SEM image of a Khoot oil shale sample (Avid and Purevsuren, 2001).

In the pyrolysis studies conducted by Avid et al (2000), Khoot oil shales were determined to be the best oil shale deposits among all oil shale deposits in Mongolia with 14.5-28.8 wt.% TOC. The shale oil yield of Khoot oil shales is 13.3 wt% to 15.6 wt% of the raw oil shale. These results were obtained at pyrolysis temperature of 550 °C and at a heating rate of 92 °C/min (Avid et al., 2000). Hard residue from the pyrolysis is between 73.4 wt% and 75.5 wt%. Compared to this, Estonian oil shales have a 25.5 wt% shale oil yield and a hard residue wt% of 63.8 %. Green River oil shale has 10.3 wt% shale oil yield and the hard residue is 85.8 wt%. The Khoot oil shale was determined to be an aluminosilicate-carbonate type oil shale with 51% clay minerals, 25% organic matter, and 10% calcite and dolomite (Avid and Purevsuren, 2001) (Figure 2.5). X-ray diffraction patterns of Khoot oil shale is shown to have calcite, dolomite, quartz, illite, smectite, getite, halloysite, feldspar, and hydromica (Figure 2.6).

Until recently, Khoot deposits were considered coeval with the extensively distributed Early Cretaceous lacustrine oil shale-rich Shinekhudag Formation. However, a recent study by Li et al. (2014) reassessed the biostratigraphic (Figure 2.7) timeframe of the Khoot oil shale deposits and discovered that Khoot oil shales were deposited during the Middle Jurassic instead of Early Cretaceous as previous studies had concluded.

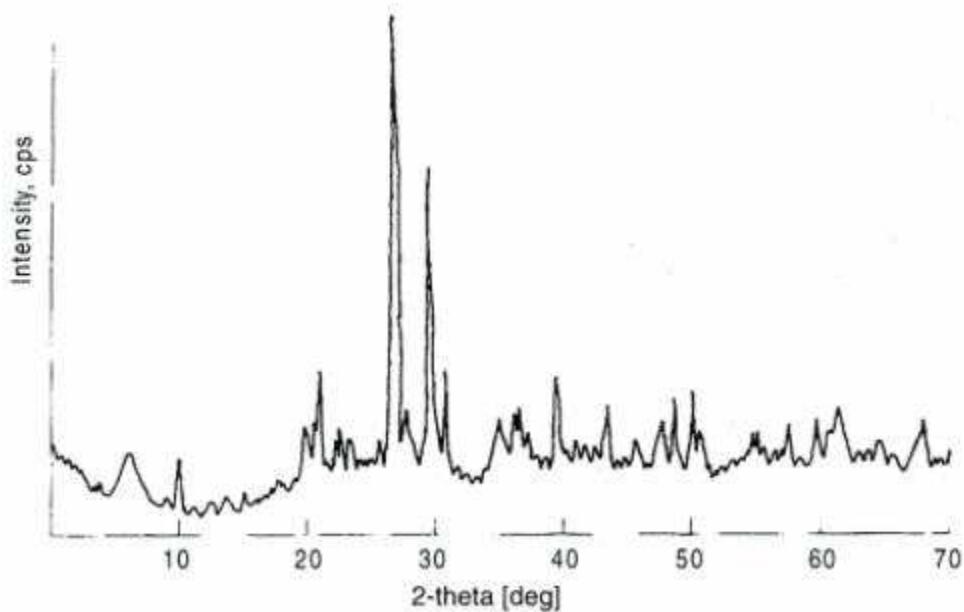


Figure 2. 6 The X-ray diffraction analysis result of a Khoot oil shale sample under $\text{CuK}\alpha$ radiation on a Siemens D-5000 diffractometer (Avid and Purevsuren, 2001). The minerals identified by Avid and Purevsuren (2001) are calcite ($d=3.03, 2.08, 1.87 \text{ \AA}$, e.g.), dolomite ($d=2.89, 1.78, 2.19 \text{ \AA}$), quartz ($d=3.34, 1.81, 1.54, 1.37, 2.45, 2.12 \text{ \AA}$), illite ($d=2.57, 1.49 \text{ \AA}$), smectite ($d=1.495, 4.45 \text{ \AA}$), getite ($d=2.45 \text{ \AA}$), halloysite, feldspar ($3.21, 3.18, 3.95 \text{ \AA}$) and hydromica ($d=2.54, 4.41, 1.48 \text{ \AA}$). This study showed no kaolinite.

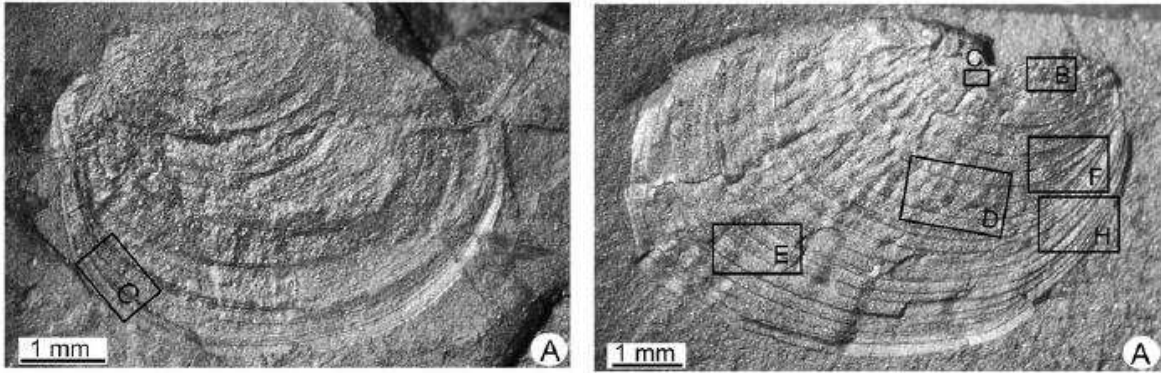


Figure 2. 7 A) Shallow depth core sampling from the Eedemt (Khoot) locality has proven that the Eedemt Formation is abundant in *Triglypta eedemtensis* Li *sp. nov.* (Left) and B) *Dundgobiestheria mandalgobiensis* Li *gen. et sp. nov.* (Right), which are typical of Middle Jurassic lacustrine deposits of northern Hebei, and the Junggar and Turpan basins of northwestern China (Li et al., 2014).

A similar conclusion was drawn from a palynostratigraphic study of the underlying coal-bearing deposits (Khootiin Khotgor Formation) after assessing the Khootiin Khotgor Coal Mine deposits (Ichinnorov et al., 2008). Li et al. (2014) has thus assigned a new name for the oil shale formation in the Eedemt (Khoot) area to distinguish it from the Early Cretaceous Shinekhudag Formation.

CHAPTER 3

SUBSURFACE ARCHITECTURE OF THE KHOOT BASIN

3.1 Tectonic and Depositional Architecture from Seismic Data

The Khoot basin was drilled for the first time between 2010 and 2014. The first seismic data were also obtained during the same time. The seismic line used in this study was shot along Drill Holes 1, 2, 3, and 4 in NE-SW direction (Figure 3.1). The proposed tectonic regime here is extension, however, it could also be transtension (Figure 3.2). The extensional direction is NE-SW (Figure 3.2), which is the opposite direction of the Early Cretaceous regional extensional direction (NW-SE), which formed the larger EMBP basins, such as East Gobi, Tamsag and Choir-Nyalga.

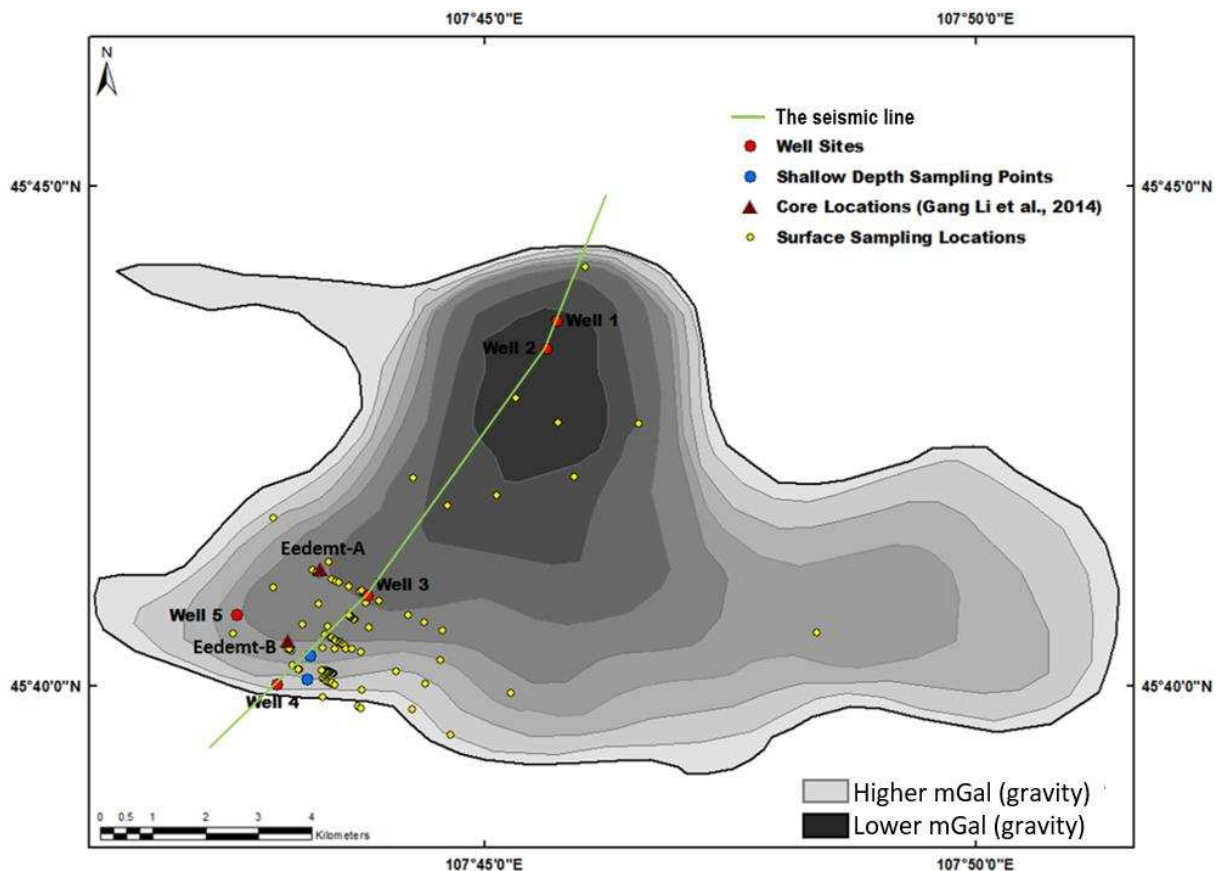


Figure 3. 1 Position of the seismic line in the Khoot basin. The seismic line was shot through DH 1, DH 2, DH 3, and DH 4.

Tectonic structures that formed because of this NE-SW extension are listric normal faults, a graben and a rollover anticline (Figure 3.2, Figure 3.2D). The graben that is located towards the southwestern region of the basin is approximately 1500 m long. DH 3 was drilled in this graben. The outcrops located to the northeast of DH 3 in the area of DH 1 and DH 2 contain a stratigraphically thicker section than the outcrops located to the southwest of DH 3.

The lacustrine strata in this section overlie a retrogradational thin mounding pack of strata that covers the entire area. Between these mounds and the lacustrine strata is an erosional surface, which is characterized by the sharp change in sediment succession, where the oil shale layers directly overlay thin layers of coal and silty sandstone-conglomerate. In the well logs, this erosional surface is at the point where the gamma ray crosses the resistivity log below Sequence 1.

It was previously assumed from gravity data that Drill Holes 1 and 2 were drilled in the basin depo-center. In this section, the previous assumption is proven from seismic data interpretation. The basin depo-center is identified as a depression formed over the thinning section of a stratigraphic wedge that underlies the lacustrine deposits. Sediments filled the main depo-center from two sides. The prograding delta foresets are relatively gently dipping (10-12°) and most likely made of muddy fine-grained materials, as opposed to steeply dipping coarse-grained Gilbert-type delta. Aside from the bi-directional deltaic features, the basin depo-centers have basin-floor mounds interpreted to be deep lake submarine fans (encircled in blue) (Figure 3.2C, 3.2D).

To the northeast of DH 1, there is a topographic high, which leads to another small depo-center behind the topo high. The biggest structural architectural element in this part is a rollover anticline associated with a listric fault almost at the edge northeastern edge of the basin. The previously mentioned two graben-forming normal faults are also listric normal faults. The displacement caused by these listric faults is relatively small (approximately 50 m).

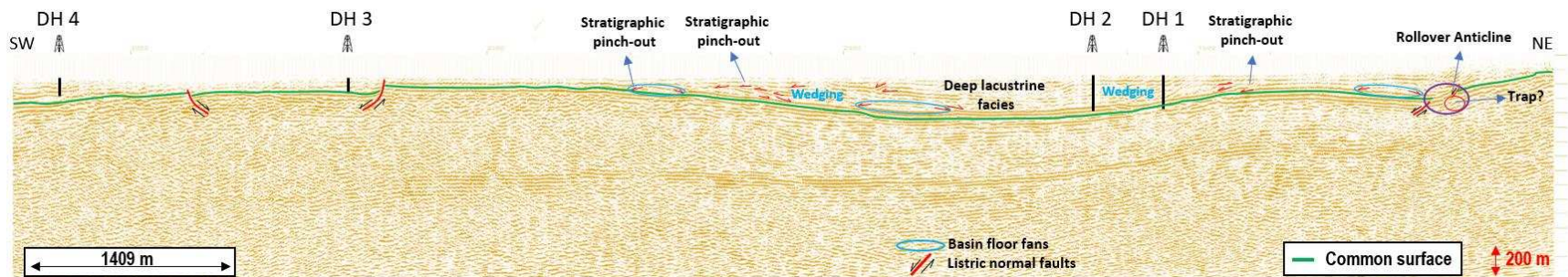


Figure 3. 2 A) The interpreted seismic line of the Khoot Basin. The seismic line was shot along the line of DH 1, DH 2, DH 3 and DH 4.

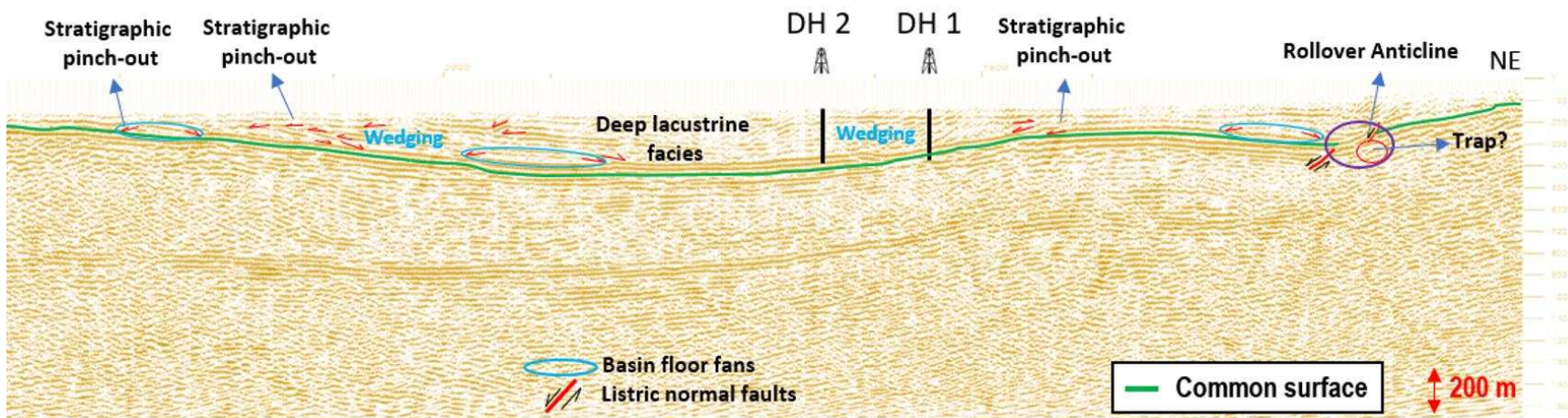


Figure 3. 2 B) Enlarged image of the selected area in Figure 3.2 A.

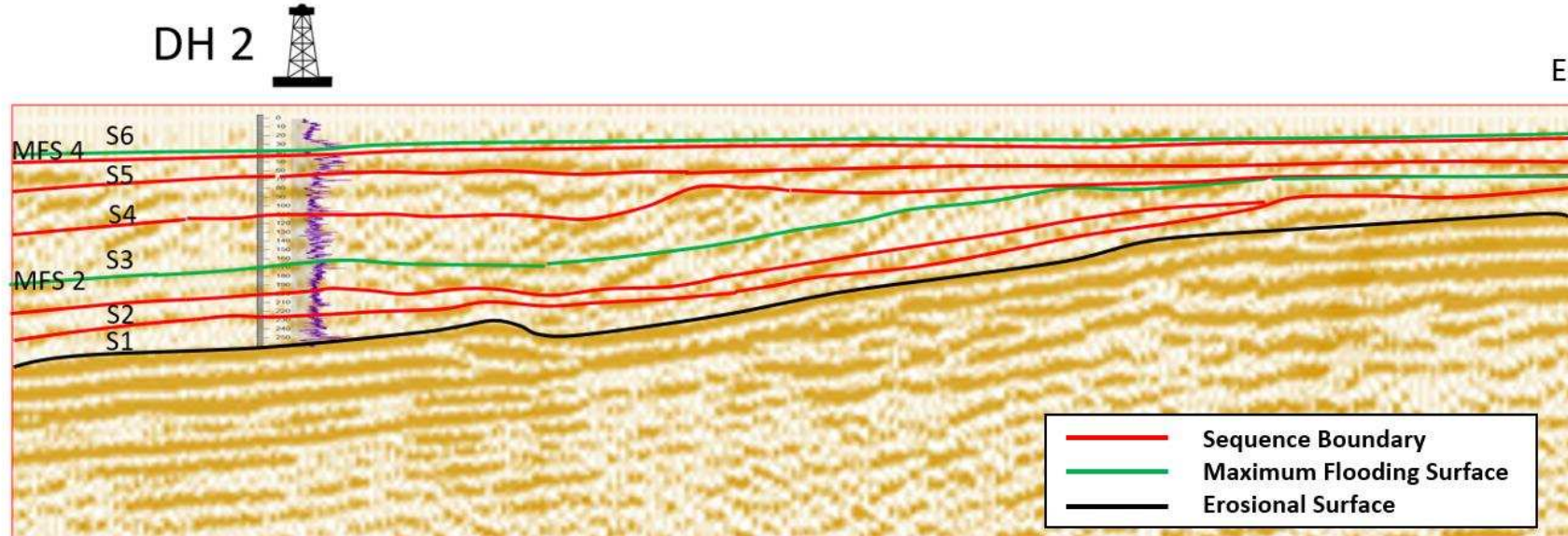
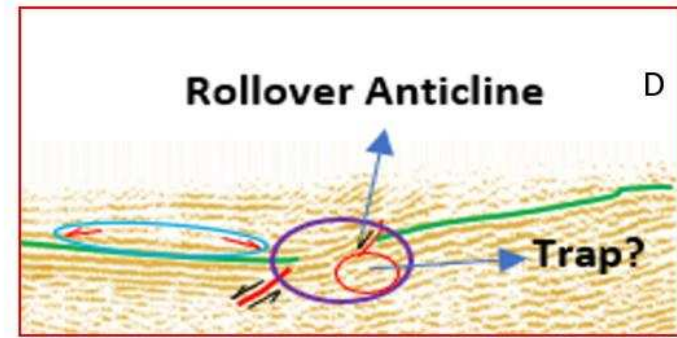
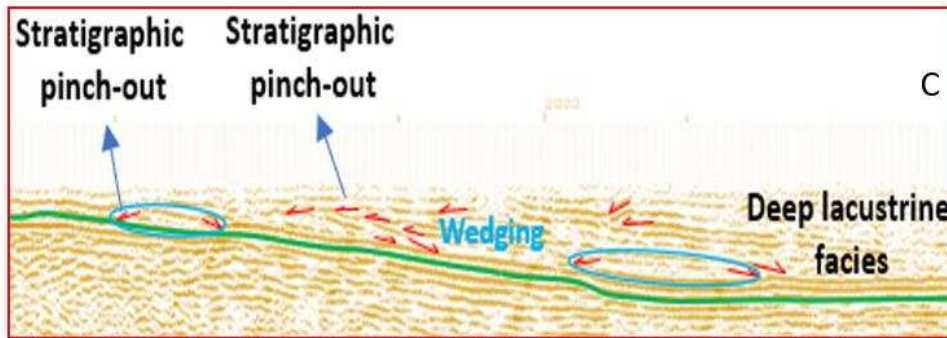


Figure 3. 2 C) Southwestern slope of the Khoot basin depo-center D) Northeastern side of the Khoot basin (See Figure 3.2B for legend.) E) Identified stratigraphic sequences and sequence boundaries in the Khoot basin.

3.2 Stratigraphic Successions of the Jurassic and Cretaceous Strata in Mongolia

As stated above there was no pre-existing interpretation and published materials on the Khoot basin subsurface architecture and stratigraphy. It was previously mentioned in Chapter 2 that the age of the Khoot basin is controversial. Figure 3.3 shows the Early-Middle Jurassic and Early Cretaceous stratigraphic successions in the neighboring Ongi River basin.

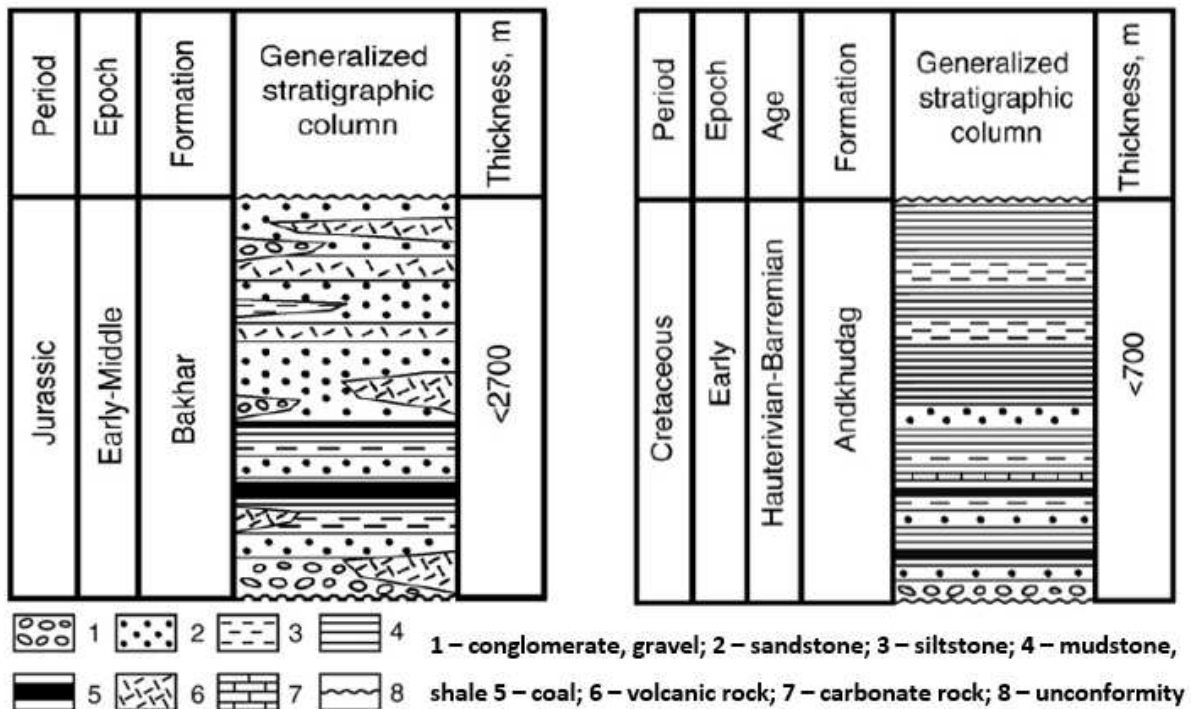


Figure 3. 3 The general stratigraphic successions of the Early-Middle Jurassic Bakhar Formation and the Early Cretaceous And Khudag Formation in the Ongi River basin (From Erdenetsogt et al., 2009). The stratigraphic succession of the Early Cretaceous Shine Khudag Formation is similar to the And Khudag Formation.

The Early-Middle Jurassic strata in Mongolia are dominated by continental red beds and volcanic rocks. However, it was found that southern and southeastern Mongolia has some 500 m thick bituminous coals and interlayered floodplain and lacustrine mudstones (Sladen and Traynor, 2001). The total thickness of the preserved Early-Middle Jurassic strata in Mongolia is less than 2700 m (Sladen and Traynor, 2001). A simplified stratigraphic events of the Early-Middle Jurassic time was proposed

by Genyao et al (2014), where the Jurassic strata was divided into pre-coal strata, coal-bearing strata and post-coal strata. There is very little information on the Jurassic oil shales in Mongolia. Previous workers such as Erdenetsogt et al (2009) suggested that the Jurassic strata in Mongolia has very little to no oil shale. But, Sladen and Traynor (2001) noted oil shale grade lacustrine deposits (Tsagan Obo and Sayan Obo localities) from the Ongi River basin as well as the Har Horin basin (Har Horin deposits). The depositional environment in the Early-Middle Jurassic was proposed as dry and arid as evidenced by the abundance of red beds in the area (Traynor and Sladen, 2001). See Chapter 2 for detailed locations of the oil shale deposits.

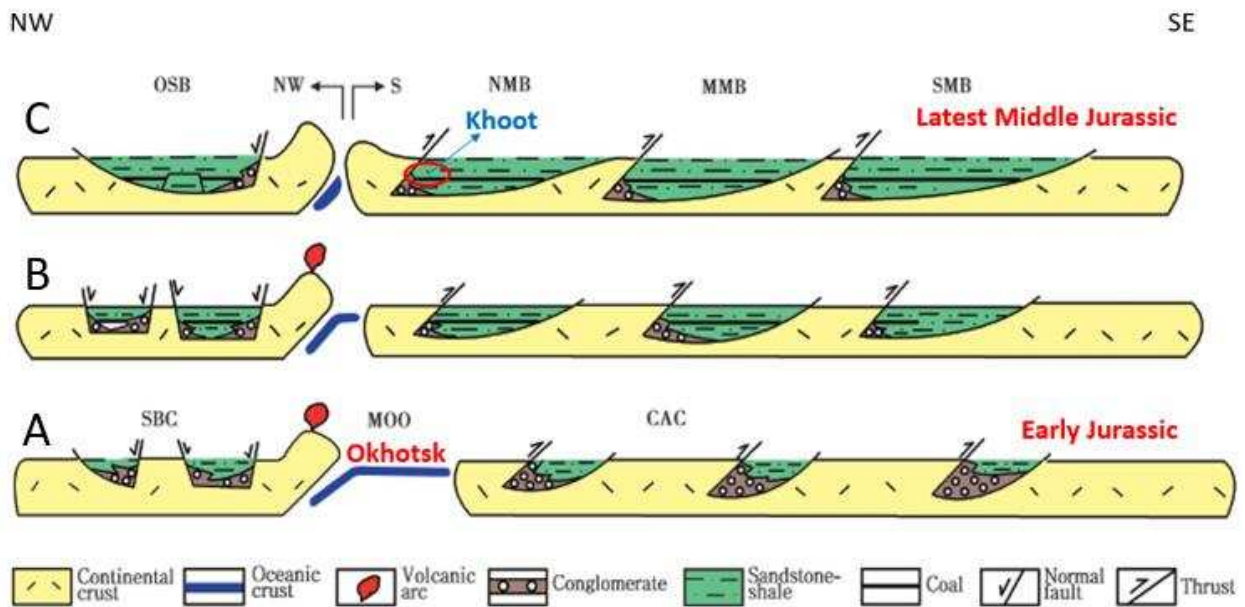


Figure 3. 4 Cross section view of the Jurassic tectonic events and deposits in Mongolia. A) Early Jurassic or the pre-coal stage, B) coal-bearing stage, C) Latest Middle Jurassic or the post-coal stage (Modified from Genyao et al., 2014). See Chapter 2 for the detailed Early-Middle Jurassic basins in Mongolia.

The Early Cretaceous in Mongolia, especially in the eastern part of the country, was dominated by coal deposits, thick oil shales and mudstones. The And Khudag deposit in the Ongi River basin is less than 700 m thick. The Shine Khudag deposit in the Eastern Mongolian Basinal Province is 300-700 m thick depending on the location. The Shine Khudag Formation is assumed to be deposited in the Choir-Nyalga Basin

(exposed at the Bayan Erkhiti location), Middle Gobi Basin (exposed at the Shawart Obo and Shine Khudag locations), and the East Gobi Basin (in the subsurface). Study of the Shine Khudag deposits at the Shine Khudag locality has provided evidence that the climate was warm and humid in the Early Cretaceous (Ando et al., 2005). See Chapter 2 for in detail locations of the oil shale deposits.

3.3 Sequence Stratigraphic Correlation in the Khoot Basin

3.3.1 Identification of Systems Tracts and Surfaces

Stratigraphic sequences were identified and correlated from gamma ray and resistivity log trends across the four wells (Figure 3.5) that were drilled along the interpreted seismic line (Figure 3.2E). The gradual decreasing intensity of the resistivity log shows an overall fining upward trend from the bottom of the drill hole to the upper section. Individual sequences and para-sequences within each sequence is better observed in the gamma ray log trend. Flooding surfaces and systems tracts were also identified from the gamma ray logs.

- **Maximum flooding surfaces:** A maximum flooding surface defines the furthest landward shift of the basin shoreline. In the Khoot basin's correlated sections, the maximum flooding surfaces were identified as distinct high sharp gamma-ray spikes.
- **Sequence boundary:** Sequence boundary was assumed to be an erosional surface that separates a highstand depositional cycle from a lowstand depositional cycle. Sequence boundaries were identified by abrupt changes in gamma-ray response, which indicates unconformity.
- **Transgressive systems tract (TST):** Transgressive systems tract records increasing water level. The transgressive systems tracts were easily identified in the Khoot basin logs from the 10-12 m retrograding third-order parasequences in the gamma-ray logs. The gamma-ray pattern has a sharp base and has a bell shape (Figure 3.5).

- Highstand systems tract (HST): Highstand systems tract is a stratal package that was deposited during water level high. The highstand systems tracts were identified by the maximum flooding surfaces at the bottom and at the top by low gamma-ray readings before the next high, which is marked by the sequence boundary. Although, this stratal package is called the highstand systems tract, it records an overall basin water level decrease from the highest point at the maximum flooding surface to the next lowstand. The HST is identified by serrated patterns in an overall funnel shaped patterns in the gamma-ray log.
- Lowstand systems tract (LST): Lowstand systems tracts are stratal packages deposited during low basin water level. The lowstand systems tracts are marked by sequence boundaries at the bottom. However, lowstand systems tracts are not pronounced in the Khoot basin logs. The LST appears as a funnel shaped pattern in the gamma-ray log.
- Datum: The unconformity surface identified at the bottom of the drill holes was chosen as the datum. In the logs, it is identified at the point at which the gamma-ray log crosses the resistivity log. Strata above the datum are lacustrine oil shale, the strata below the datum is a thin coal surface, coaly siltstone, sandstone and conglomerate at the very bottom.

3.3.2 Interpretation and Correlation of the Khoot Basin Sequences

As previously mentioned DH 3 and DH 4 were drilled in the southwestern part of the paleo basin-margin. DH 1 and DH 2 were drilled in the paleo-basin depo-center (Figure 3.1). Six fining upward parasequences were identified in DH 2. Sequence 1 has the first five parasequences, however, in DH 1 the sixth parasequence is absent. Basin-margin drill holes DH 3 and DH 4 have fewer sequences. Sequence 1 and Sequence 2 were identified in DH 3 and DH 4. Sequence 3 is only partially present in DH 3 and DH 4. Sequences 4, 5 and 6 are absent in DH 3 and DH 4.

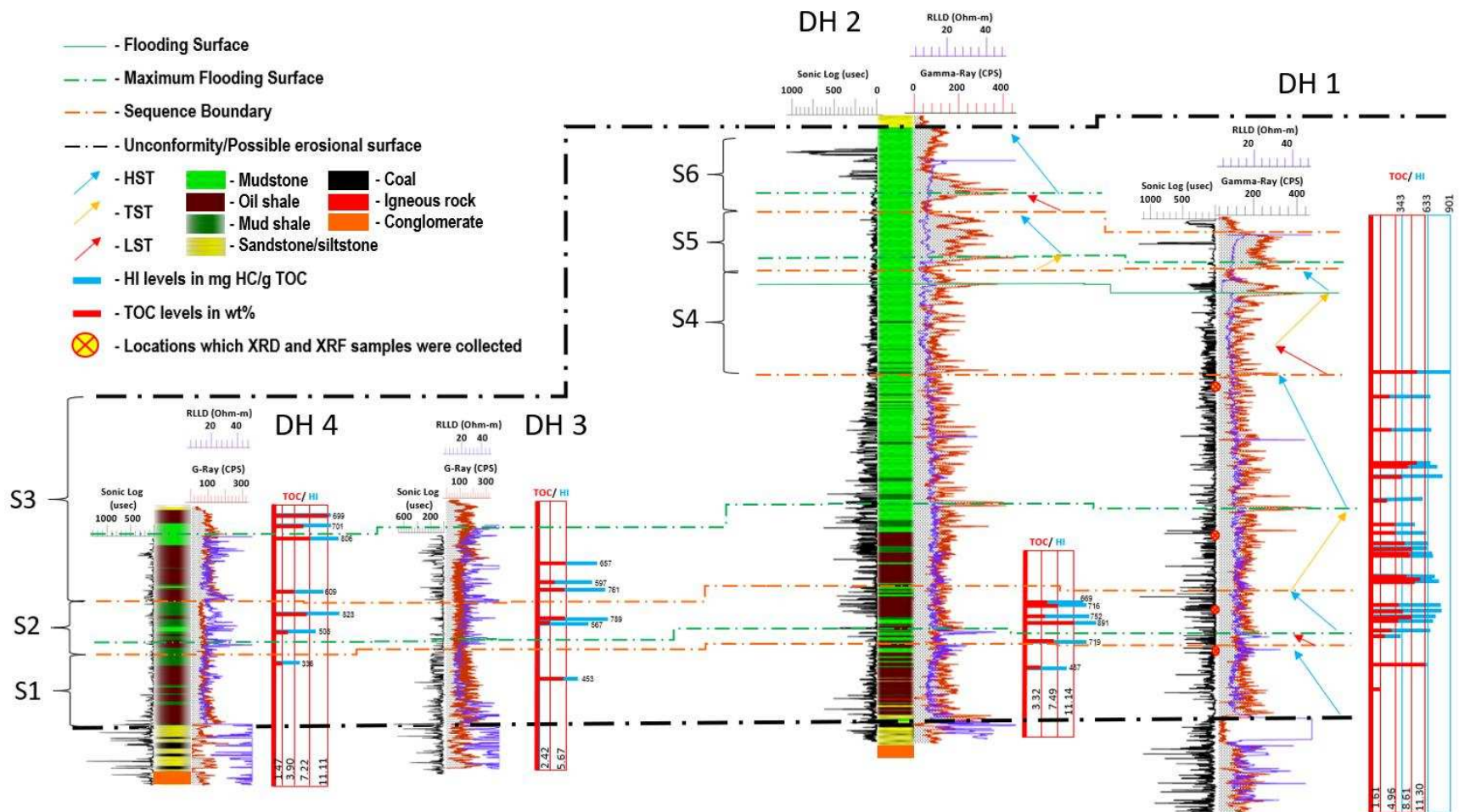


Figure 3. 5 The interpreted well log correlation of Khoot subsurface intervals.

The same observation can be made from the interpreted seismic data; the thick sequences (especially Sequence 3 to Sequence 6) of DH 2 and DH 1 pinch out in the basin depo-center and are absent in drill holes DH 3 and DH 4. The six sequences are described below:

Sequence 1 is 24 meters (DH 2) to 29 meters (DH 1) thick. It is bounded by an erosional surface at the bottom. Sequence 1 almost exclusively consists of HST and lacks TST and has a thin LST. Sequence 1 has a 1 m thick sandstone base and fines upward into 3 m thick interlayered siltstone and mudstone. There is also <0.6 m thick igneous rock interlayer. The oil shale interval begins after this siltstone/mudstone package. The oil shale deposit contains <0.1 m thick light brownish colored marl layers in between. The upper oil shale section has more interlayers of blue greenish or blue greyish colored mudstone. Oil shale in this section contains some pyrite. The overall HI in this sequence is low, it ranges between 24 mg HC/g TOC and 633 mg HC/g TOC, but the average HI across the four wells is 400 mg HC/ g TOC. And the average TOC is 3-4 wt%. The HI level indicates Type II kerogen. Sample-1 was selected from this sequence.

Sequence 2 is 24 meters thick (DH 2) and 22 meters thick in DH 1. Sequence 2 begins with interlayered brownish grey colored oil shale and light blue-greenish colored mudstone. The middle section is dominantly darkish brown grey colored oil shale. The middle part of the HST is a continuous layer of oil shale, which is 8 m. The upper section, like the base, also has interlayered mudstone and oil shale. Sample-2 was collected from this oil shale layer. The HI and the TOC in this sequence show an overall increasing trend in DH 1, DH 3 and DH 4. The HI increases from Type II kerogen (343-567 mg HC/g TOC) to Type I kerogen (700-900 mg HC/g TOC) towards the top of the sequence. The overall TOC is also higher in this sequence, where it ranges from 4 wt% to 11 wt%, with the dominant TOC being 7-8 wt%.

Sequence 3 is 88 meters thick in DH 2 and 89 meters thick in DH 1. This sequence has a thick TST, indicating increasing water level and a thick HST, which means that the lake was deep. The LST and the base of the TST in DH 2 consist of brown grey, grey colored oil shale with thin layers of very soft clay and blue-greenish

grey colored mudstone. The TST then grades into dark brown mud shale, dark brown oil shale and blue-greenish grey colored mudstone. The HST is mostly dark brown colored mudstone. The lithology in DH 4 has more dark brown mud shale than blue-greenish grey colored mudstone. In DH 2, the HI continuously decreases until it reaches the maximum flooding zone and increases back to Type I kerogen in the HST. The TOC in this sequence is more uniform in the oil shale zone, which is about 18 m thick, but it is non-uniform in the mudstone. In some parts, the TOC is as high as 8.8 wt%, but in some sections, the TOC is 4 wt%. Sample 3 was collected from the TST and Sample 4 was collected from the HST in Sequence 3.

Sequence 4 is 42 meters thick in DH 2 and 44 meters thick in DH 1. It has a thin HST and thick TST. Sequence 5 is 24 meters thick in DH 2 and 16 meters thick in DH 1. Sequences 5-6 are almost exclusively black greenish colored mudstone with <20 m thick few interlayers of black grey colored mud shale. No Rock-Eval data is available from these sections. Gamma-ray reading in this section is very high, but the sonic log reading is very low. Sequence 6 is 36 meters thick in DH 2, however, this sequence is incomplete in DH 1; and only a 6 meters thick LST is preserved.

CHAPTER 4

ROCK-EVAL 6 PERFORMANCE AND DATA VERACITY

Sample weight is an essential factor in programmed pyrolysis analysis and data quality. Peters (1986) and Thul (2012) demonstrated that samples under 40-60 mg usually show non-uniform, erratic and unreliable results. Thul (2012) recommended that a minimum of 40 mg sample must be used to obtain optimal results for the measured parameters on Rock-Eval 2, while Peters (1986) recommended a minimum of 60 mg to reach optimum programmed pyrolysis results (Figure 4.1 and Figure 4.2).

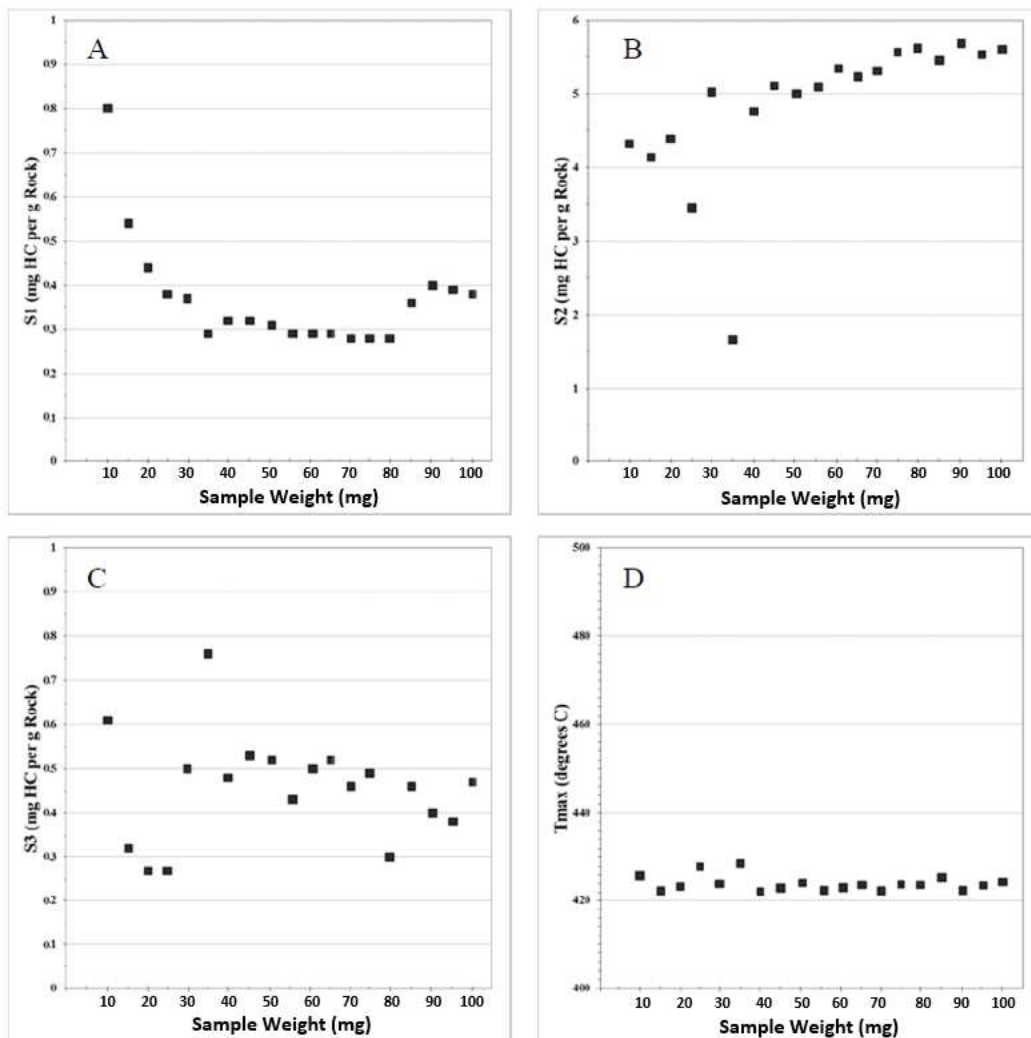


Figure 4. 1 Rock-Eval 2 programmed pyrolysis sample results from the Niobrara Formation, Denver Basin. Measured parameters stabilize at 40 mg (Thul, 2012).

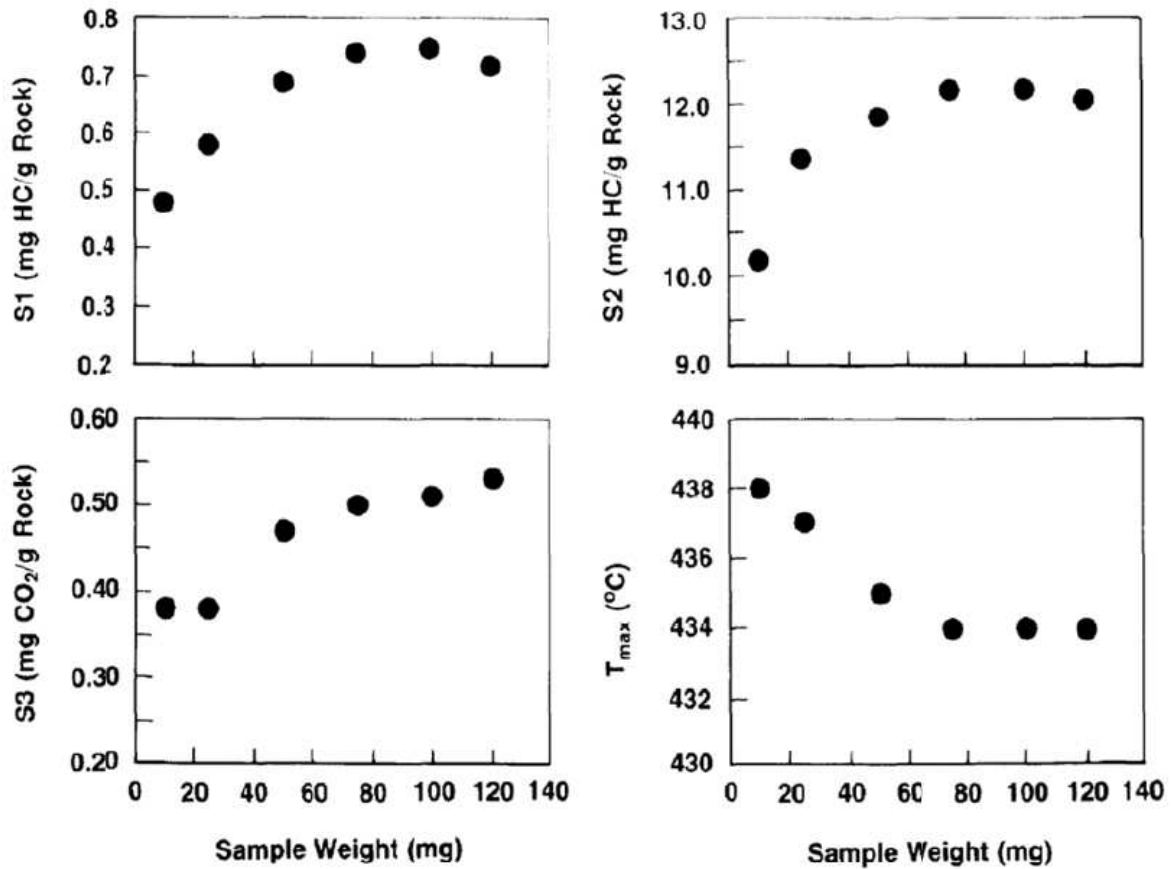


Figure 4. 2 Programmed pyrolysis analysis results from Peters (1986). Measured parameters start to show consistency at 60 mg (Peters, 1986; Thul, 2000).

Unfortunately, the majority of the Khoot samples collected for this study barely meet the recommended 40 mg minimum weight, except for some samples from DH 1. Samples from DH 1 range in weight between 24 mg and 74 mg. Table 4.1 shows the sample weight range and the number of samples collected from each drill hole and surface sampling campaign. Hence, it is possible that sample weight has affected the pyrolysis results. Figures 4.3 through 4.11, measured and calculated parameters from Rock-Eval 6 parameter results, show that sample weight has significant effect on programmed pyrolysis results.

Table 4. 1 Tabulated sample weight range and number of collected samples from each drill hole and outcrop sampling campaigns.

Sample Group	Weight Range (in mg)	Number of Samples
DH 1	24-74	85
DH 2	16-46	72
DH 3	18-37	78
DH 4	18-44	84
DH 5	18-42	135
SHALLOW DEPTH	22-59	40
CAMPAIGN 1	20-42	41
CAMPAIGN 2	20-40	32
CAMPAIGN 3	21-44	58

4.1 Veracity of Drill Hole 1 (DH 1) Samples and Data Calibration

4.1.1 Quality of Drill Hole 1 (DH 1) Samples

There is almost negligible data variation in the measured and calculated samples from DH 1. The only visibly noticeable difference occurs in S2 values, where the S2 values for underweight samples range between 0 to 150 mg/g while the S2 values for the calibrated samples tend to be less than 100 mg/g. This is especially true for samples that are over 60 mg, which is the recommended minimum weight for programmed pyrolysis analysis by Peters (1986). Hydrogen index, a parameter derived from S2, also shows shrinkage in data range and standard deviation.

4.1.2 Data Calibration and Selection

Except for DH 1 samples, all measured and calculated parameters from the rest of the samples showed strong dependence on sample weight (Figure 4.4 through Figure 4.11).

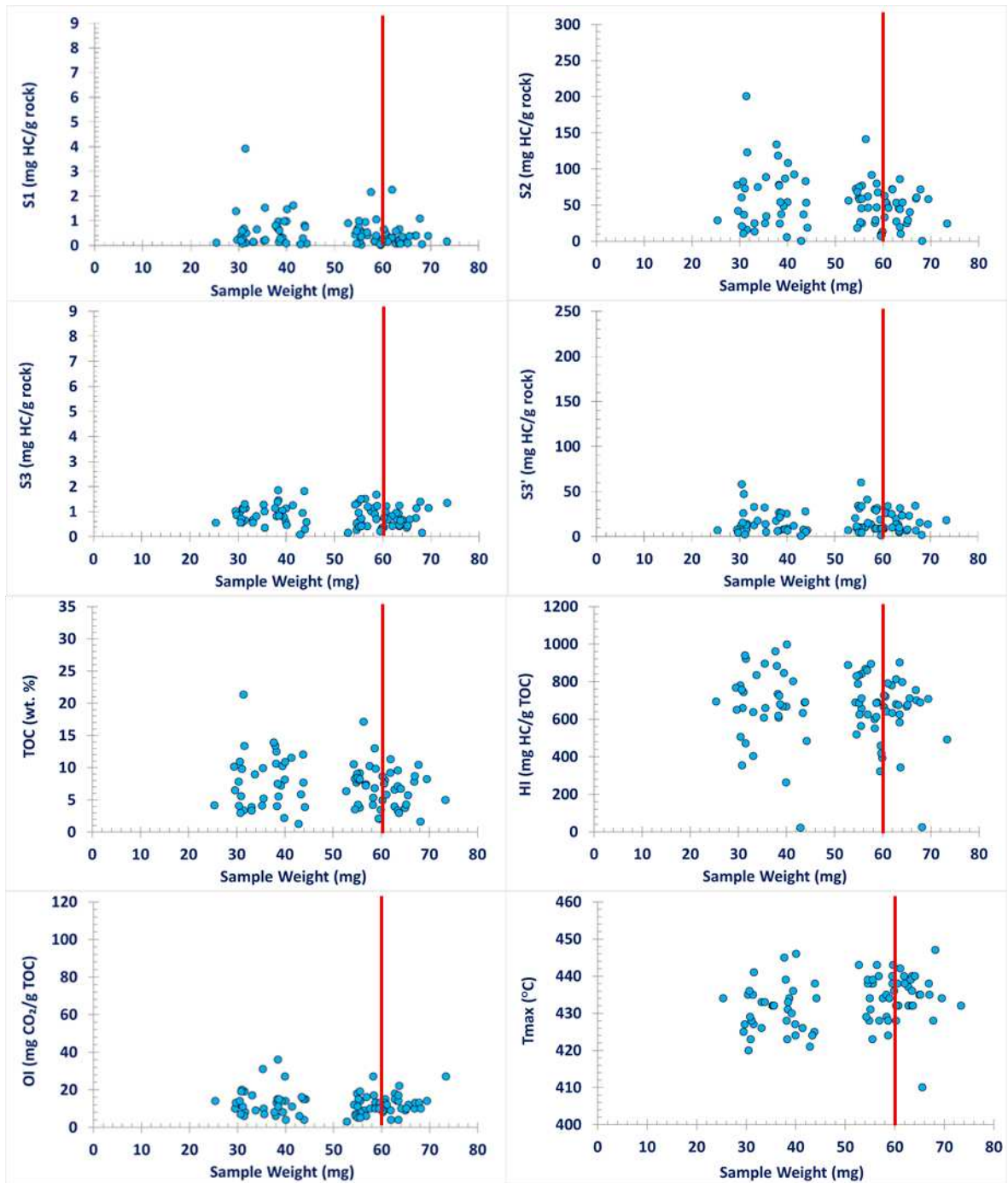


Figure 4. 3 Cross-plots of the measured and calculated Rock-Eval 6 programmed pyrolysis parameters vs. sample weight for DH 1 samples. The threshold weight is the minimum recommended weight (60 mg) by Peters (1986).

Since most Khoot samples are less than 60 mg and 40 mg, which are the minimum weights recommended by Peters (1986) and Thul (2012), respectively, a threshold weight point was chosen for each group of samples as a result of analyzing the Rock-Eval parameter vs Weight cross-plots (Figure 4.4 through Figure 4.11). This weight corresponds to a weight where most, if not all, parameters start to show consistent results. For DH 2 samples, this threshold weight is the recommended 40 mg in Thul (2000). For all other samples, the threshold weight is between 34 mg and 38 mg.

4.2 Veracity of Drill Hole 2 (DH 2) Samples

For DH 2 samples, parameter values stabilize around 40 mg as previously mentioned. DH 2 samples show an odd behavior between 30 mg and 40 mg, where S1, S2, S3', HI, OI, and TOC values artificially spike up. On the contrary, Tmax values artificially drop for the same samples which have 30 mg-40 mg weight range (Figure 4.4).

However, at 40 mg, the erratic behavior of the measured and calculated parameters stabilizes (Figure 4.4). The standard deviation for each parameter also narrows down for the standard weight samples, which are over 40 mg (Table 4.2).

Table 4. 2 Data range and standard deviations of DH 2 samples. The threshold weight is 40 mg.

Parameter	Data range < 40 mg	Data range ≥ 40 mg	SD < 40 mg	SD ≥ 40 mg
S1	0.02-0.79	0.08-4.41	0.65	0.22
S2	0.61-117.5	16.16-99.24	29.32	26.21
S3	0.18-1.95	0.6-0.83	0.34	0.09
S3'	1.7-83.0	4.6-70.1	14.25	24.85
TOC	0.41-14.88	3.32-11.14	3.26	2.56
OI	5-44	7-19	6.10	4.50
HI	29-1186	487-891	206.39	119.68
Tmax	406-553	425-439	16.43	4.93

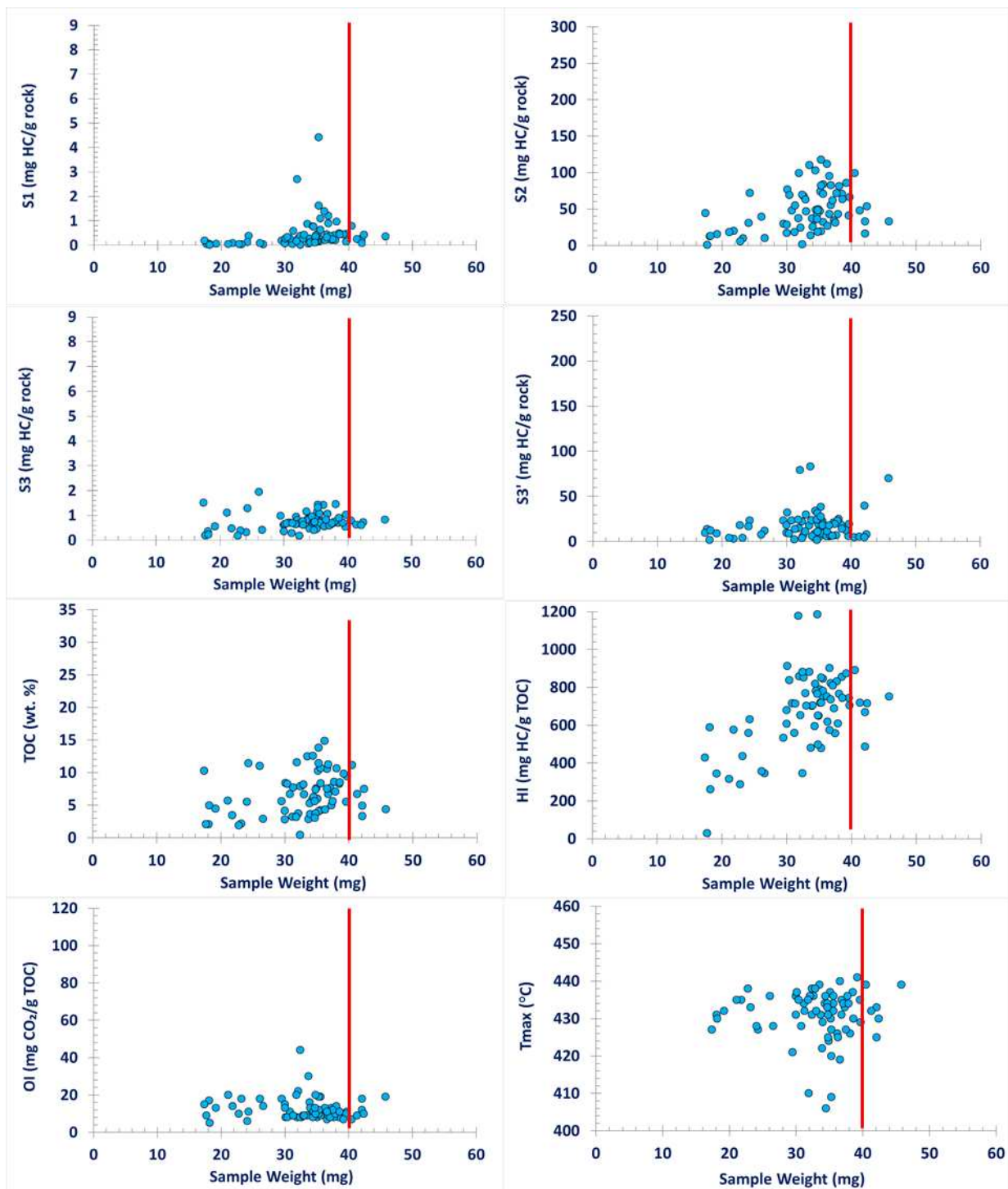


Figure 4. 4 Cross-plots of the measured and calculated Rock-Eval 6 programmed pyrolysis parameters vs. sample weight for DH 2 samples. The threshold weight is the minimum recommend weight (40 mg) by Thul (2000).

4.3 Veracity of Drill Hole 3 (DH 3) Samples

The effects of sample weight start to show at 33 mg for the DH 3 samples. Underweight samples have high S1 values, but all standard weight samples have lower S1 ($S < 1$ mg HC/g rock). The maximum remaining ability to generate hydrocarbon (S2) is 200 mg HC/g rock in the underweight samples. However, the true S2 values for DH 3 samples range between 13.72 mg HC/g rock and 43.26 mg HC/g rock as indicated by the S2 range in the standard weight samples. The organically sourced carbon dioxide values (S3) do not show much change (Figure 4.5), but its derived parameter OI shows evident change. The OI values shrink for samples over 33mg, and so does the standard deviation, which decreases to 3.71 from 8.91 (Table 4.3).

Table 4. 3 Data range and standard deviations of DH 3 samples. The threshold weight is 33 mg. SD stands for Standard Deviation.

PARAMETER	DATA RANGE		STANDARD DEVIATION	
	Weight < 33 mg	Weight ≥ 33 mg	SD < 33 mg	SD ≥ 33 mg
S1	0.03-5.91	0.11-0.73	0.96	0.23
S2	1.39-181.73	13.72-43.26	39.43	12.24
S3	0.3-1.74	0.50-1.10	0.28	0.20
S3'	3.8-97	22.7-45.5	17.73	8.77
TOC	0.67-18.35	2.42-5.67	3.81	1.25
OI	5-58	14-25	8.91	3.71
HI	190-995	453-789	204.44	114.92
Tmax	409-443	427-438	6.38	3.68

Tmax, which is an indicator of source rock thermal maturation, is another important parameter affected by weight. The Tmax values for samples over the threshold value (33 mg) range between 424°C and 438°C. Compared to that, the Tmax values for some of the underweight samples are as low as 409°C.

The most affected parameter is the TOC and S2. The TOC significantly drops from a high of 18.35 wt.% to 5.67 wt.% for the calibrated samples (over 33 mg).

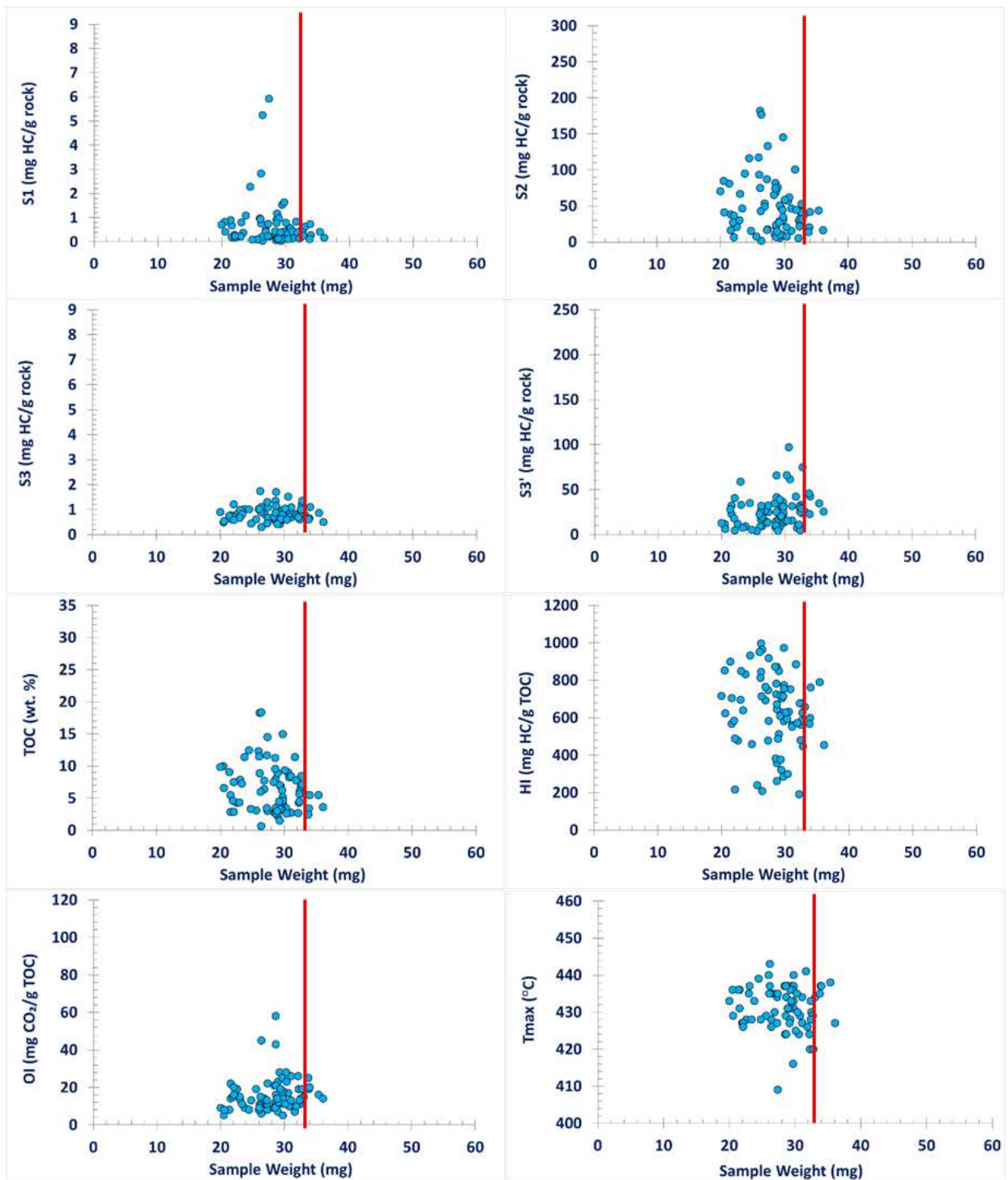


Figure 4. 5 Cross-plots of the measured and calculated Rock-Eval 6 programmed pyrolysis parameters vs. sample weight for DH 3 samples. The threshold weight was chosen as 33 mg.

4.4 Veracity of Drill Hole 4 (DH 4) Samples

DH 4 samples do not show as obvious change in parameter results as DH2 and DH3. However, measured samples S2 and Tmax, and calculated sample HI show more change with increasing weight. The threshold weight is 34.5 mg. Standard deviations of parameters S1, S3 and OI only increase when weight increases. However, the overall data range of S1 and OI decreases.

Table 4. 4 Data range and standard deviations of DH 4 samples. The threshold weight is 34.5 mg.

Parameter	Data range < 34.5 mg	Data range ≥ 34.5 mg	SD < 34.5 mg	SD ≥ 34.5 mg
S1	0.03-3.21	0.05-2.01	0.60	0.62
S2	2.78-173.32	4.94-77.7	33.52	22.86
S3	0.44-4.3	0.55-4.34	0.71	1.2
S3'	4.1-68.5	17.6-49	15.38	11.34
TOC	1.32-17.75	1.47-11.11	3.39	2.83
OI	7-62	9-39	10.33	11.32
HI	211-976	336-823	180.78	149.61
Tmax	404-445	422-438	8.48	5.07

4.5 Veracity of Drill Hole 5 (DH 5) Samples

Having the most number of samples, this group of samples from DH 5 show the strongest dependence of parameter value on sample weight (Table 4.5). There is only one sample that has a weight over 40 mg from the DH 5 samples. However, each parameter's data range decrease as they get closer to the recommended 40 mg

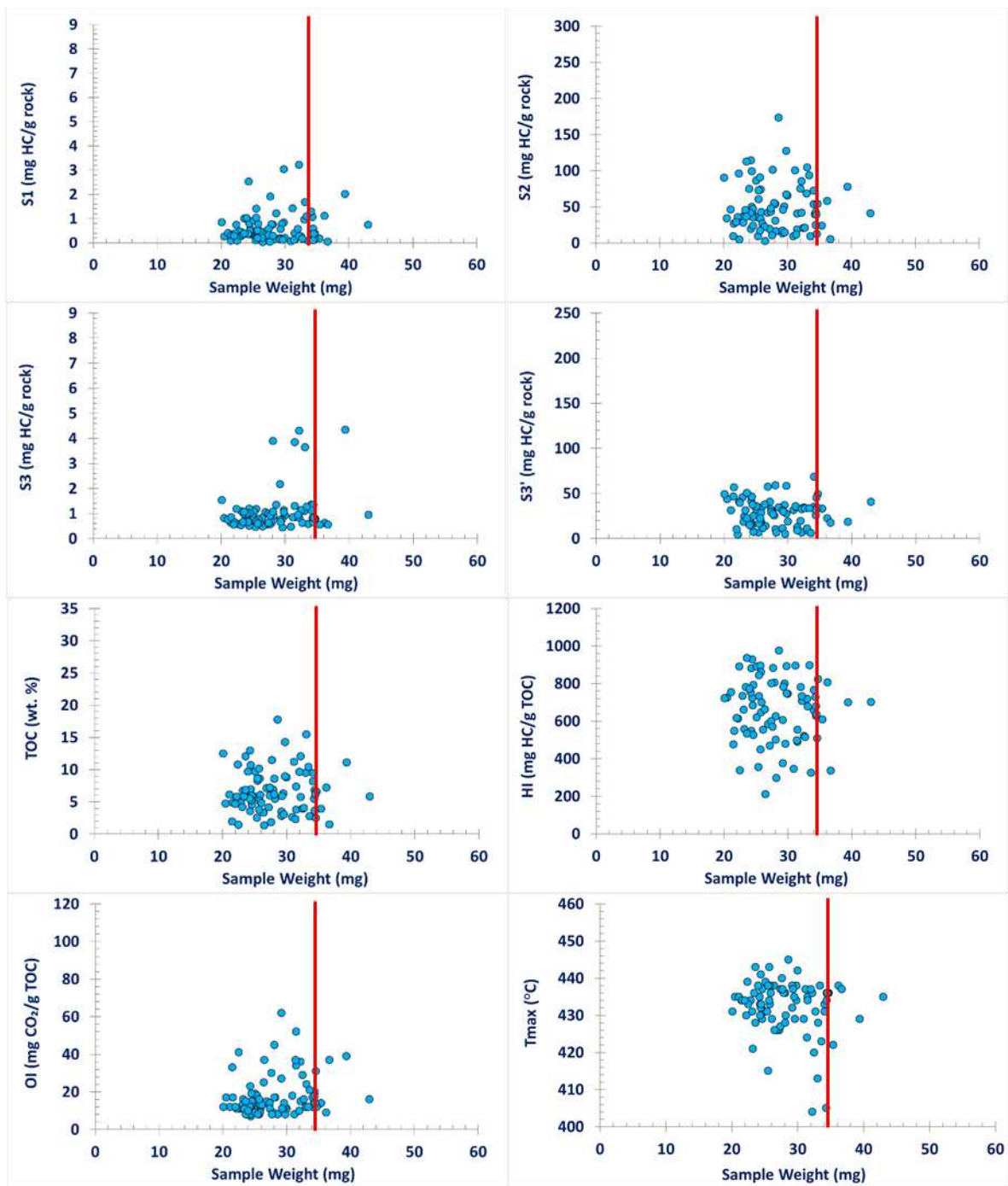


Figure 4. 6 Cross-plots of the measured and calculated Rock-Eval 6 programmed pyrolysis parameters vs. sample weight for DH 4 samples. The threshold weight is 34.5 mg.

minimum weight by Thul (2012). The threshold weight was chosen as 38 mg based on the data merging point of each Parameter vs Sample Weight cross-plot in Figure 4.7.

Table 4. 5 Data range and standard deviations of DH 5 samples. The threshold weight is 38 mg.

Parameter	Data range < 38 mg	Data range ≥ 38 mg	SD < 38 mg	SD ≥ 38 mg
S1	0.04-8.32	0.18-0.44	1.20	0.095
S2	1.29-211.24	13.82-47.29	43.89	11.56
S3	0.29-4.16	0.62-0.96	0.45	0.11
S3'	2.8-198.2	34-55.6	26.25	7.76
TOC	0.83-22.42	2.69-5.82	4.38	1.13
OI	4-91	12-23	9.77	3.93
HI	122-1018	489-813	176.85	114.59
Tmax	407-445	427-438	7.01	4.22

S1 values to the left of the threshold range between 0.04 mg HC/g rock and 8.32 mg HC/g rock, the values to the right of the threshold are 0.18-0.44 mg HC/g rock. As shown on Figure 4.7, the high S1 values are influenced by the lower than required sample weights. Similar conclusions can be drawn from the S2, S3, S3', and TOC vs Sample weight plots, in which the highest parameter values correlate to the lowest sample weight (Figure 4.7). The Tmax and HI vs Sample weight plots show the reverse pattern, where the lowest Tmax and HI values are associated with low sample weights.

The same conclusion can be drawn from the reduced standard deviation of each parameter over 38 mg samples (Table 4.5).

4.6 Veracity of the Shallow Depth Samples

Approximately a quarter of the shallow depth (20 m) samples are over 40 mg. The data range for the measured and calculated parameters shrink for samples over 40 mg, although it does not look as evident as it was for the DH 5 samples.

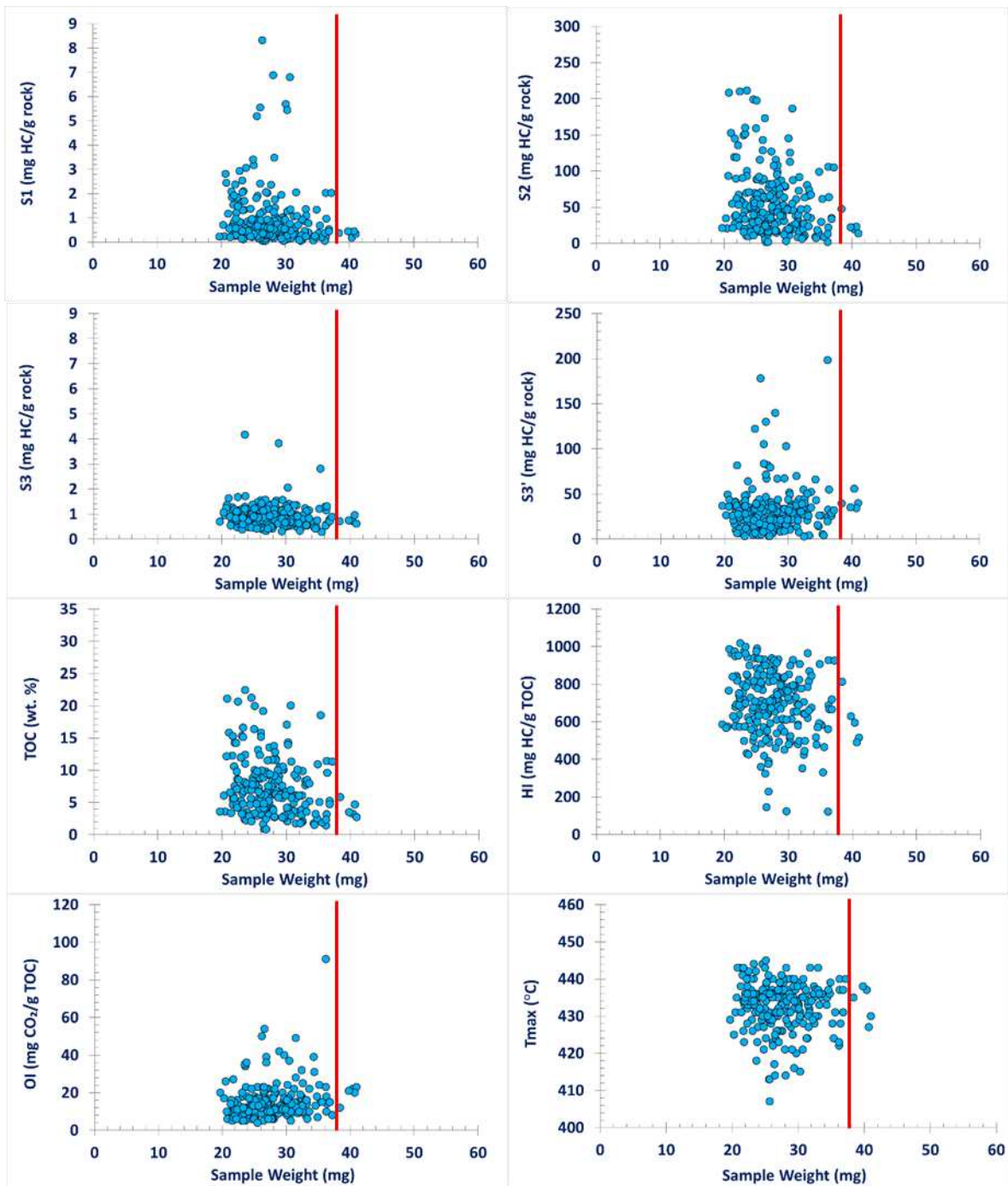


Figure 4. 7 Cross-plots of the measured and calculated Rock-Eval 6 programmed pyrolysis parameters vs. sample weight for DH 5 samples. The threshold weight is 38 mg.

The S1 parameter data range shrinks from 0.16-5.16 mg HC/g rock to 0.21-1.17 mg HC/g rock. Similar trends are observed for the S3, OI, HI, and the Tmax parameters (Figure 4.8). For some parameters, like S2, the lowest value corresponds to samples that are over 40 mg, but this happens because the overall data values decrease for samples with higher weight (Table 4.6). This is also supported by the decreased standard deviations values (Table 4.6).

Table 4. 6 Data range and standard deviations of the two shallow depth drill hole samples (SD1 and SD2). The threshold weight is 40 mg.

Parameter	Data range < 40 mg	Data range ≥ 40 mg	SD < 40 mg	SD ≥ 40 mg
S1	0.16-5.16	0.21-1.17	1.00	0.29
S2	15.91-272.39	11.48-72.8	52.25	17.08
S3	0.49-9.31	0.76-1.68	1.69	0.29
S3'	9.3-42.9	13.0-47.6	10.05	8.59
TOC	3.59-29.09	2.18-9.41	5.18	1.92
OI	6-65	12-42	13.06	9.49
HI	365-936	330-774	144.67	112.85
Tmax	422-441	427-436	4.22	2.63

The reverse trend is observed for S3', where the highest value of S3' corresponds to a sample over 40 mg weight, which shows that the overall data values for S3' increases with increasing sample weight for the near surface samples (Table 4.6).

4.7 Data Veracity of the Outcrop Samples

Like the subsurface samples, the outcrop samples (Campaigns 1-3) are mostly under 40 mg. Hence, 35 mg, 34 and 35 mg were chosen as the threshold weight for the Campaign 1, Campaign 2 and Campaign 3 outcrop samples, respectively.

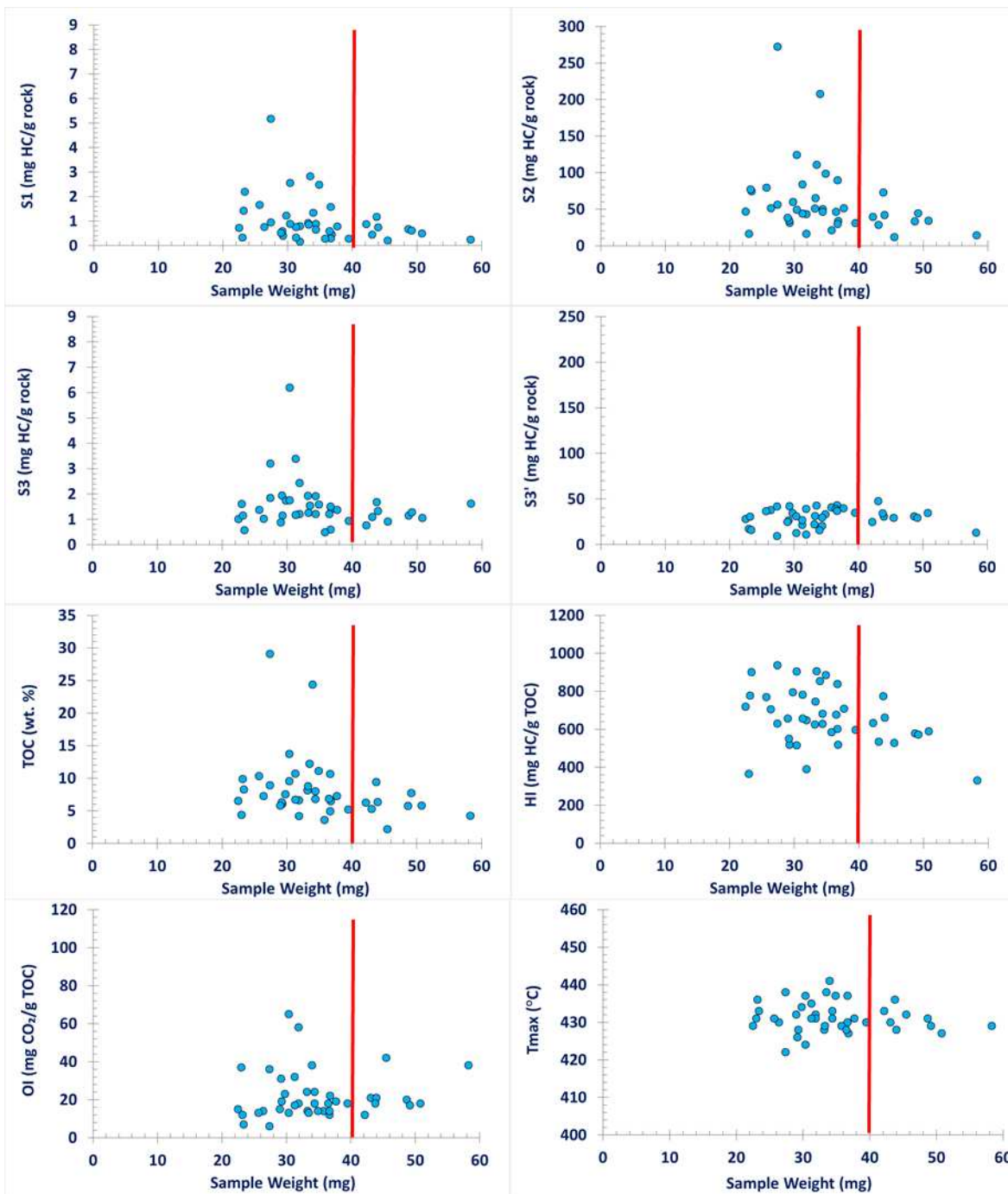


Figure 4. 8 Cross-plots of the measured and calculated Rock-Eval 6 programmed pyrolysis parameters vs. sample weight for the two-shallow depth SD1 and SD2 samples.

The change in standard deviations do not correspond with the change in data range for Campaign 3 parameters. However, it can be observed from both the data table (Tables 4.7-4.9) and the corresponding cross-plots (Figures 4.9- 4.11) that the data range narrows down very well for samples over the threshold points.

Table 4. 7 Data range and standard deviations of Campaign 1 outcrop samples. The threshold weight is 35 mg.

Parameter	Data range < 35 mg	Data range ≥ 35 mg	SD < 35 mg	SD ≥ 35 mg
S1	0.18-3.79	0.39-1.63	0.89	0.45
S2	21.29-272.39	40.31-134.18	65.11	32.77
S3	2.33-13.69	3.77-9.24	2.57	1.99
S3'	6.8-23.9	7.7-12.8	4.54	1.99
TOC	3.62-30.83	7.26-15.55	6.75	2.73
OI	15-104	34-95	15.13	21.66
HI	409-1146	524-863	133.49	129.81
Tmax	423-444	429-438	4.68	3.16

Table 4. 8 Data range and standard deviations of Campaign 2 outcrop samples.

Parameter	Data range < 34 mg	Data range ≥ 34 mg	SD < 34 mg	SD ≥ 34 mg
S1	0.13-2.7	0.64-2.12	0.59	0.51
S2	16.75-306.01	100.77-223.7	64.21	41.50
S3	2.71-13.64	4.37-9.22	2.77	1.88
S3'	6.3-20	12.8-21.3	3.87	2.75
TOC	3.47-33.54	12.0-24.75	6.77	4.23
OI	33-78	35-50	10.72	5.21
HI	432-912	779-904	151.71	39.11
Tmax	428-444	435-446	6.40	3.42

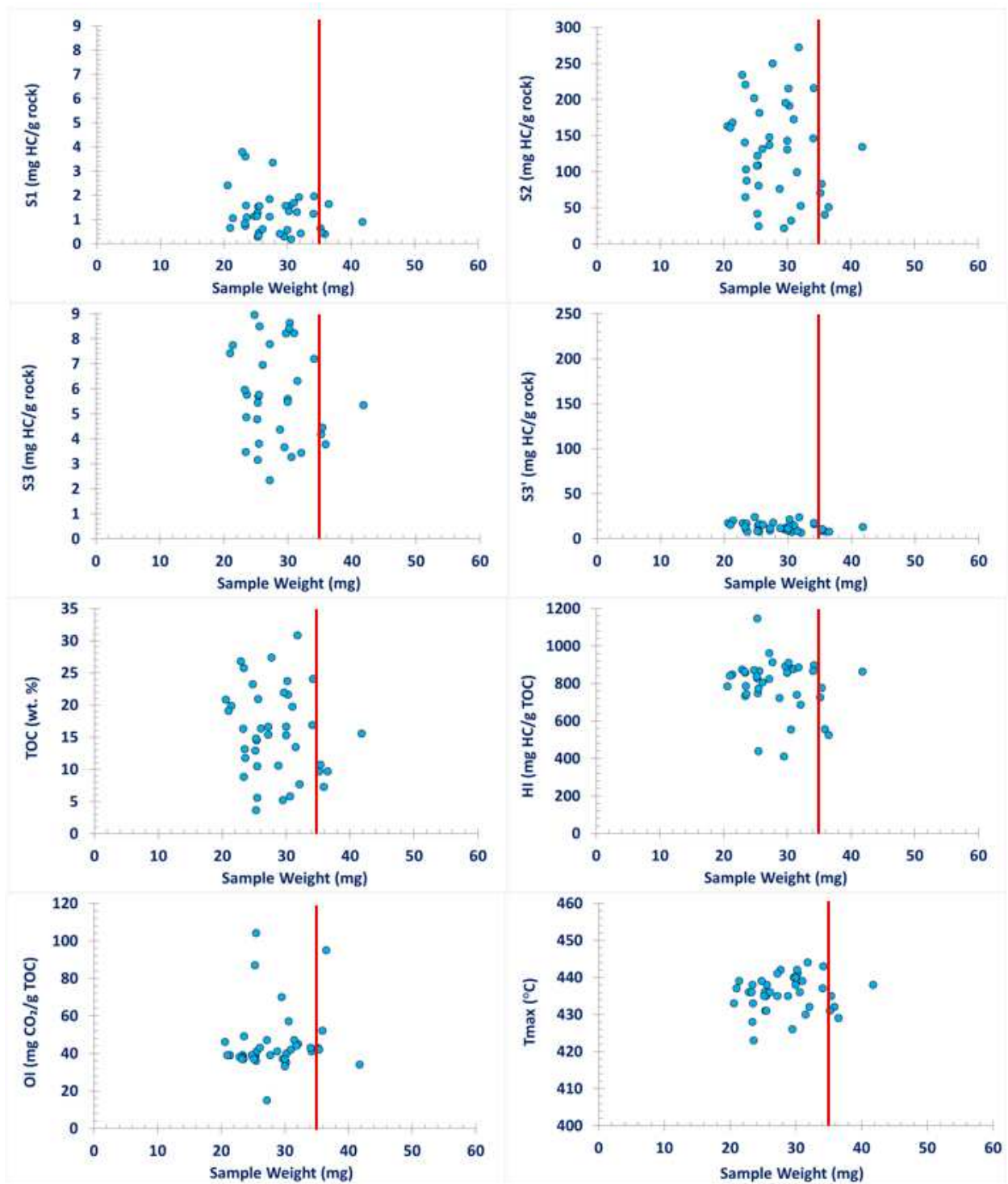


Figure 4. 9 Cross-plots of the measured and calculated Rock-Eval 6 programmed pyrolysis parameters vs. sample weight for Campaign 1 samples. The threshold weight was chosen as 35 mg.

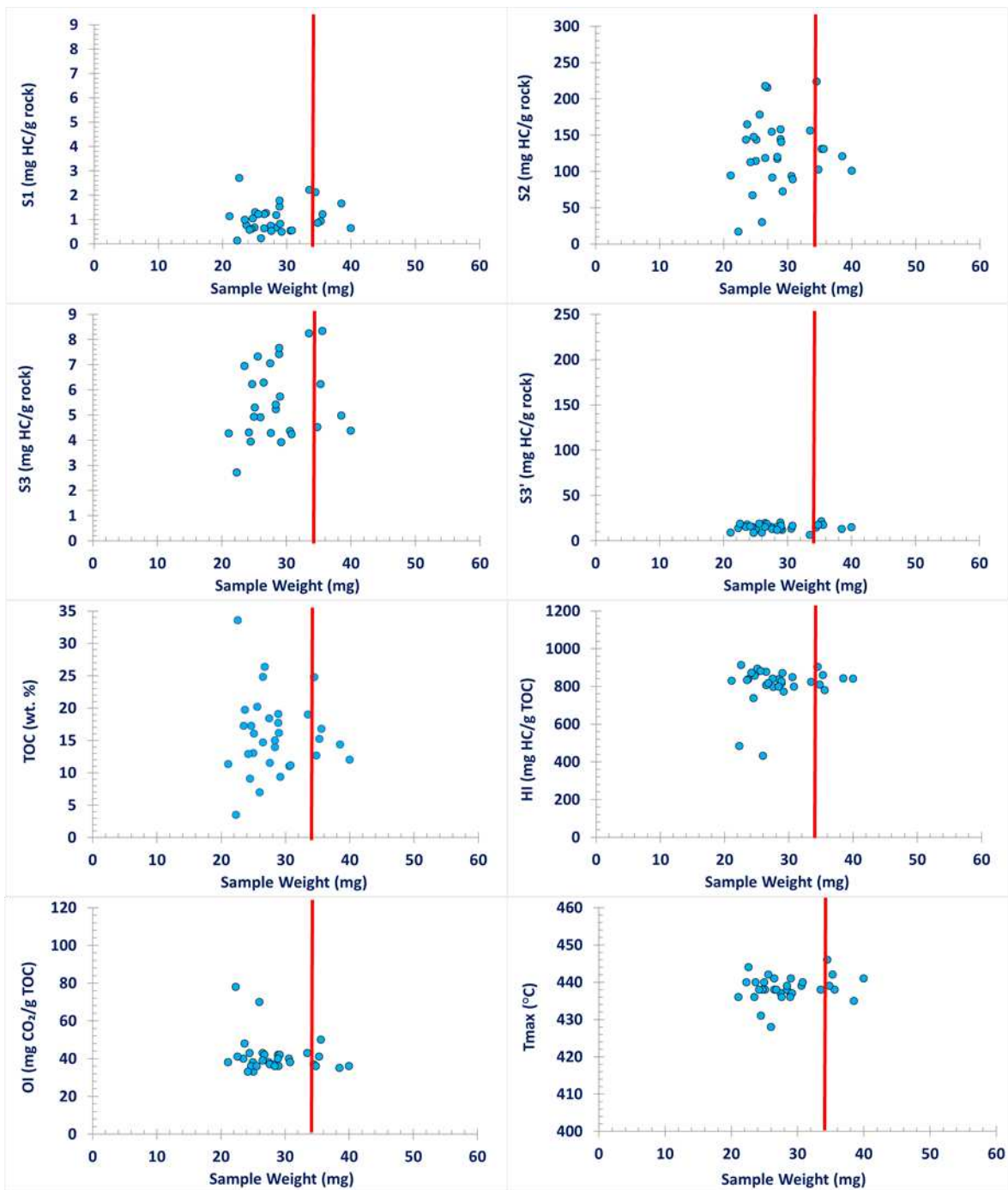


Figure 4. 10 Cross-plots of the measured and calculated Rock-Eval 6 programmed pyrolysis parameters vs. sample weight for Campaign 2 outcrop samples. The threshold weight was chosen as 34 mg.

Judging from the new data range, Campaign 2 and Campaign 3 surface samples are even better quality than they were previously thought. For example, the maturity indicator Tmax started at 419-428 for the original data range, which corresponds to immature source rock. However, the narrowed down data range suggest that the lowest Tmax value is 435, which makes all Campaign 2 and Campaign 3 samples early mature to mature source rock. The same can be said about the TOC values (Tables 4.8 and 4.9).

Table 4. 9 Data range and standard deviations of Campaign 3 outcrop samples. The threshold weight is 35 mg.

Parameter	Data range < 35 mg	Data range ≥ 35 mg	SD < 35 mg	SD ≥ 35 mg
S1	0.11-2.69	0.53-1.82	0.57	0.53
S2	14.36-243.76	82.73-211.10	61.05	67.31
S3	1.13-11.37	3.93-9.66	2.62	3.05
S3'	5.2-26.7	8.9-17.8	5.98	3.75
TOC	3.2-27.7	10.27-24.44	6.08	6.97
OI	8-87	34-44	15.03	6.55
HI	166-923	806-921	169.86	175.41
Tmax	419-444	435-444	7.05	9.27

The narrowed down data range much better aligns with previous studies conducted by Avid et al (2000) and Yamamoto et al. (1993), where they reported the TOC levels of Eedemt (Khoot) samples to be 14.8-28.8 wt% and 5.83-21.31 wt%, respectively. It is also evident that extremely high HI and Tmax values as well as the extremely low HI and Tmax values in the original data set were caused by inadequate sample weight. HI and Tmax are crucial factors in determining source rock quality and calculating hydrocarbon potential of a basin. Therefore, in the next chapters the non-calibrated samples will be eliminated.

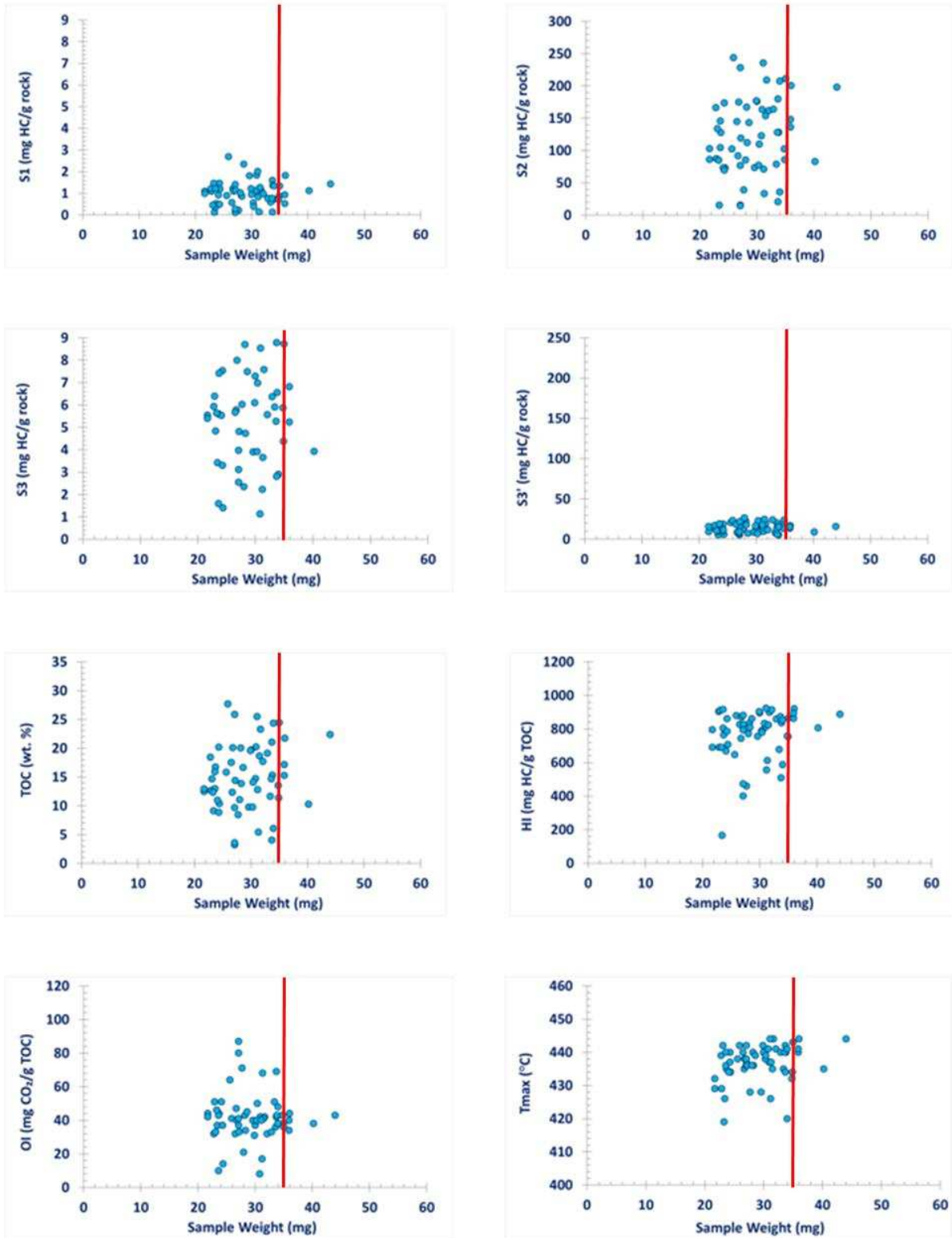


Figure 4. 11 Cross-plots of the measured and calculated Rock-Eval 6 programmed pyrolysis parameters vs. sample weight for surface samples collected during Campaign 3. The threshold weight is 35 mg

CHAPTER 5

SOURCE ROCK POTENTIAL BASED ON ROCK-EVAL DATA

5.1 Organic Matter Richness

5.1.1 Total Organic Content (TOC) of the Non-Calibrated Samples

Evaluating the source rock is an essential part of hydrocarbon exploration. Figure 5.1 and Figure 5.2 show the measured TOC range for the non-calibrated Khoot samples. Values in this dataset show very little variation among the five Khoot drill hole samples, despite the wells being in various positions in the basin (Figure 5.1). The near surface SD1 and SD2 core samples exhibit overall higher TOC levels than the five deep drill hole samples, but broadly lower TOC than the outcrop samples (Figure 5.2).

The outcrop samples demonstrate much higher TOC levels as well as greater data range (Figure 5.2). Moreover, the outcrop samples' results closely align with the Rock-Eval study conducted by Yamamoto et al. (1993) in the same basin. The exact location of their study is unknown, hence samples from their study will be referred to as Eedemt (Eidemt). The key difference between the Khoot outcrop samples and the Eedemt samples is that the Khoot outcrop samples have much broader data range, which is skewed by underweight sample measurements (Figure 5.2).

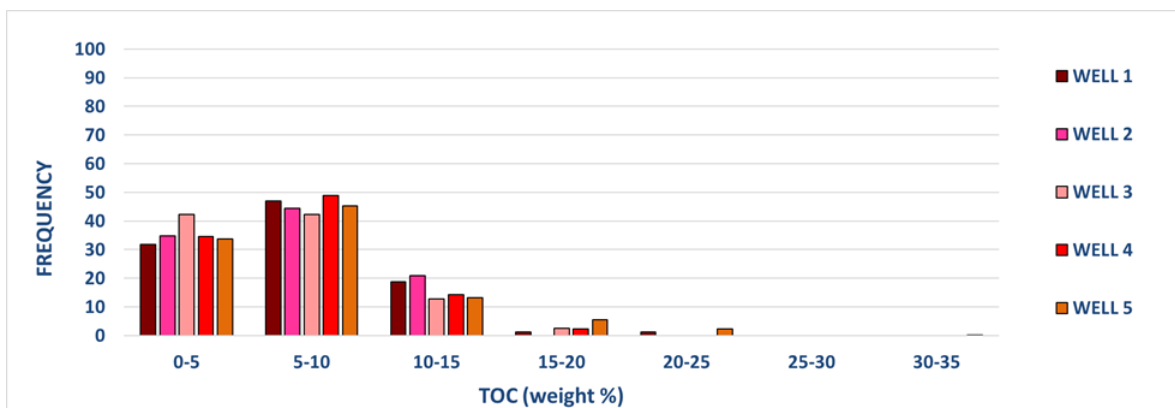


Figure 5. 1 TOC frequencies in the non-calibrated subsurface samples.

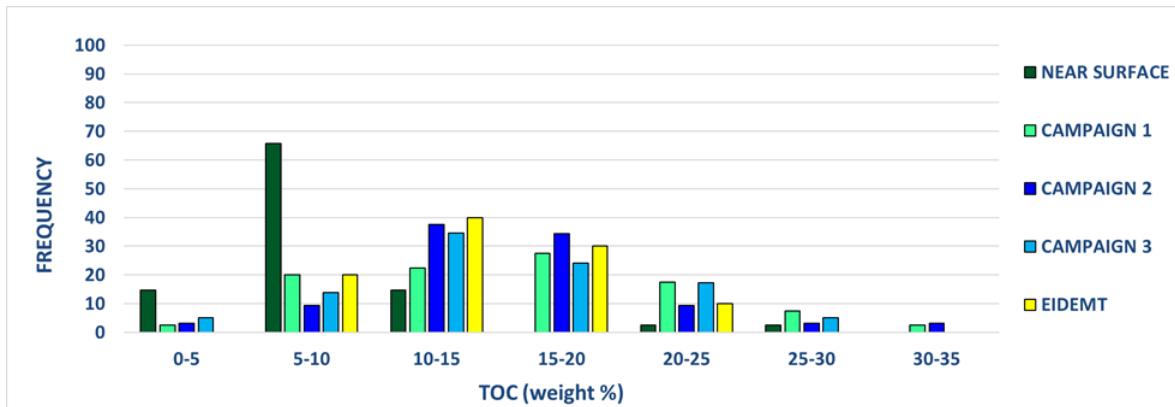


Figure 5. 2 TOC levels in the non-calibrated Khoot near surface and outcrop samples as well as the Eidemt (Eedemt) samples from Yamamoto et al. (1993).

5.1.2 True Organic Richness from the Calibrated Samples

Contrary to the TOC range in the non-calibrated samples, the calibrated subsurface samples show much lower organic content (Table 5.1). The true TOC range for samples from these five drill holes starts around 2-4% (the lows) and ends at 7-11% (the highs). Readings from DH 3, DH 4 and DH 5 are especially low, which is consistent with observations from Green River source rock analysis, where source rocks located at basin-margin show consistently lower TOC than the basin-center rocks (Feng, 2011).

The calibrated shallow depth drill hole (SD1 and SD2) samples are very similar to the five deep drill hole samples (Table 5.1). The true TOC range for the shallow depth drill hole samples is 2-10% (Table 5.1) as opposed to 2-25% (Figure 5.2). The previously recorded high TOC levels from SD1 and SD2 were only recorded from the underweight samples.

The outcrop samples show the exact opposite trend, where the low TOC values (<7%) are exclusively associated with the underweight samples. Additionally, the remarkably high TOC levels (>25%) are also associated with low weight samples. The true TOC range (7-25%) of the outcrop samples match the previously studied Eedemt samples' TOC, which is between 7% and 25% (Table 5.1, Figure 5.2). The Shinekhudag Type Samples have lower TOC than the Khoot (Eedemt) outcrop samples, their TOC range is closer to the Khoot subsurface samples'. The Central

Mongolian Source Rocks (Har Horin, Sayan Obo and Tsagan Obo), on the other hand, have much similar organic richness (Table 5.1) to the Khoot (Eedemt) outcrop samples. The Tavan Har and Noyon Uul samples are clearly not associated with the Khoot Basin samples.

Table 5. 1 TOC range of the calibrated Khoot oil shale samples as well as Mongolian oil shale and shale samples from various basins in Mongolia. See Chapter 2 for Mongolian Basin locations. *These three are considered the same deposition, thus will be referred to as the Shinekhudag Type Samples. **This is the age that was assigned by Li et al (2014) to the cores which were drilled nearby SD1 and SD2 of this study. Before this study, Khoot oil shales were considered to the same age as the Shinekhudag Type Samples. ***These three samples will be referred to as the Central Mongolian Shales. Sladen and Traynor (2000) considered them to be of oil shale quality.

SAMPLE GROUP	TOC	BASIN	AGE
DH 1	2-11 %	Khoot/Central Gobi	Unknown
DH 2	4-11 %	Khoot/Central Gobi	Unknown
DH 3	4-7 %	Khoot/Central Gobi	Unknown
DH 4	2-8 %, 11 %	Khoot/Central Gobi	Unknown
DH 5	2-7 %	Khoot/Central Gobi	Unknown
NEAR SURFACE	2-10 %	Khoot/Central Gobi	Middle Jurassic**
CAMPAIGN 1	7-16 %	Khoot/Central Gobi	Unknown
CAMPAIGN 2	12-25 %	Khoot/Central Gobi	Unknown
CAMPAIGN 3	10-23 %	Khoot/Central Gobi	Unknown
EEDEMT	6-22 %	Khoot/Central Gobi	Same as Khoot
SHAWART OBO*	4-10 %	Central Gobi Basin	Late Early Cretaceous
BAYAN ERKHIT*	3-10 %	Choir-Nyalga Basin	Late Early Cretaceous
SHINEKHUDAG*	4-10 %, 15 %	Central Gobi Basin	Late Early Cretaceous
TAVAN HAR	1-3 %	East Gobi Basin	Mid Early Cretaceous
HAR HORIN	7.9-18.7 %	Har Horin Basin	L.Jurassic-E.Cretaceous
TSAGAN OBO	20.6 %	Ongi River Basin	Lower Middle Jurassic
SAYAN OBO	13-23 %	Ongi River Basin	Lower Jurassic
NOYON UUL	3-5 %	South Gobi Basin	Triassic-Jurassic

Figure 5.3A and Figure 5.3B are the Inverse Distance Weighted (IDW) interpolation maps (TOC) of the Khoot basin (Plotted in ArcMap). IDW interpolation assumes that points that are close to one another have more similar values than points that are further away. The IDW interpolation maps show that the areas with specifically low TOC values are also the locations where the two cores were extracted by Li et al. (2014). The locations of these two cores are provided in Figure 1.3. The age of the

Khoot oil shale was established as Middle Jurassic based on shrimp fossils found in these cores.

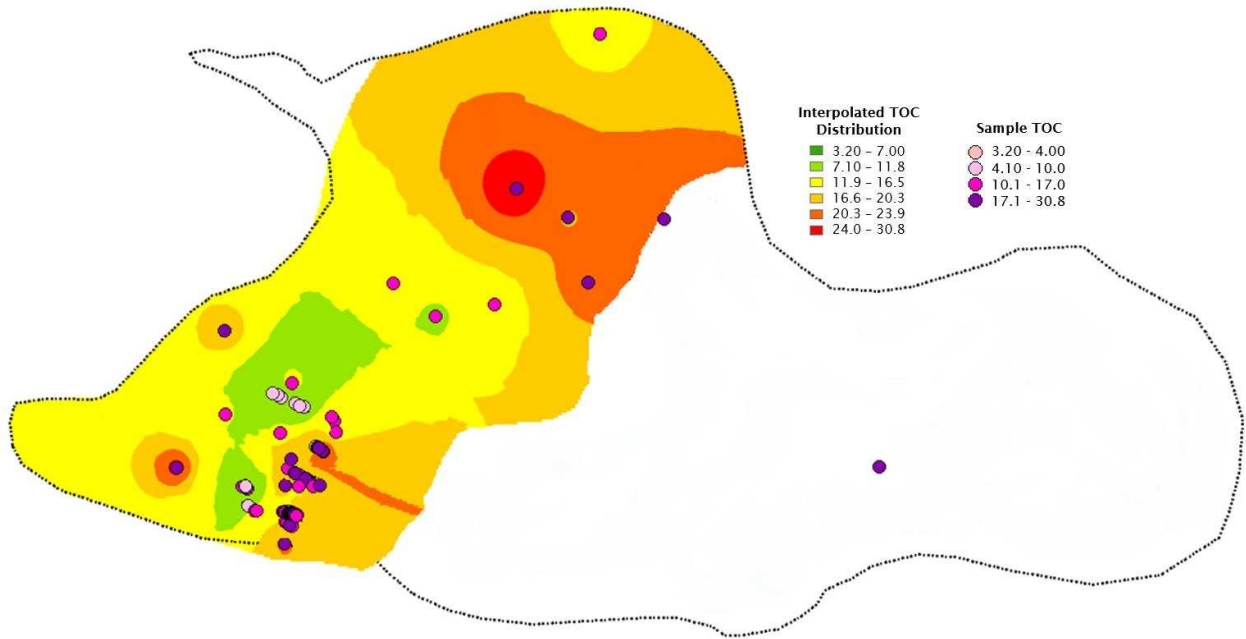


Figure 5. 3 A) Interpolated (IDW) TOC map of the Khoot basin from the non-calibrated samples.

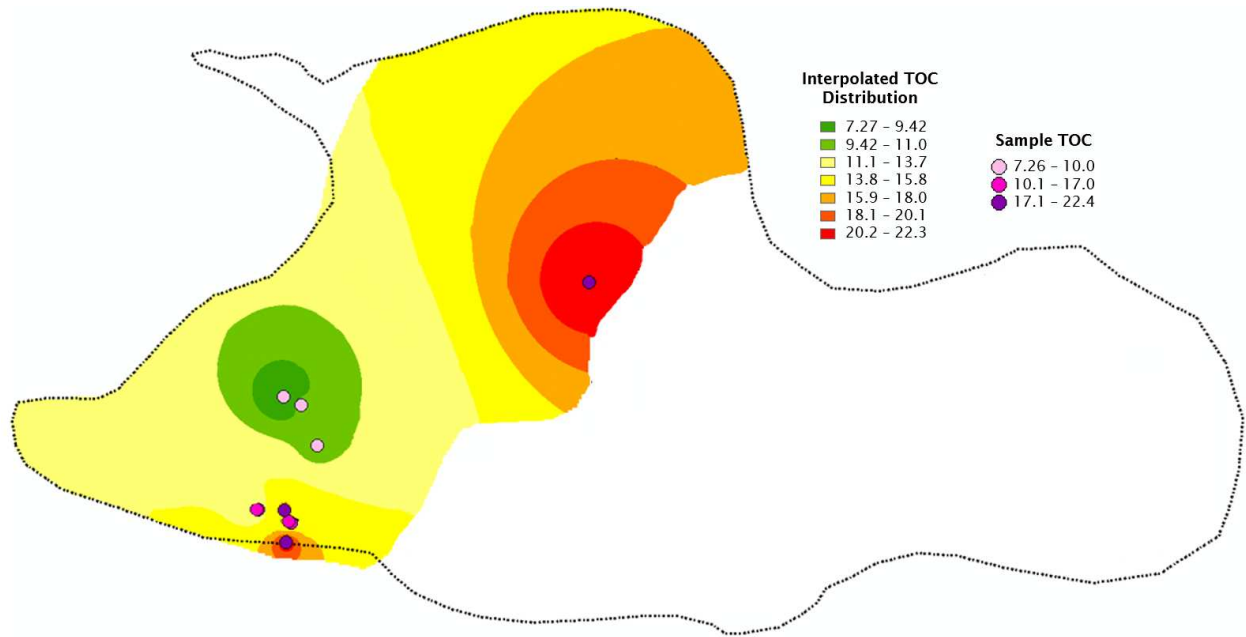


Figure 5. 3 B) Interpolated (IDW) TOC map of the Khoot basin from the calibrated samples.

5.1.3 Potential for Oil Shale Development

The primary purpose for studying the Khoot oil shales was to study its potential for shale oil development via in-situ retorting. During this process, the kerogen in the oil shale is first thermally cracked into low degree hydrocarbon molecules, it is then gradually upgraded by in-situ hydrogenation (Bartov, 2014).

While source rocks with 2-4 wt% TOC are considered good to excellent quality source rock, oil shales under 10 wt% are not suitable nor economically viable for production. The ideal oil shale must have at least 10 wt% TOC and must be at least 100 meters thick (Bartov, 2014). The classification scheme for oil shales is also different. For example, Israeli oil shales are classified as low quality when TOC is 11 wt%, medium-grade when TOC is 14 wt%, and high-grade when the TOC is greater than 17 wt% (Grinberg et al., 2000).

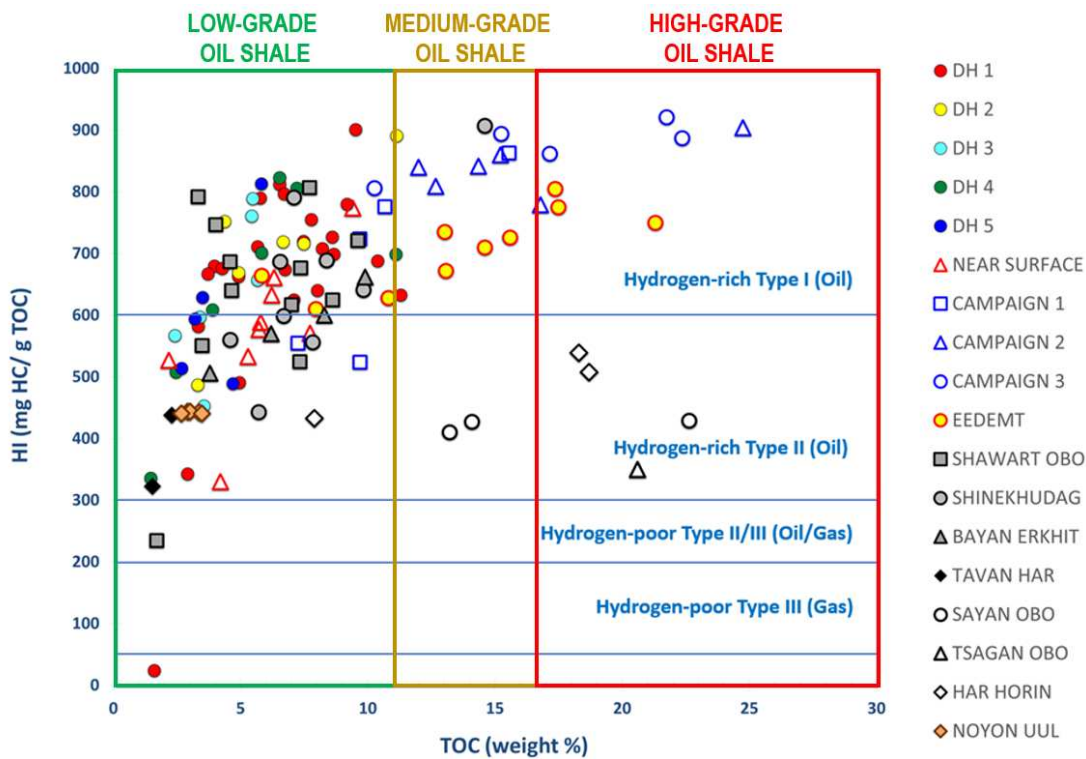


Figure 5. 4 HI plotted against TOC for weight calibrated Khoot samples (core and outcrop). Additionally, nine different shale and oil shale samples from various locations in Mongolia are plotted for comparison. This plot indicates the kerogen type and oil shale quality of the studied samples. Non-Khoot sample locations are available in Chapter 2 (Figures 2.1, 2.3).

On this oil shale classification scale, subsurface Khoot oil shales are ranking in the lowest range (Figure 5.4), so does all the Shinekhudag-type (Zuunbayan Group Formation) oil shales from Bayan-Erkhit, Shawart Obo and Shinekhudag. These two basins are in Central Mongolia. The Eedemt/Khoot outcrop samples have much better quality, medium to high-grade TOC levels suitable for oil shale development, than the Khoot core samples. The Early-Middle Jurassic samples from the Ongi River basin (Tsagan Obo and Sayan Obo) and Late Jurassic-Early Cretaceous Har Horin basins are also of the same quality.

5.2 Kerogen Type

Kerogen types are characterized by HI vs OI (Figure 5.6), HI vs Tmax (Figure 5.9), and S2 vs TOC (Figures 5.11A and 5.11B) plots. Additionally, kerogen types can be determined by S2/S3 vs TOC (Figure 5.5) and PCI vs TOC (Figure 5.17). All HI-dependent diagrams show the same or comparable results. The difference is that some studies classified kerogen Type I starting at 600 mg HC/g TOC while others used 700 mg HC/g TOC.

On the HI-dependent graphs, all Khoot outcrop samples belong to kerogen Type I, so does the Eedemt samples (Figures 5.4, 5.5, 5.6 and 5.9), except for two samples with low HI (524 mg HC/g TOC and 555 mg HC/g TOC) that were collected from the southwestern corner (green region) of the Khoot basin (Figure 5.3A, 5.3B). These samples also have the lowest TOC and Tmax values (Figures 5.8A, 5.8B, 5.10A, and 5.10B).

The near surface samples are more complex, showing a mixture of Type I and Type II. On the modified Van Krevlen diagram (Figure 5.6) and on the HI vs TOC graph (Figure 5.4), the near surface samples are a mixture of Type I and Type II kerogen. On the S2/S3 vs TOC plot (Figure 5.5), however, the near surface samples are dominantly

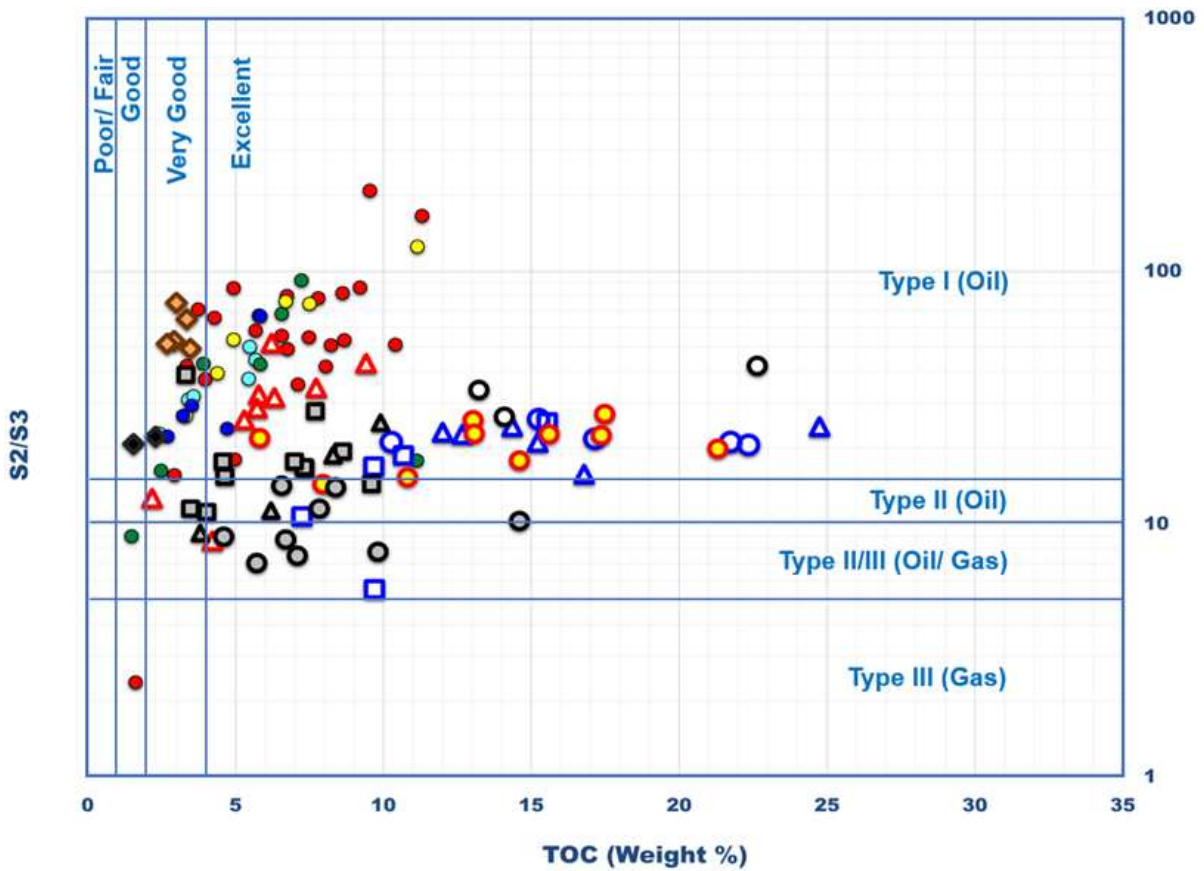


Figure 5. 5 S_2/S_3 plotted against TOC shows the overall quality of the source rocks and kerogen type. Plotted on the graph are the weight calibrated subsurface and outcrop samples from the Khoot Basin and additional samples from literature. See Figure 4.4 for legend.

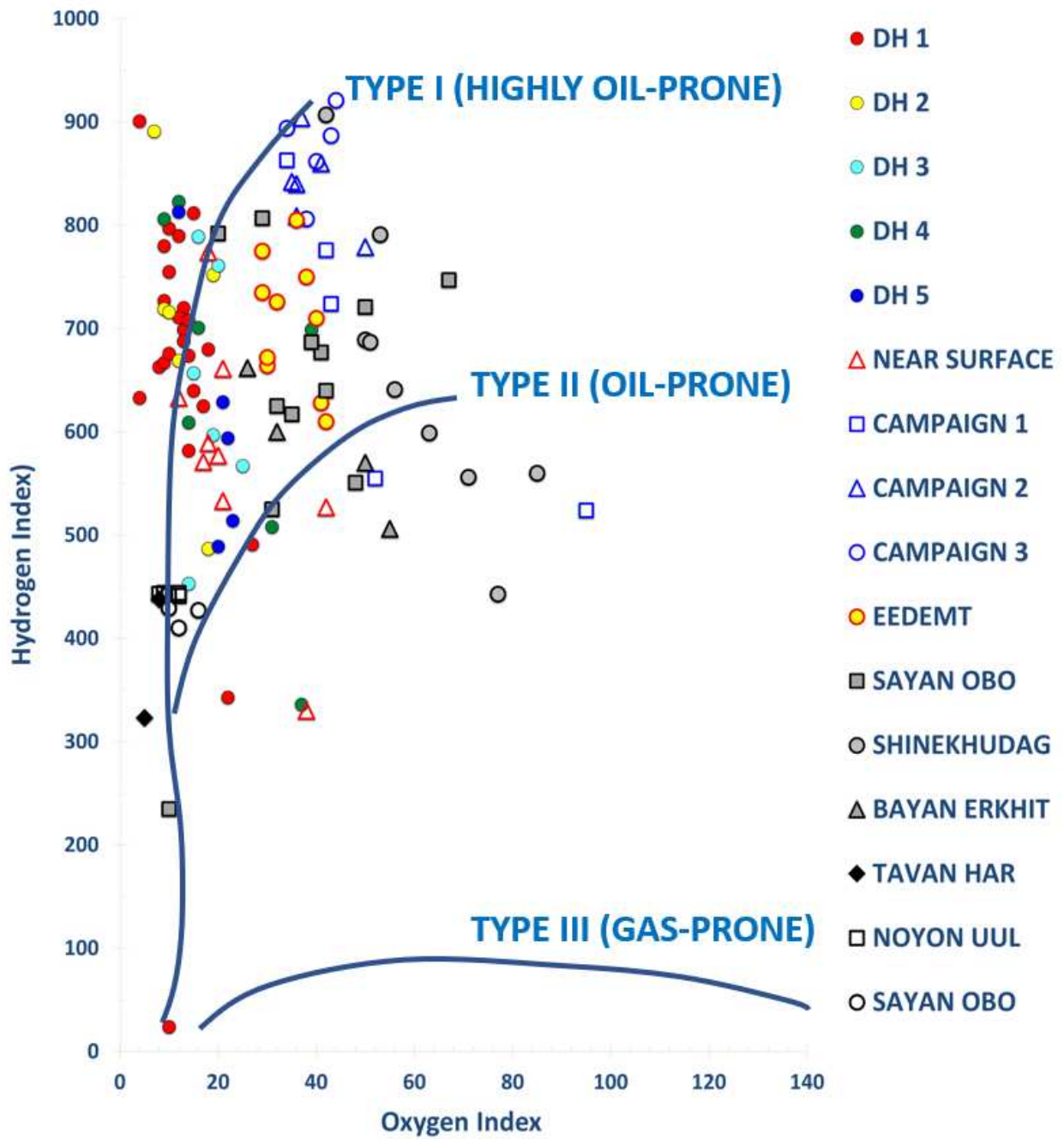


Figure 5. 6 Modified Van-Krevelen diagram shows the organic matter type of the studied samples. All Mongolian samples have exclusively oil-prone Type I/Type II kerogen.

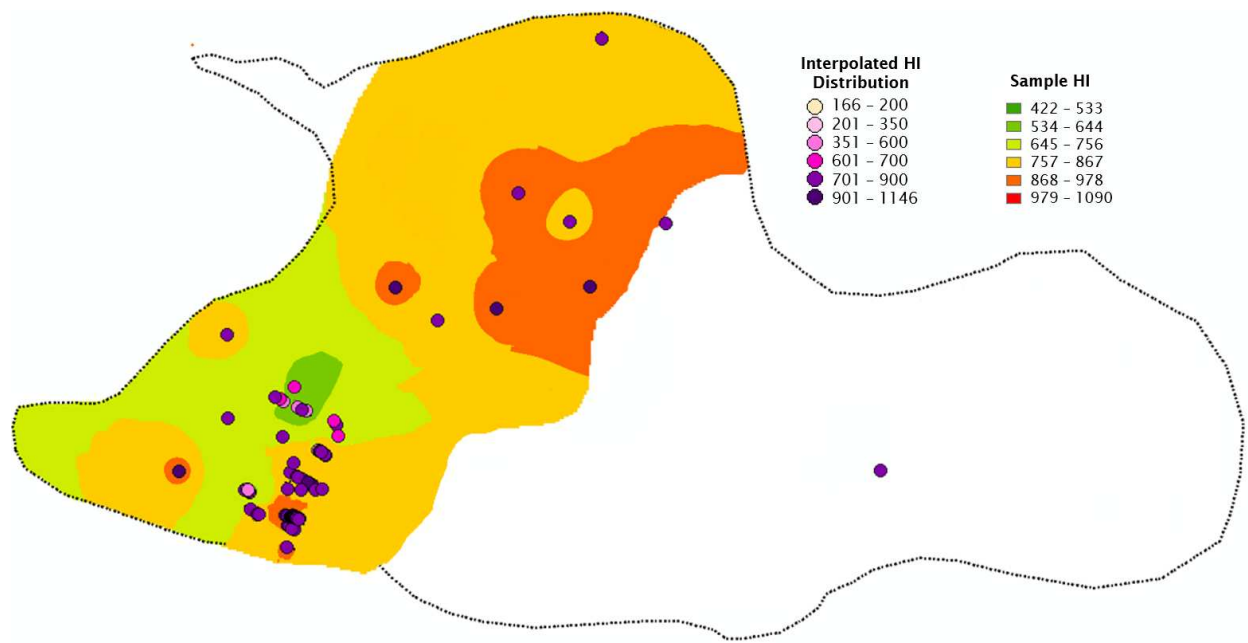


Figure 5. 7 A) Interpolated (IDW) HI distribution map of the Khoot basin from the non-calibrated outcrop samples.

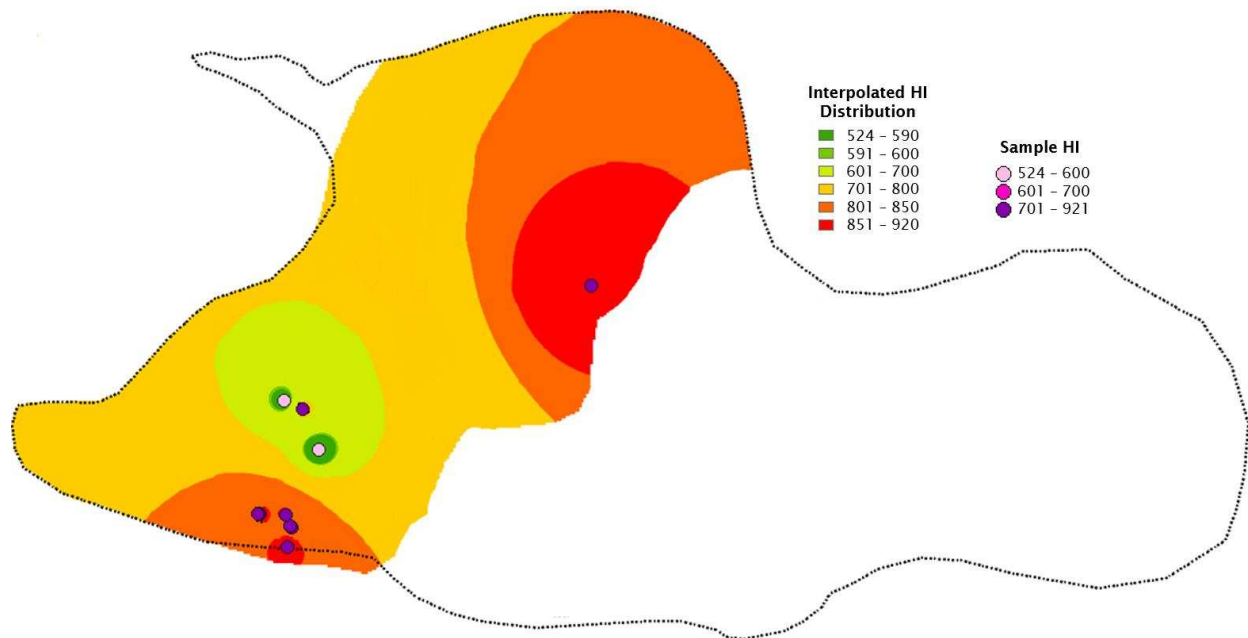


Figure 5. 7 B) Interpolated (IDW) HI distribution map of the Khoot basin from the calibrated outcrop samples.

Type I (Figure 5.5), except for two samples with the lowest TOC levels. From this plot, it is also observed that lower TOC levels correspond to lower S2 value and low S2/S3 ratio.

Figures 5.8A and 5.8B are the IDW maps of hydrogen index (HI). HI is calculated as $HI = (S2 / TOC) \times 100$. Like the previous TOC interpolation map, the southwestern region around Eedemt-A and Eedemt-B are again the lowest HI regions, where the kerogen type is more Type II than Type I. The highest HI values are recorded from the eastern side of the paleolake depo-center. Relationship between OI and HI are shown on Figure 5.7. The oxygen index (OI) is the reflection of the amount of CO₂ created per gram of TOC and calculated as $OI = (S3 / TOC) \times 100$.

5.3 Thermal Maturation

Thermal maturity is measured by Tmax and vitrinite reflectance. Both parameters are highly dependent on the organic matter type (Peters, 1986). In the absence of vitrinite reflectance, it can be calculated from Tmax. The top oil window ranges between 435-445°C depending on the type of organic matter. Tmax ≥ 440°C is usually considered mature for Type I source rocks (Sari et al., 2015). However, for most shale gas plays 435°C is accepted as early mature (Cardott, 2014).

5.3.1 Thermal Maturation of Mongolian Samples

Figure 5.8, Tmax plotted against HI, shows that the Khoot subsurface samples are immature to early mature Type I and Type II rocks, so are the Campaign 1 surface samples. Only one sample from DH 1 plots as Type III mature oil shale. Khoot surface samples collected during Campaign 1 and Campaign 2 are better quality than their subsurface counterparts. The outcrop samples are early mature to mature Type I oil shales.

The Eedemt and Shinekhudag-type samples are again showing comparable results to the Khoot surface samples (Figure 5.8), despite having an overall lower HI values (500-850 mg HC/ g rock) and slightly higher Tmax (441-452°C) values. It can be said that the Eedemt and Shinekhudag-type samples have lower HI values due to their maturity because Hydrogen Index decreases as Tmax increases. There are two Eedemt

samples that have very low Tmax values (422°C and 429°C). However, the S1 values corresponding to these two samples are the highest (10.19 mg/g and 10.52 mg/g).

Figure 5.6 and Figure 5.8 also show that the Lower-Middle Jurassic Sayan Obo and Late Jurassic-Early Cretaceous Har Horin samples are immature to early mature Type II rocks, while the Triassic Jurassic Noyon Uul samples are mature Type I kerogen-bearing rocks.

5.3.2 Thermal Maturation from Calculated Vitrinite Reflectance

Vitrinite reflectance provides the true maturity of source rocks. In the absence of directly measured vitrinite reflectance, it is calculated from Tmax. In the following plots, vitrinite reflectance is calculated as $R_o = 0.0165 \cdot T_{max} - 6.5143$ (Jarvie, 2018). Although using this calculation is discouraged for Type I source rocks, the outcome closely resembled the results in previous sections.

DH 2, DH 3, DH 4, DH 5, and Campaign 1 samples are immature to early mature (Figures 5.21, 5.22). DH1 samples as well as Campaign 2 and Campaign 3 samples are mostly in their peak maturation oil window. The near surface samples are the least mature out of all subsurface samples (Figure 5.21).

The Eedemt, Shawart Obo, Shinekhudag, and Noyon Uul samples are also in the same range. Only the Bayan Erkhite samples are in the volatile oil zone (VOZ) (Figure 5.23).

Vitrinite reflectance is showing that Sayan Obo and Tavan Har samples are the least favorable out of all studied samples. The Sayan Obo samples are immature and the Tavan Har samples are barely fitting in the early mature zone (Figure 5.23).

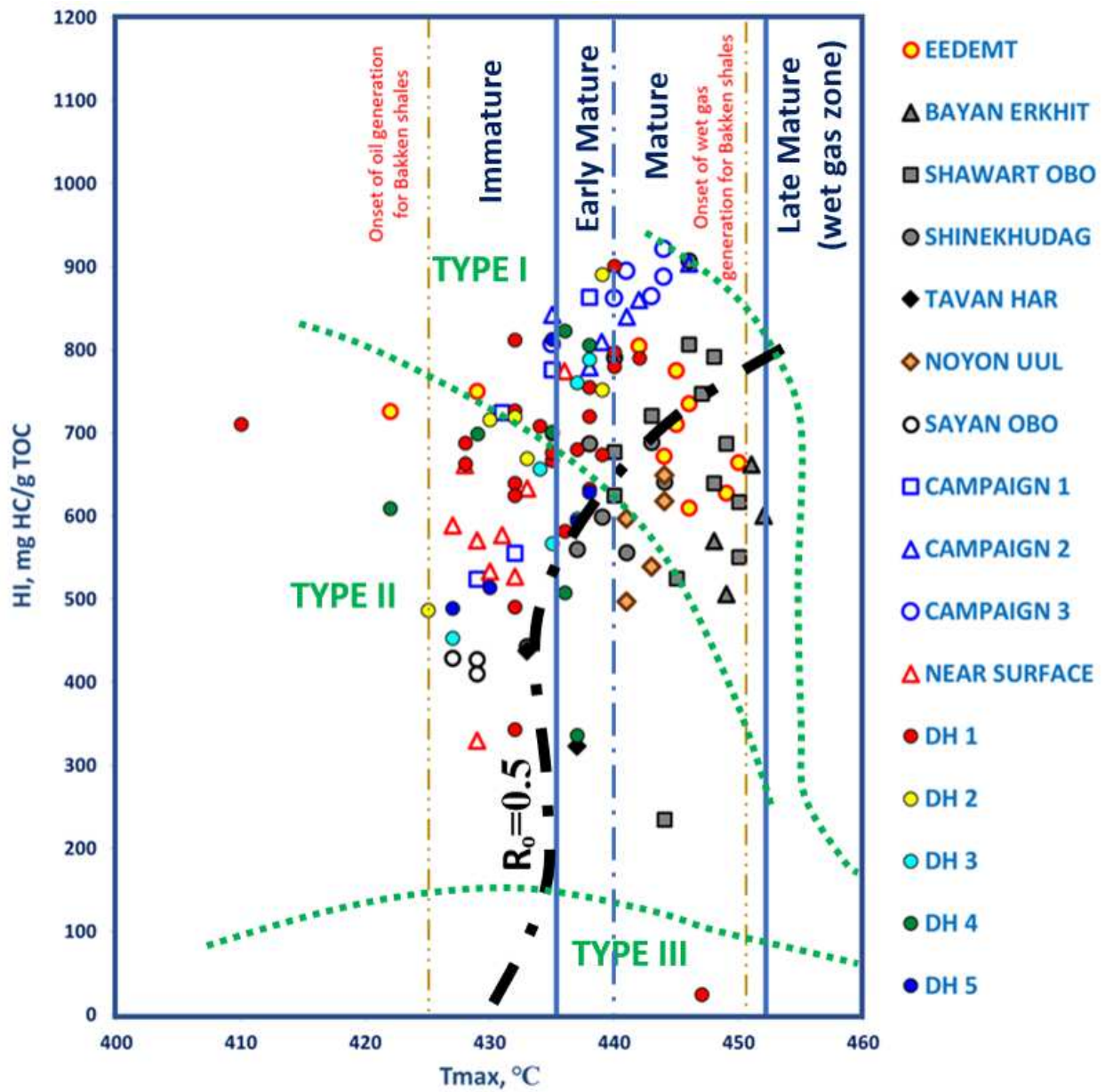


Figure 5. 8 HI plotted against Tmax shows the maturity of each sample. The subsurface Khoot samples are immature to early mature while the outcrop samples are early mature to mature.

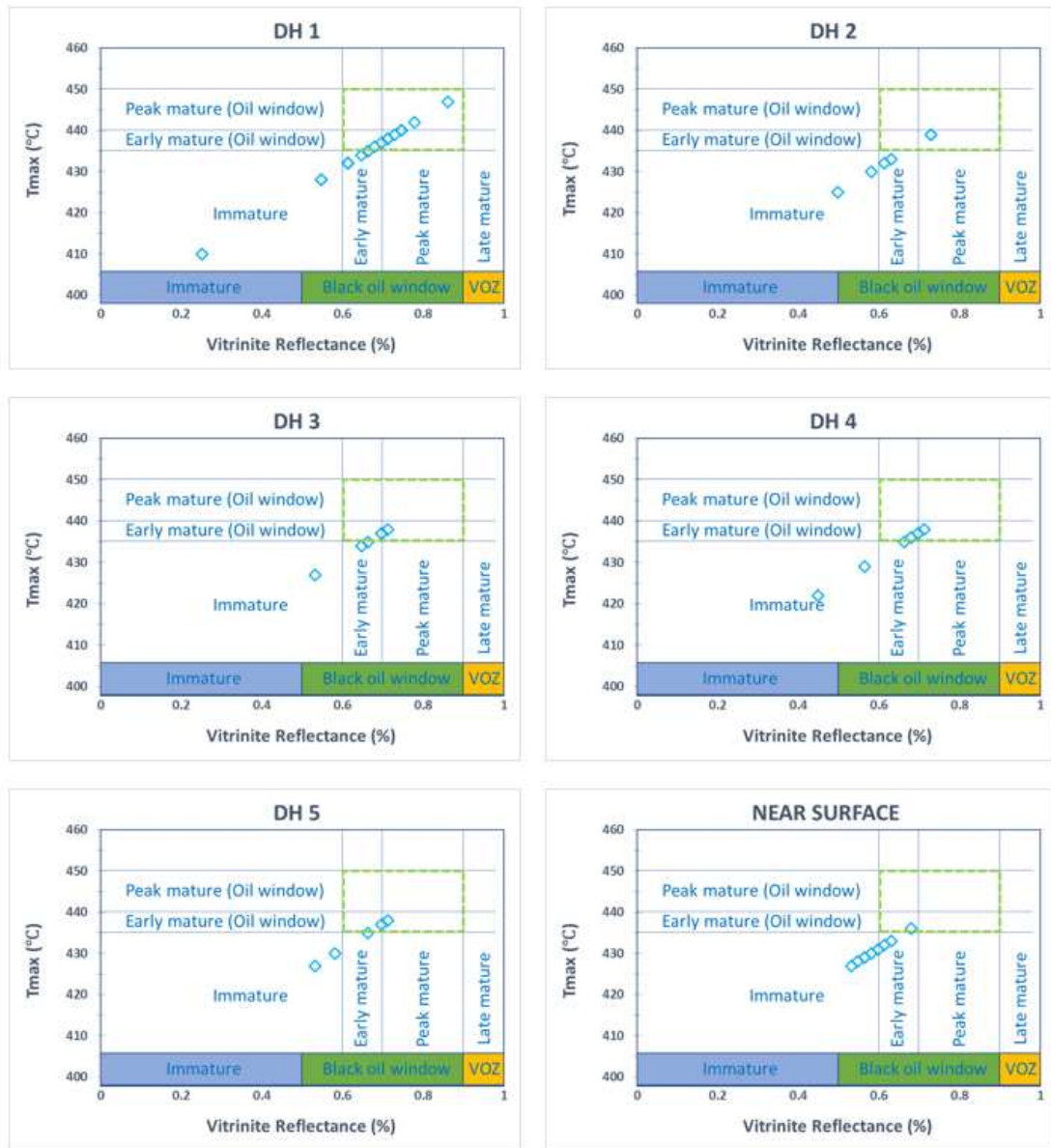


Figure 5. 9 Tmax vs Vitrinite Reflectance (%) plot of subsurface Khoot oil shale samples. VOZ stands for volatile oil zone.

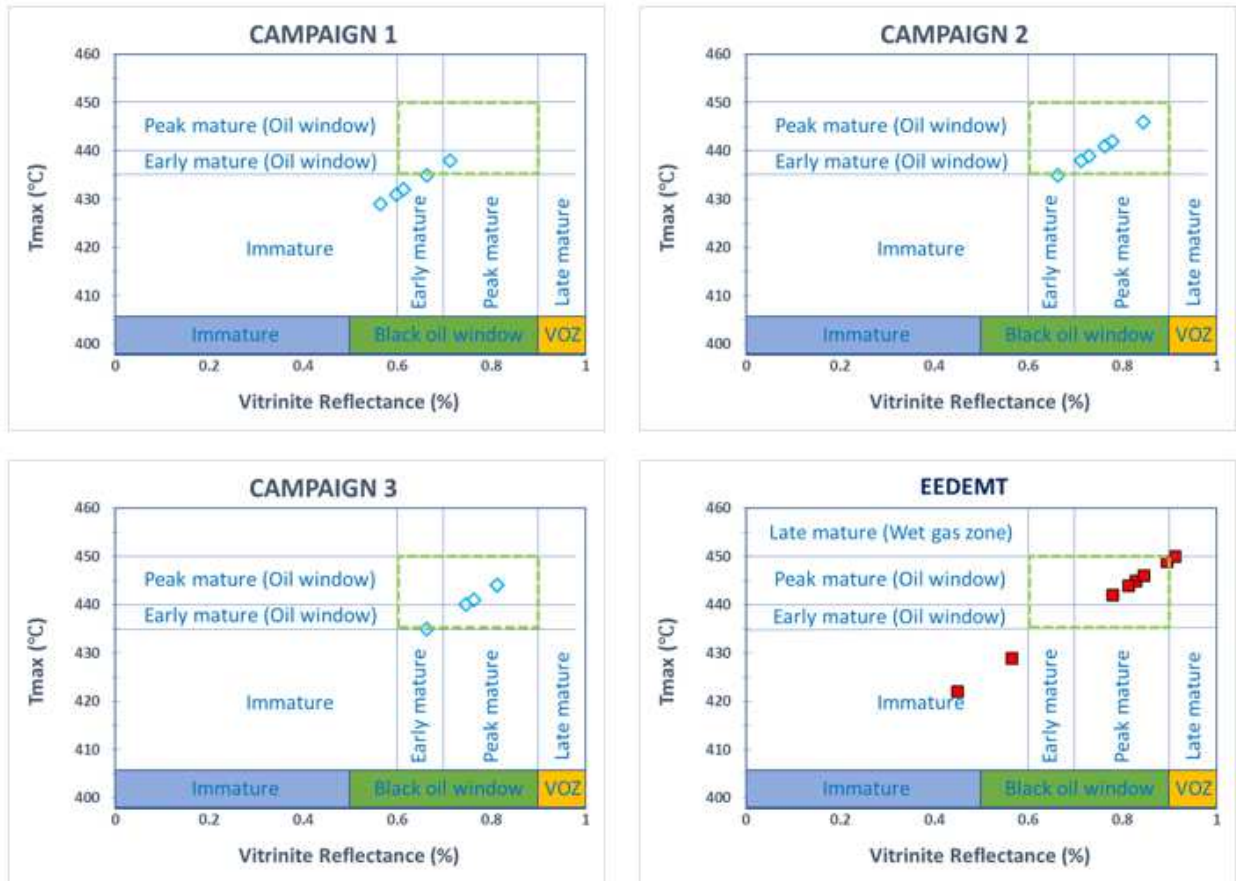


Figure 5. 10 Tmax vs Vitrinite Reflectance (%) plot of outcrop Khoot oil shale samples compared to Eedemt samples. VOZ stands for volatile oil zone.

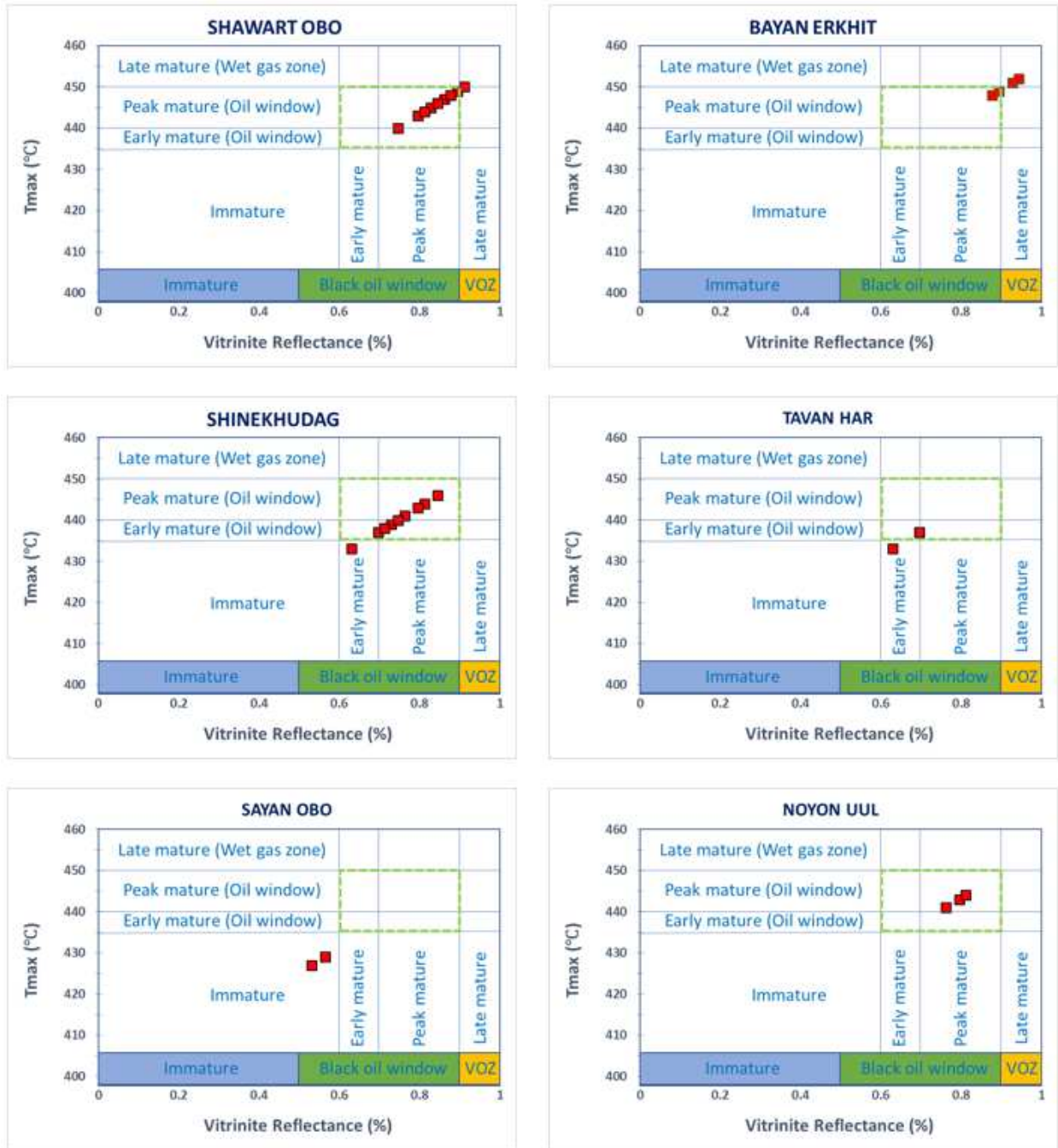


Figure 5. 11 Tmax vs Vitrinite Reflectance (%) plot of Mongolian oil shale and shale deposits. VOZ stands for volatile oil zone.

5.3.3 Thermal Maturation Map of the Surface Samples

Figure 5.12 is the interpolated surface Tmax maps of the Khoot Basin. Figure 5.12 was created using all available non-calibrated surface samples.

The southwestern area of the basin, where Eedemt-A and Eedemt-B cores were obtained again shows the lowest Tmax values, which fall below 435°C. These low values extend into the surrounding DH 3 area (Figure 5.12). The lowest Tmax value recorded in this area is 426°C. Thermal maturity of the outcrop samples increases back towards the very edge of the paleolake where DH4 and DH5 were drilled. The Tmax for the rocks in this region is 435-441°C.

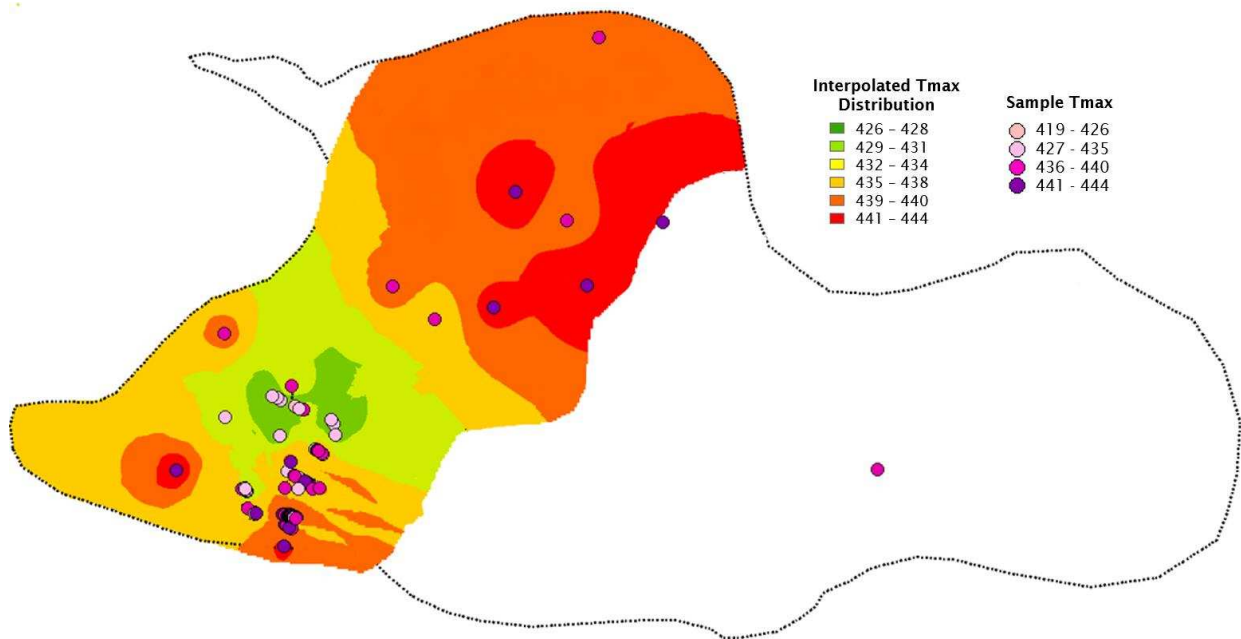


Figure 5. 12 A) Interpolated (IDW) Tmax map of the Khoot Basin from the non-calibrated outcrop samples.

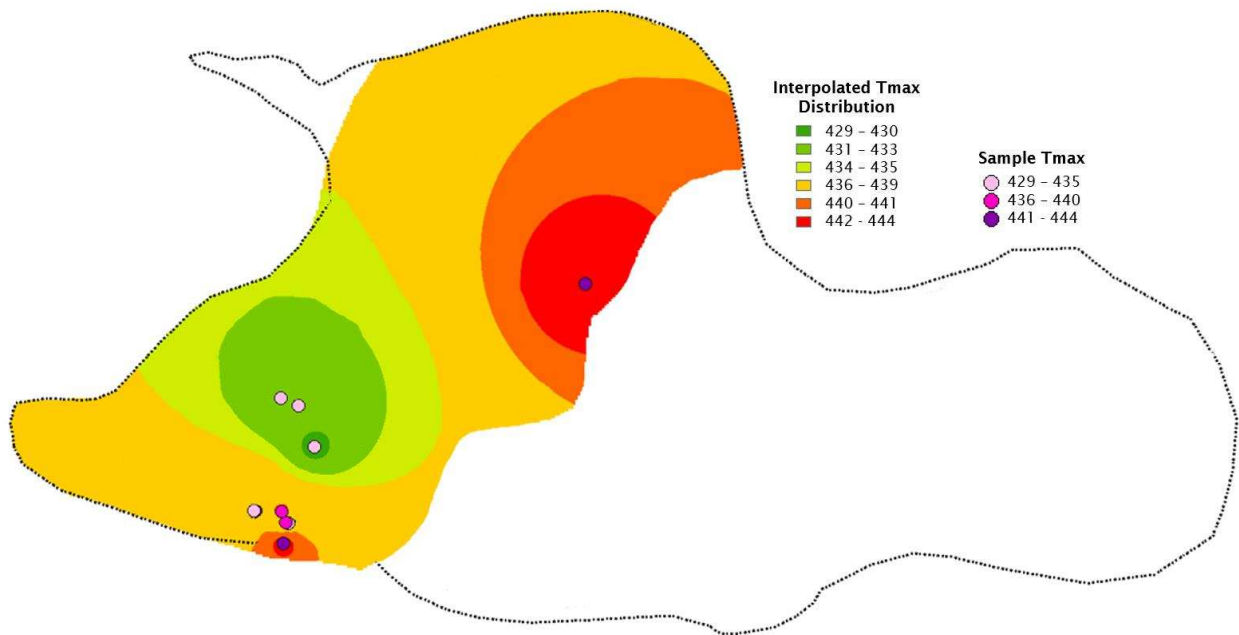


Figure 5. 12 B) Interpolated (IDW) Tmax map of the Khoot basin from the calibrated outcrop samples.

5.4 Influence of Mineral Matter on Thermal Maturation and Organic Richness

In Section 5.2, it was established that the S2/S3 values for the subsurface samples are very high due to their low S3 (CO₂ created by burning carbon with the oxygen within from organic source) (Figure 5.13 A).

On this graph, it shows that the Khoot shallow depth samples have slightly higher S3 values and lower Tmax values than most deep drill hole samples. The Eedemt and Shinekhudag samples have very high S3 values together with the Khoot outcrop samples (Figure 5.13 A). Tavan Har and Noyon Uul samples show the lowest S3 readings. The Shawart Obo, Bayan Erkhrit and Sayan Obo samples are in the middle (S3=1 to 4 mg CO₂/g rock).

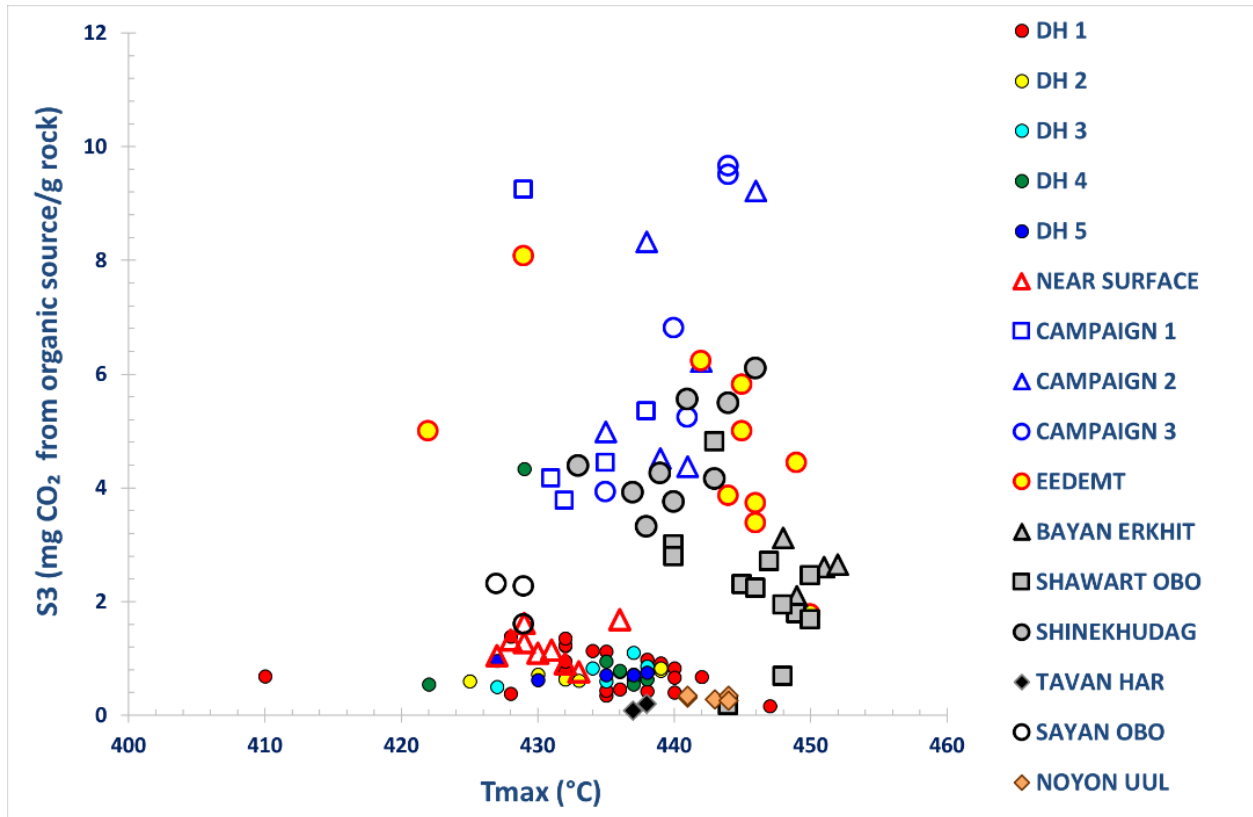


Figure 5. 13 A) Plot S3 vs Tmax serves to show the relationship between thermal maturity and CO₂ created from organic content. Displayed on the graph are core and outcrop samples from the Khoot Basin and Mongolian samples from seven different locations.

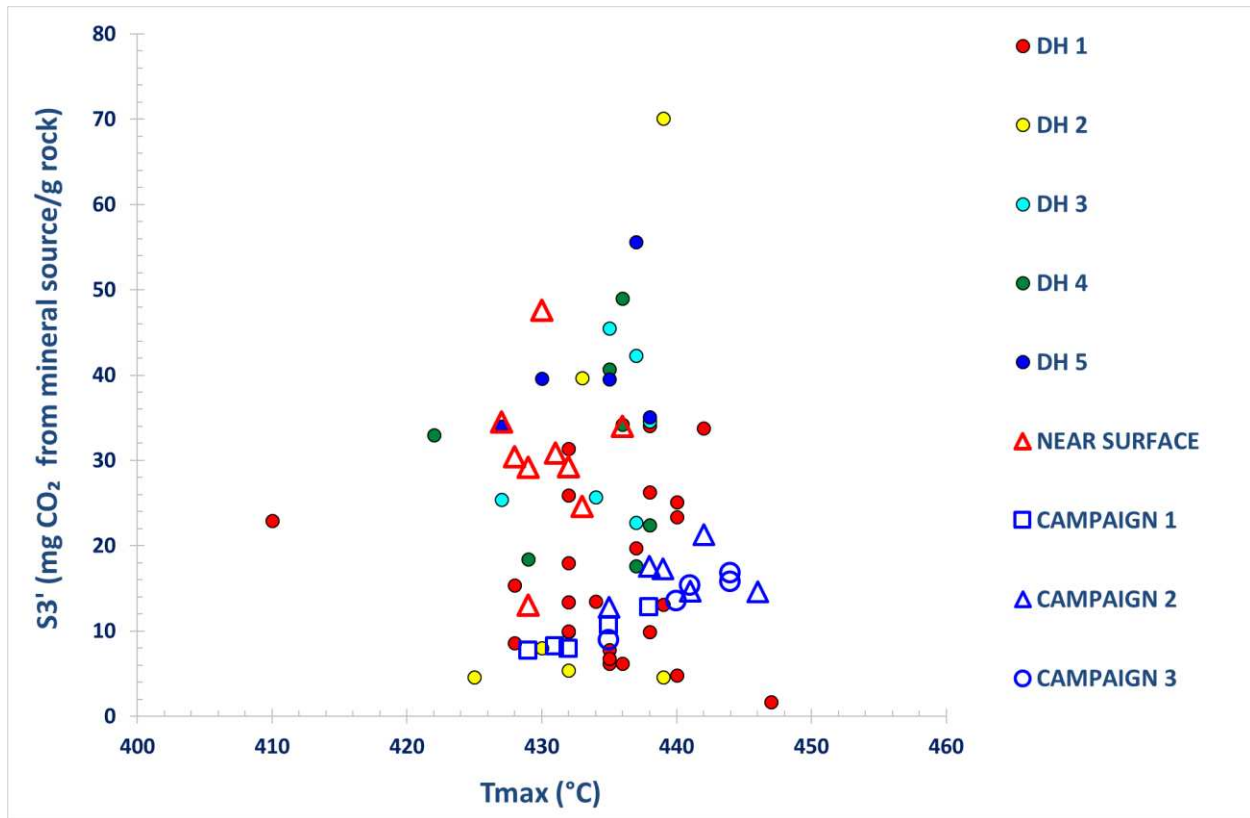


Figure 5.13 B) Plot S3' vs Tmax serves to show the relationship between thermal maturity and CO₂ created from mineral contents in the samples. Displayed on the graph are core and outcrop samples from the Khoot Basin.

Contrary to that, the amount of CO₂ created from mineral source (S3') is much higher for the subsurface and near surface samples (Figure 5.13 B). The S3' values are especially high for samples from DH 3, DH4 and DH5. From Figure 5.2 and Figure 5.13 B, it is evident that drill holes with the highest amount of mineral content (16-82 mg CO₂/g rock) has the lowest amount of organic matter (Figure 5.13). Lafargue et al (1998) suggested in their Rock-Eval 6 Application Manual that siderite is present when S3'CO is greater than 5 mg CO/g rock and S3' CO₂ is greater than 10 mg CO₂/g rock. While most samples meet the S3' CO₂ >10 mg CO₂/g rock requirement, none of the samples exceed 5 mg CO/g rock for both S3CO and S3'CO, which suggests that the Khoot samples have no siderite or very low amount of siderite.

Figures 5.14, 5.15 and 5.16 show the S3' vs TOC, HI and Tmax plots. It was previously shown in Figures 5.13 A and 5.13 B that the Khoot outcrop samples have higher S3 (CO₂ released from organic matter) while the Khoot subsurface samples had higher S3' (CO₂ created from minerals). Hence, Figures 5.14-5.16 were plotted to see if there was any relationship between organic richness, thermal maturity and mineral content in the Khoot samples.

Figure 5.14 shows five groups of Khoot samples, which cluster together according to their TOC and S3' values.

- 1) Organic-lean (2-8 wt% TOC), mineral-rich (S3'=37-70) Type I/II samples that are immature to early mature.
- 2) Organic-low (1-10 wt% TOC), average mineral content (S3'=21-37) Type I/II samples that are immature to early mature. Within this group, the shallow depth drill hole samples are dominantly Type II and immature, while DH 1 samples are dominantly Type I and early mature.
- 3) Organic-low (1-10wt%), moderate-mineral content (S3'=11-21). This group which has the least number of samples has dominantly DH 1 samples.
- 4) a. Organic-lean (1-5 wt% TOC), low-mineral content (S3'=0-11) Type II samples (immature to early mature). Within this group, DH 1 samples are almost exclusively Type II kerogen samples.
b. Organic-low (6-12 wt% TOC), low-mineral content (S3'=0-11) Type I/II samples (immature to early mature). Within this group, DH 1 samples are almost exclusively Type II kerogen samples.
- 5) Organic-rich, moderate-mineral content samples. This group is made entirely from the Campaign 1 and Campaign 2 surface samples, except for one sample each from DH 1 and DH 4. Additionally, these samples are entirely Type I with high HI values (Figure 5.13) and are early mature to mature.

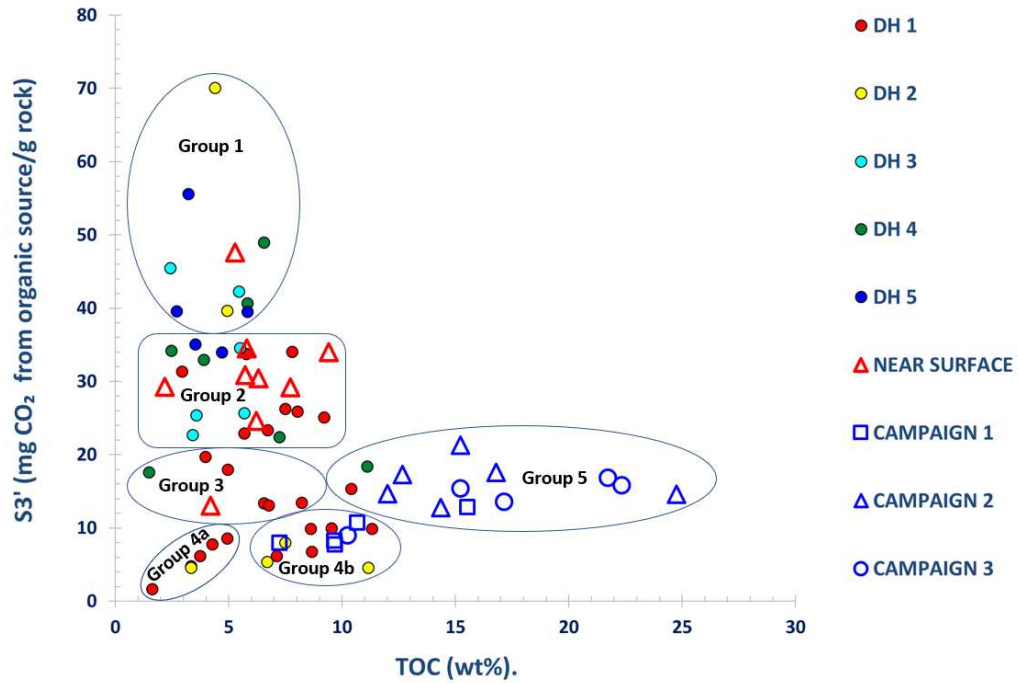


Figure 5. 14 S3' vs TOC plot shows the relationship between organic richness and CO₂ created from mineral matter. Higher mineral content is associated with lower level of organic richness.

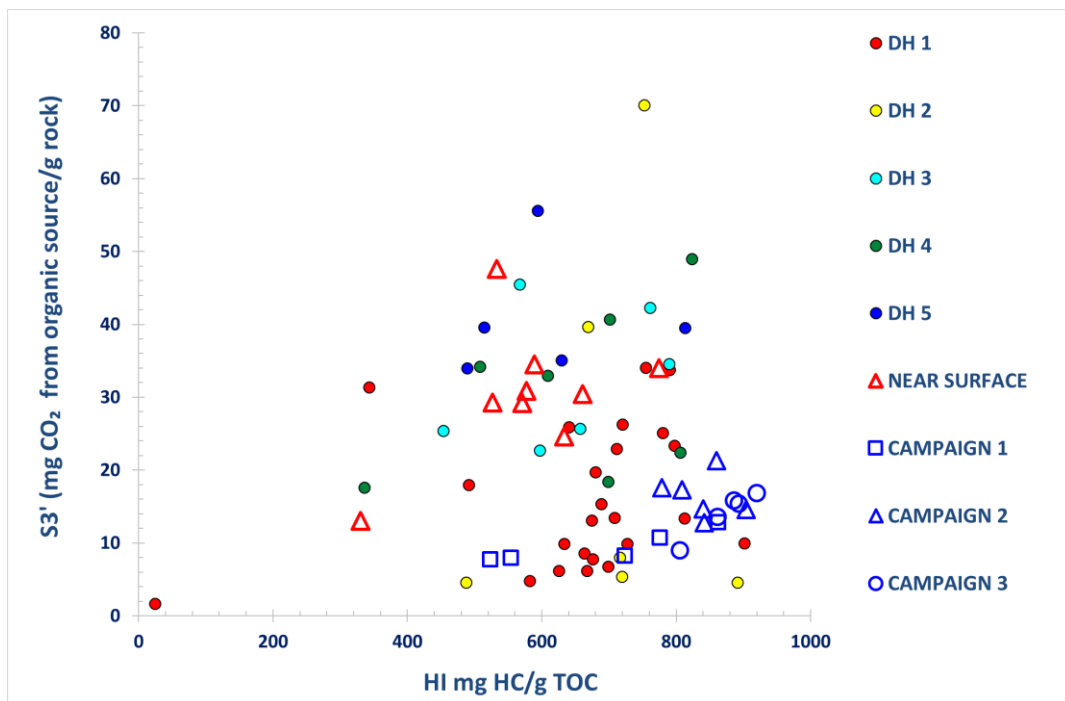


Figure 5. 15 S3' vs HI plot shows the relationship between hydrogen index and CO₂ created from mineral matter in the Khoot samples.

Some of the samples fluctuate between the facies groups, however, most of the samples belong to one of the five groups specified above. Unlike the Green River oil shale, where the richest layer Mahogany zone is several hundreds of feet and buried at an ideal temperature and pressure, the richest part of the Khoot oil shale is exposed at the surface and there is no layer comparable to this Group 5 sample at the subsurface, at least in the studied Khoot basin.

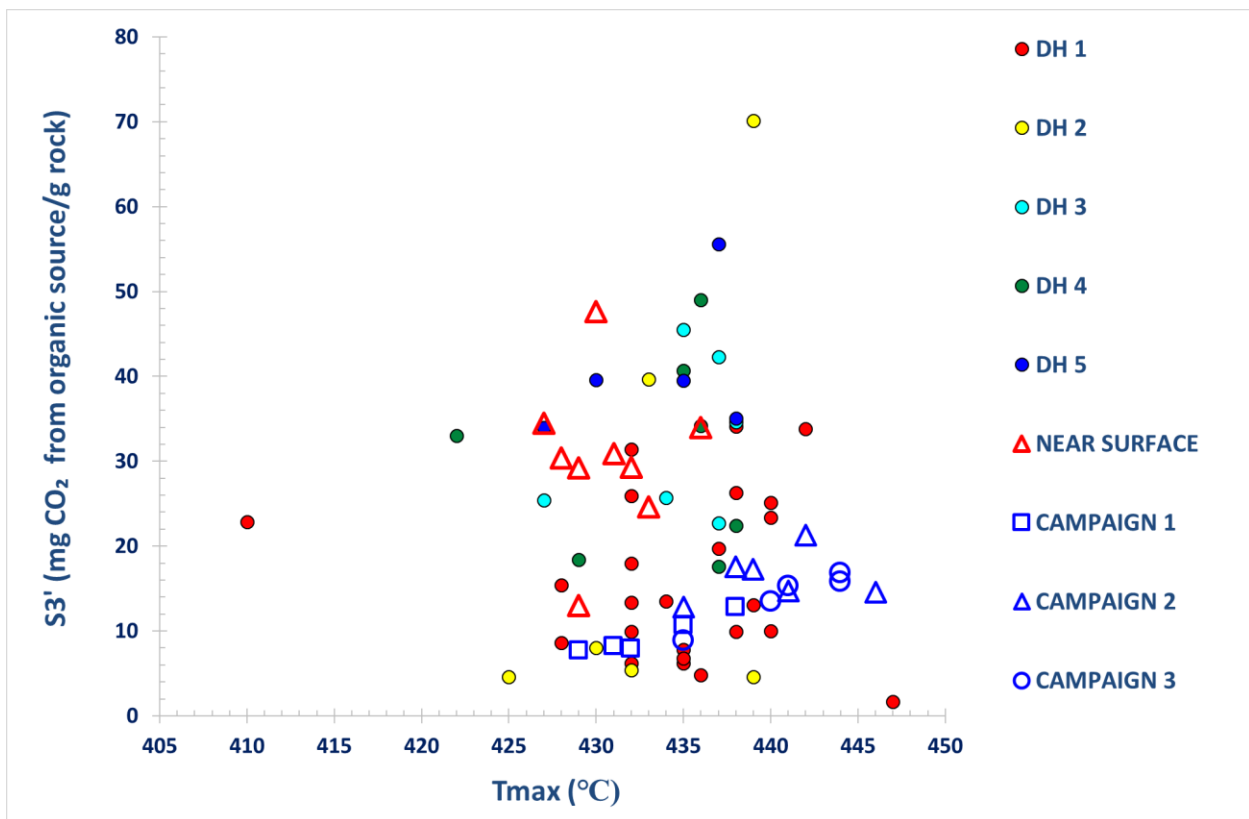


Figure 5. 16 S3' vs Tmax plot shows the relationship between source rock maturation and CO₂ created from mineral matter in the Khoot samples.

5.5 Hydrocarbon Generating Capacity

The S2 peak, measured in mg HC/g rock, is the indicator of pyrolyzed hydrocarbons generated through cracking the kerogen in a rock. However, unlike S1, S2 is measuring the amount of new hydrocarbon liberated through thermal cracking.

S2 vs TOC (Figures 5.17 and 5.18) plots show the quality as well as the kerogen types present in the samples from the Khoot Basin and other basins in Mongolia. S2 values are derived from Peters (1986). Based on these numbers, Khoot outcrop samples contain exceptionally good dominantly Type I kerogen, except for 2-3 samples collected during Campaign 1.

In a study of Kabalar oil shales in Turkey, immature and mature source rocks had very different S2 values (Sari and Aliev, 2005). The mean S2 values for the immature samples were 27.13 mg HC/g rock while the S2 values for mature samples were 49.97 mg HC/g rock (Sari and Aliev, 2005). Mongolian oil shales are showing similar trends, where the immature to early mature subsurface and near surface drill hole samples have lower S2 than the early mature to mature Campaign 2, Campaign 3 and Eedemt samples have exceptionally high S2 (Figure 5.11A), although almost all Mongolian samples studied here has very low S1 (Figure 5.19).

The Khoot oil shale samples appear very similar to the North American Green River formation samples on source rock analysis diagrams, despite the Khoot Basin being much smaller in scale. Green River oil shales had similar characteristics, where the S1 values were relatively low while the S2 values were very high (Schamel, 2015). These exceptionally high levels of S2 recordings were explained by the bound oil effect, where the expelled oil is trapped inside nano-pore throats or by sorption of the kerogen (Jarvie, 2012; Schamel, 2015). This would result in decreased S1, PI, OSI, and Tmax values, but elevated S2 and HI values on the programmed pyrolysis results.

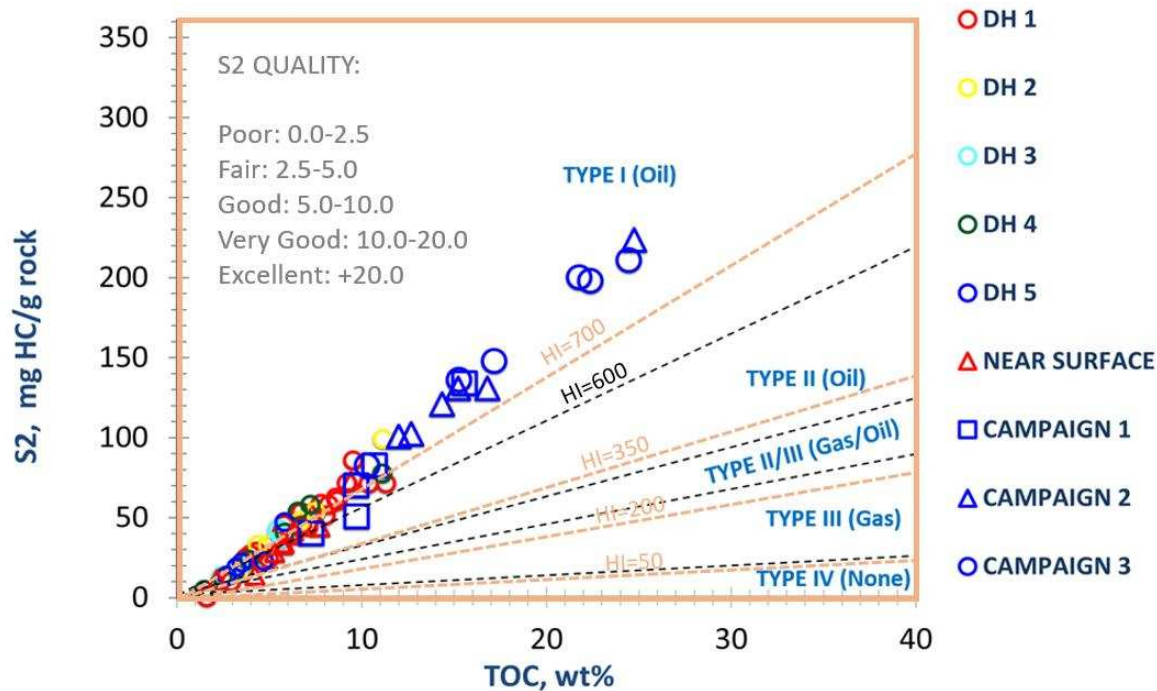


Figure 5. 17 Plot S2 vs TOC shows the source rock quality and the kerogen type. All samples plotted in this graph are the Khoot Basin samples. Levels of HI indicates the kerogen type.

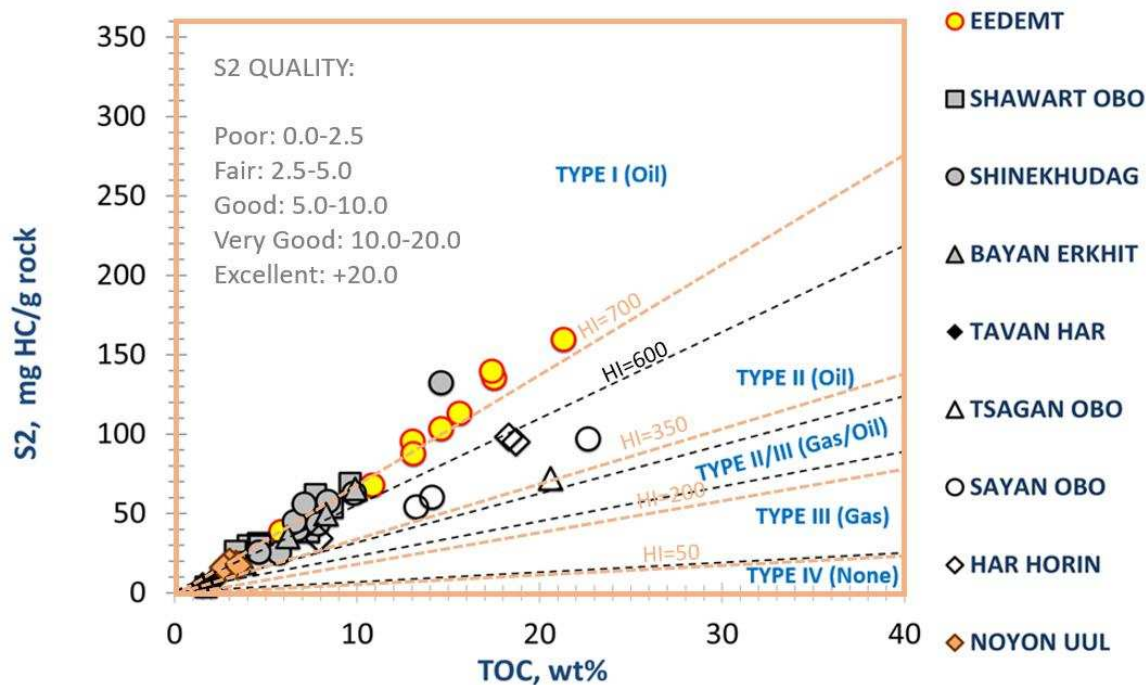


Figure 5. 18 Plot S2 vs TOC shows the source quality and the kerogen type. All samples plotted in this graph are from previous studies. Levels of HI indicates the kerogen type.

Kerogen type depends on the HI threshold value. Currently both 600 and 700 are accepted as the lower threshold value for kerogen Type I. If the threshold value is set at 700 mg HC/g, then nearly all near surface samples and DH 5 samples classify as Type II kerogen. The rest of the subsurface samples classify as Type I/II. When the threshold value is 600 mg HC/g rock, all outcrop samples become Type I.

5.5.1 Production Index

Much like the Green River oil shale and the Turkish Kabalar oil shale, Mongolian oil shales have extremely low PI values that are less than 0.1. PI is an indicator of thermal maturity as well as the producibility of the source rocks, and it is calculated as $S1/(S1+S2)$ (Peters, 1986). Figures 5.19 A and 5.19 B are the PI vs Tmax plots. Except for one DH 1 sample from the bottom of the drill hole (at 196 m), all Mongolian source rocks have $PI < 0.1$. Peters (1986) suggested that rocks with PI values under 1 are immature source rocks.

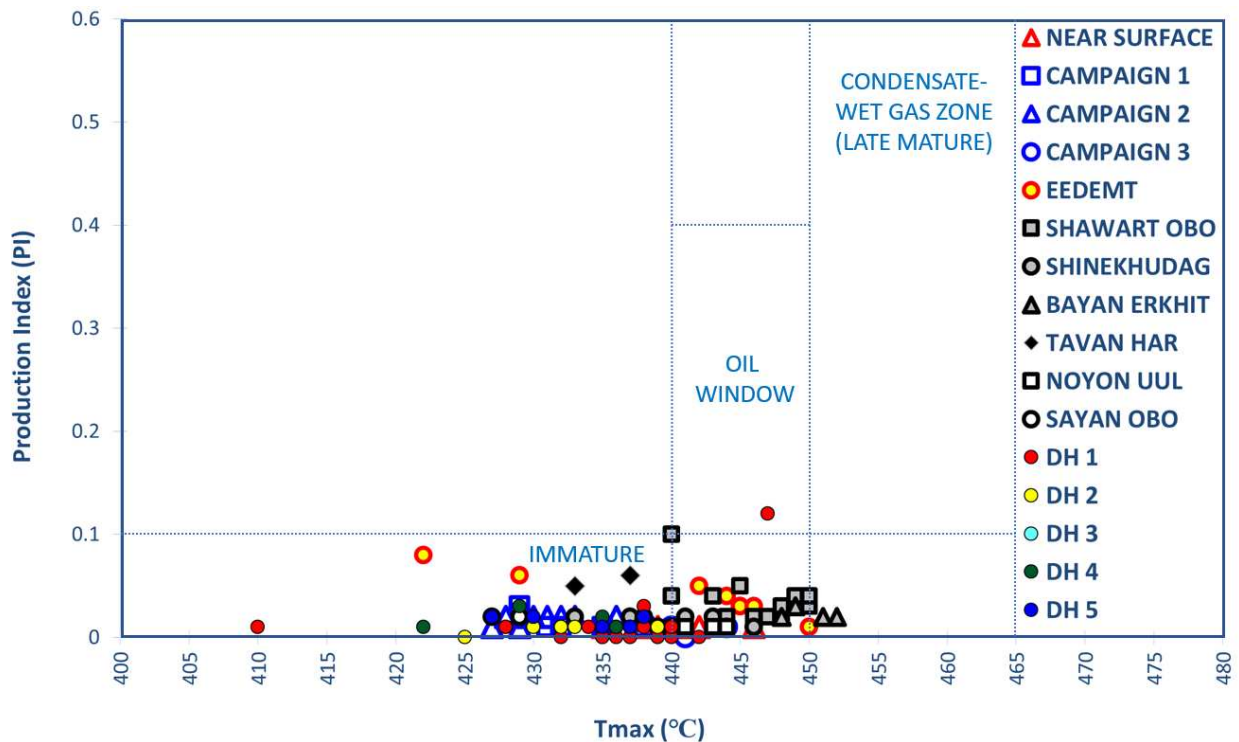


Figure 5. 19 A) The Production Index vs Tmax plot shows whether a source rock is in the oil window or immature. Production Index is calculated as $S1/(S1+S2)$. The plot indicates that almost all Mongolian source rocks have very low production index.

By contrast, Johnson et al. (2003) reported that some Mongolian source rocks, such as the Tavan Har source rocks tend to be mature for PI that equals 0.02 to 0.06. Schamel (2015) has also explained why Green River oil shales tend to mature for Tmax values as low as 425°C and for PI values less than 0.1. Because the oil generated during lower thermal heating becomes “bound oil” it does not show up on the S1 peak, but spikes up the S2 peak, as previously explained. Therefore, it is possible that Khoot Basin samples have bound oil.

Figure 5.19B is the enlarged version of Figure 5.19A. On this plot it is evident that the Eedemt, Shawart Obo and Tavan Har samples have the highest PI values (0.02-0.11). Eedemt and Khoot samples are from the same region, therefore, it seems like Rock-Eval 6 and Rock-Eval 2 are delivering different results as there have been differences in the Khoot samples and Eedemt samples throughout this study.

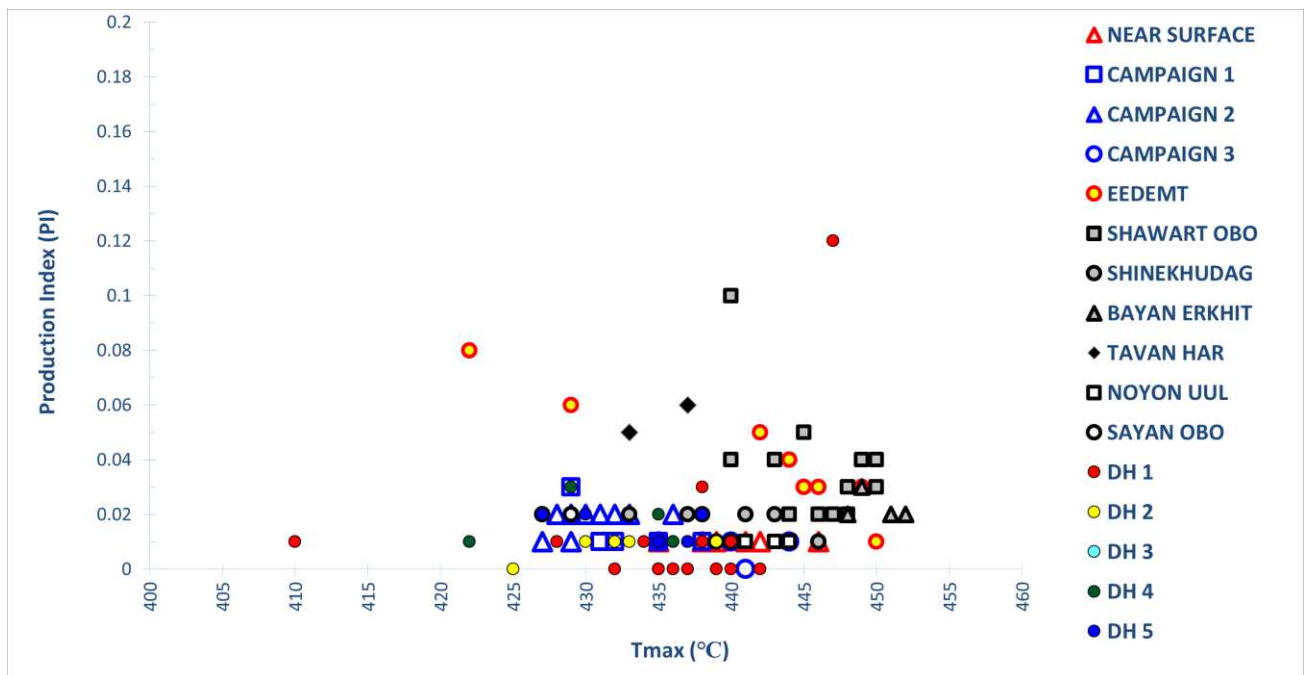


Figure 5.19 B) Enlarged PI vs Tmax plot shows that samples from literature have higher PI values than the Khoot samples.

5.5.2 Genetic Potential

The genetic potential (GP) or the total oil generating capacity of a source rock is the sum of the S1 peak and the S2 peak ($GP=S1+S2$), measured by mg HC/g rock (Schamel, 2015). Based on the values provided by Peters (1986) and Peters and Cassa (1994), Mongolian source rocks have very good to excellent genetic potential (Figures 5.20A and 5.20B). The only exception is the mid-Early Cretaceous Tavan Har samples from the East Gobi Basin and the Triassic-Jurassic Noyon Uul samples from the South Gobi basin. The lowest GP values of Mongolian oil shales and shales are higher than the lowest GP values of the Green River black shale facies and green shale facies. The highest GP values of the Khoot samples are in the same range as the Green River oil shales (Figures 5.20A and 5.20B). The red ovals demonstrate the range of the Green River oil shales according to Schamel (2015).

On a closer look, two samples from DH 4 are very similar to the mid-Early Cretaceous Tavan Har samples. Additionally, three samples each from DH 3 and DH 5 as well as one sample from DH 2 show very similar results to the Triassic-Jurassic Noyon Uul samples. All these low value samples were collected from the bottom section of each drilled hole. With that in mind, it can be said that the hydrocarbon generating capacity of the Khoot subsurface samples increase from the bottom up.

On these two plots, the Khoot outcrop samples (Campaign 3 and Campaign 2) as well as the Eedemt, Sayan Obo, Tsagan Obo and Har Horin samples demonstrate exceptionally good oil generating capacity as indicated by the high genetic potential values and high TOC values. Second to that are the DH1 samples and Campaign 1 outcrop samples. All other samples, including the shallow depth samples and the Shinekhudag-type samples are in the very good to excellent range. The hydrocarbon generating capacity also reveals that many DH 1 samples are better quality than the shallow depth samples. DH 2 samples also might have the same capacity as DH 1 samples, but there are not that many DH 2 samples from the upper parts of DH 2 in the calibrated dataset.

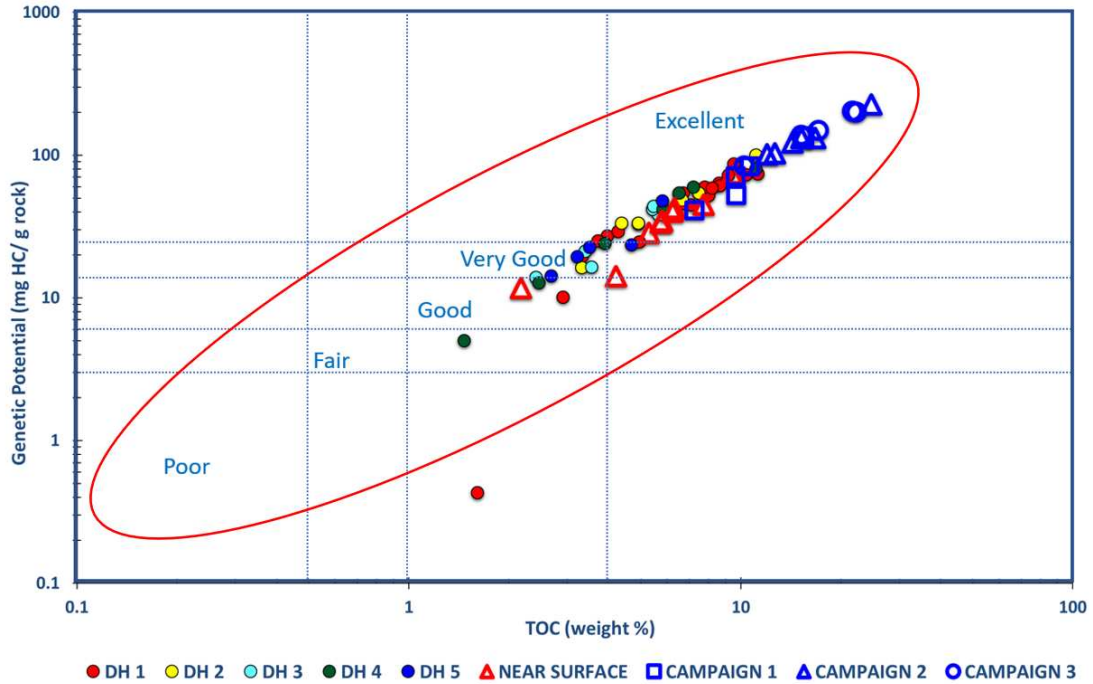


Figure 5. 20 A) The total oil generating capacity of the Khoot samples is indicated by the Genetic Potential vs TOC plot. The plot shows that most Khoot samples have very good to excellent potential.

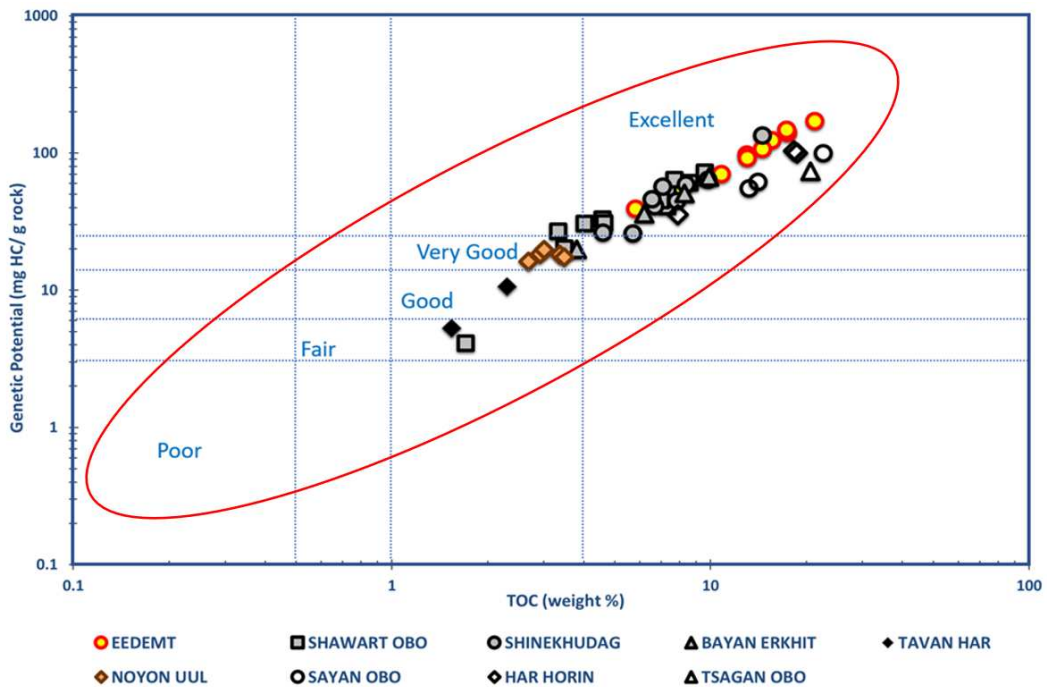


Figure 5.20 B) This plot shows the total oil generating potential of samples published in previous studies. Tavan Har samples have the lowest quality in this group.

5.5.3 Pyrolyzable Carbon Index

Pyrolyzable carbon index (PCI) reveals the maximum amount of hydrocarbon that was generated during the pyrolysis (Almansour and Al-Bazzaz, 2017). It is another parameter calculated from S1 and S2 ($PCI=0.83*(S1+S2)$). The PCI can estimate the organic matter kerogen type in a rock sample. Almansour and Al-Bazzaz (2017) has given the PCI values to characterize the distinct types of kerogen from Shaaban et al (2006). Based on this classification, all Campaign 2 outcrop samples and most of the Campaign 3 samples are pure Type I (Figure 5.21). Four DH 1 samples, two Campaign 1 samples and one sample each from Eedemt, the shallow depth drill holes and Campaign 3 samples fit in the next classification, which is Type I/II.

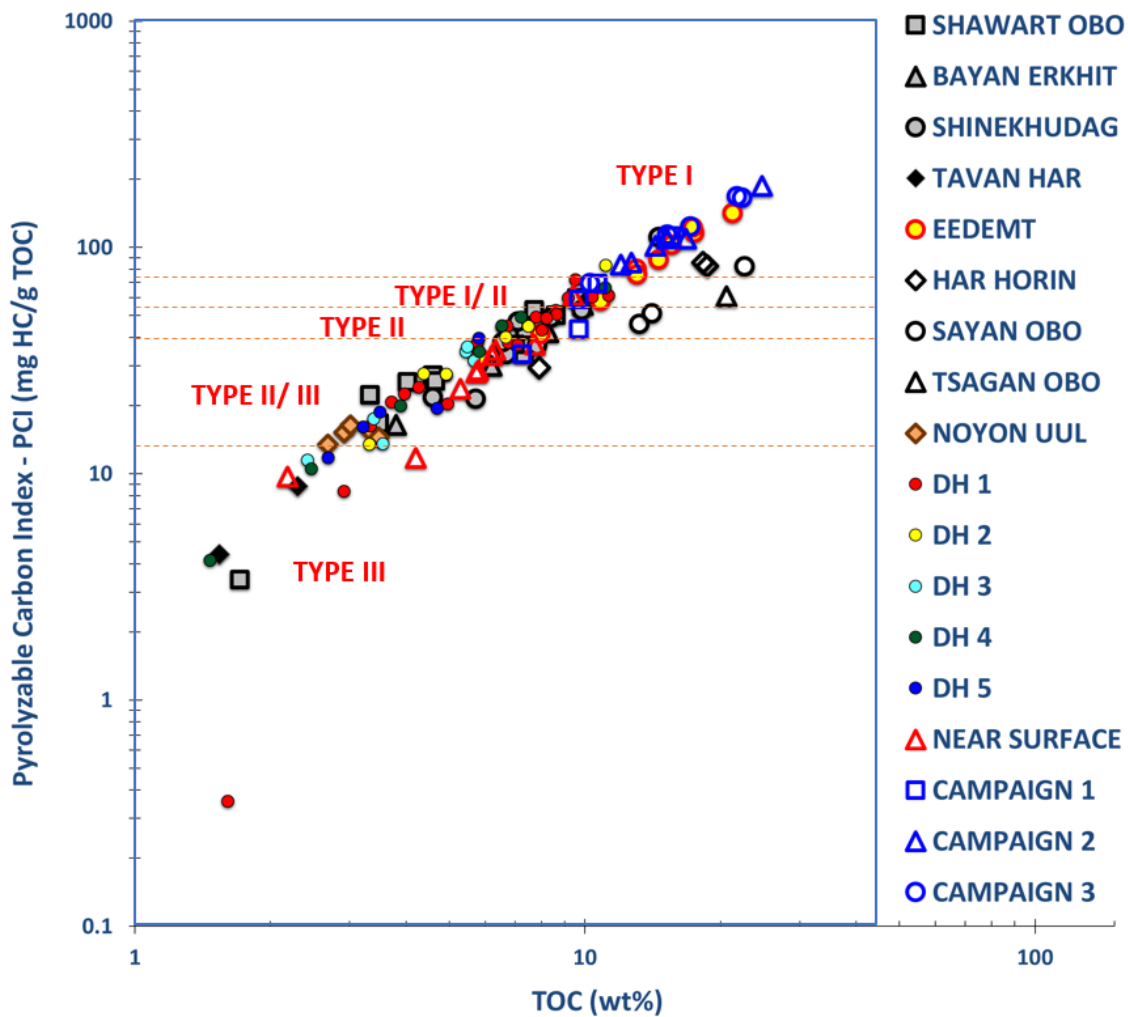


Figure 5. 21 The Pyrolyzable Carbon Index (PCI) vs TOC plot indicates the kerogen types of the source rocks.

The next cluster of samples represented by the Shinekhdag-type samples, five Khoot subsurface drill hole samples, the near surface samples and one sample from Late Jurassic-Early Cretaceous Har Horin basin is in the Type II and Type II/III zone, with PCI values greater than 25 mg HC/g TOC and less than 55 mg HC/g TOC.

Below those ranges are the Type II/III samples. The highs of this group are represented dominantly by the Shawart Obo samples and the lows are represented by the Noyon Uul samples. Samples from all five drill holes are also represented in this group, so does a couple of near surface samples.

Pure Type III samples are the mid-Early Cretaceous Tavan Har samples from the East Gobi basin. In this group there are also samples from DH 1 and DH 3 - DH 5, two shallow depth samples and one sample from Shawart Obo. These samples are of fair to good quality (Figure 5.21).

There is one sample from DH 1 which has the lowest TOC, PCI and GP values. It comes from the very bottom of drill hole 1 located at 196 m. It has a T_{max} value of 447°C, the highest T_{max} among DH 1 samples and is obviously not of the same kind as any of the Khoot samples.

5.5.4 Oil Saturation and Migration

The oil saturation index (OSI), calculated as $((S1/TOC) \times 100)$, shows that Mongolian source rocks are not producible, except for a few samples from Eedemt and one sample from Shawart Obo (Figures 5.22 and 5.23).

As explained by Jarvie (2012) and Schamel (2015), the oil saturation index from a source rock must be over 80-100 mg HC/g TOC to be considered commercial shale oil play. However, OSI values do not reflect the productivity of migrated hydrocarbons, for example the Bakken and Niobrara formations (Schamel, 2015).

On a differently scaled plot, provided by Sari et al (2015), it is shown that the Eedemt, Shawart Obo, Har Horin and Tavan Har samples have reached the oil expulsion level (Figure 5.24). Among these samples, the Har Horin samples are very

good to excellent quality, the Shawart Obo samples are fair to very good quality and the Eedemt samples are good to excellent quality (Figure 5.24).

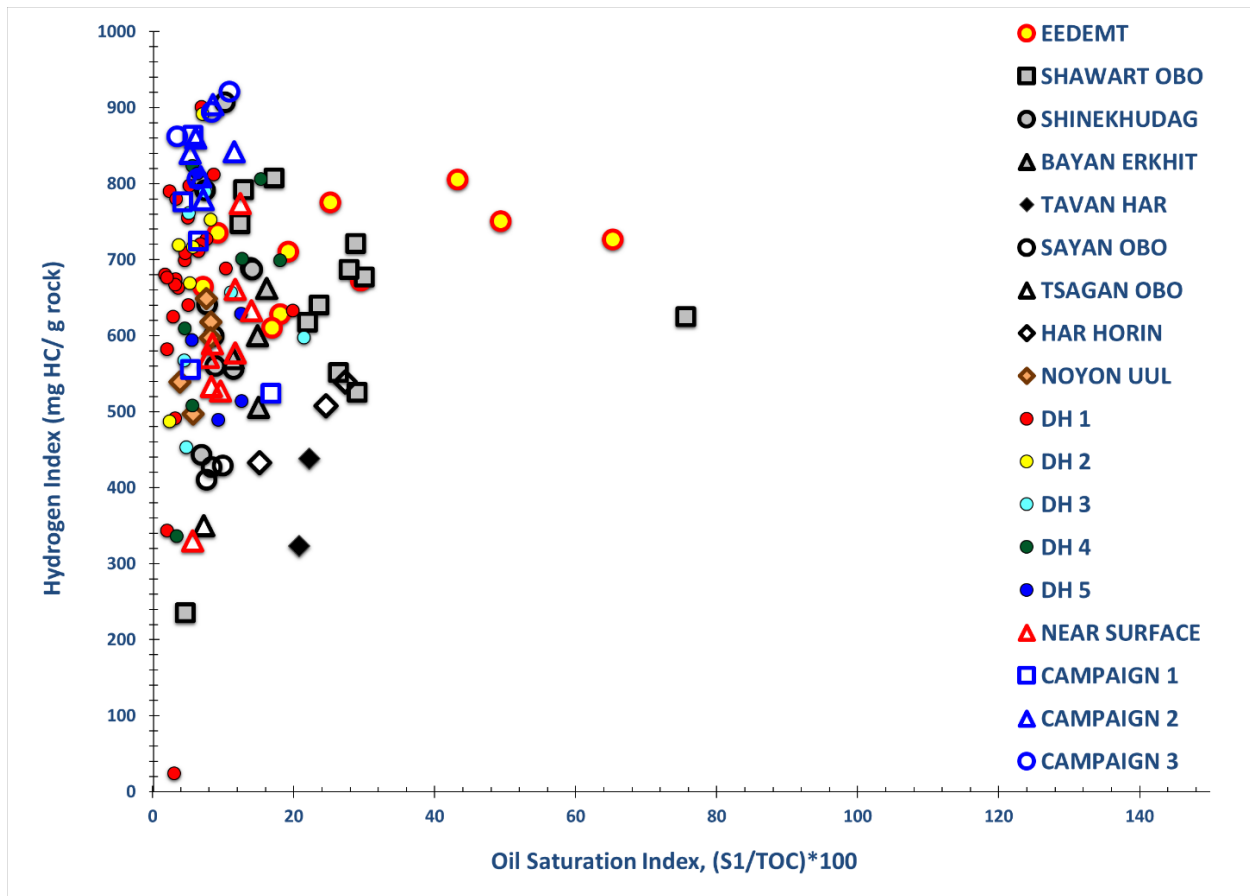


Figure 5. 22 The Hydrogen Index vs Oil Saturation Index plot shows that most Mongolian source rocks have very low oil saturation index. The oil saturation index must be over 80-100 to be considered producible.

The lowest quality of these samples are the Tavan Har samples from the East Gobi basin. According to this graph, the Khoot surface samples are fair to good quality, but no oil was expelled. The subsurface samples are of poor to good quality, with no oil expelled as well. Additionally, the Triassic-Jurassic Noyon Uul samples from the South Gobi basin are the least favorable quality.

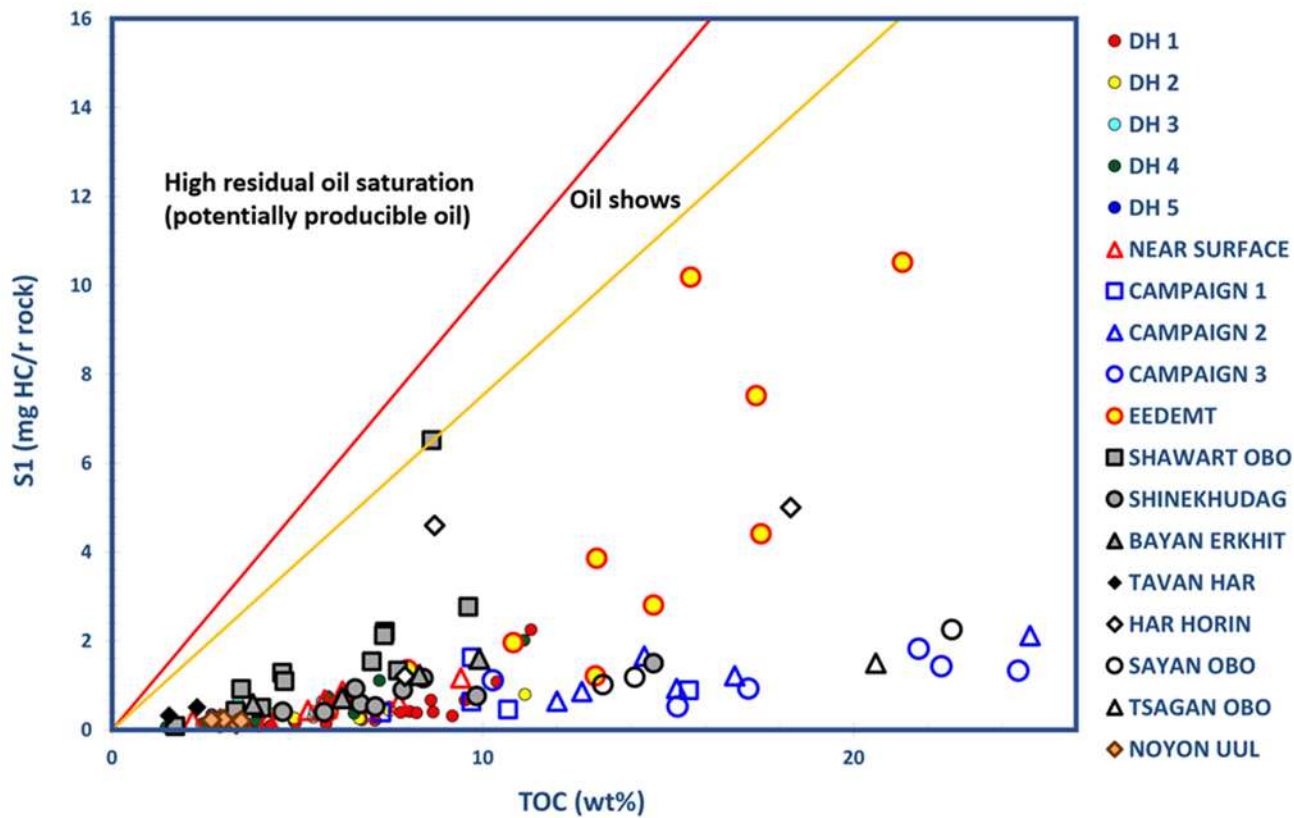


Figure 5. 23 S1 vs TOC plot of potentially producible oil from selected Mongolian oil shales and Khoot samples.

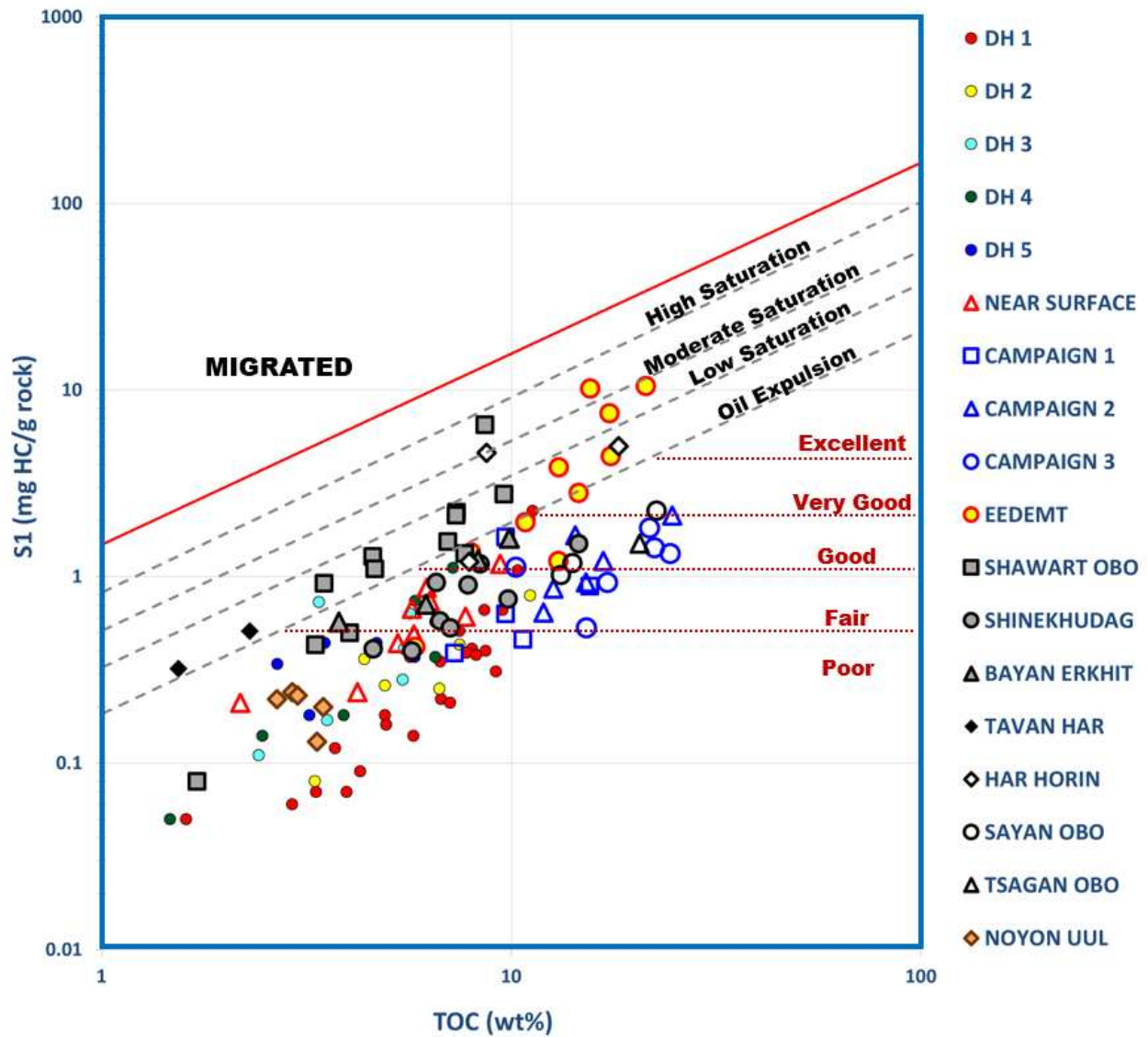


Figure 5. 24 The S1 vs TOC plot showing hydrocarbon saturation and migration qualities of selected Mongolian oil shales and Khoot samples.

CHAPTER 6

ORGANIC AND INORGANIC GEOCHEMICAL ANALYSIS RESULTS

6.1 Elemental Analysis Results

Elemental and mineralogical analysis is an effective way to understand the depositional environment, climatic change, organic enrichment, and post-depositional alteration processes in lacustrine basins. It is also a helpful tool to identify the different types of facies within the same formation.

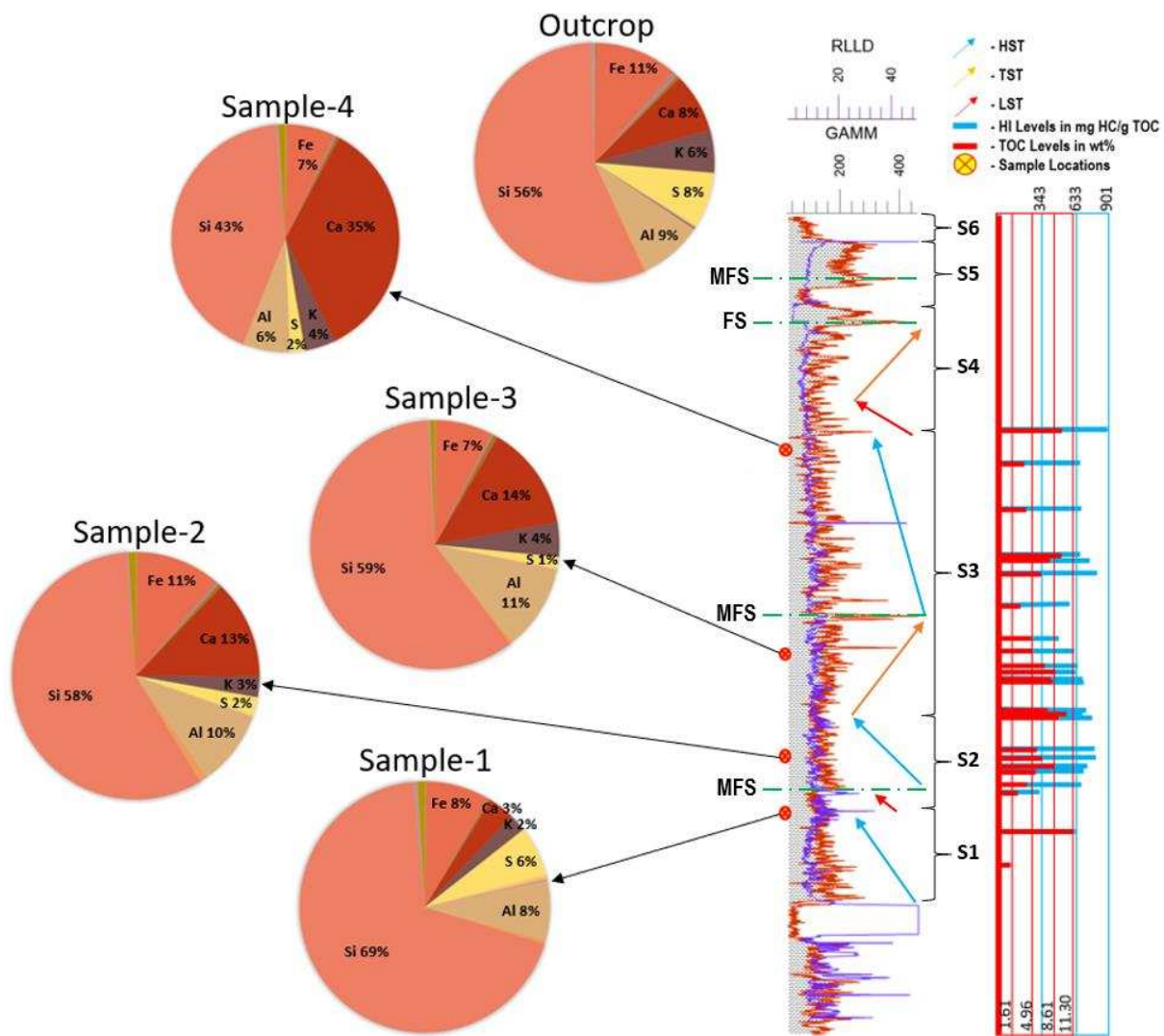


Figure 6. 1 Percentages of the major elements in the Khoot samples. The percentages of the minor and trace elements are too little to be displayed here.

The detailed amount of each element is given in Table 6.1 and Table 6.2. Out of all the samples, samples 2 and 3 have the most similar elemental composition. Based on elemental XRF analysis, the outcrop sample is drastically different from the subsurface samples, not only in organic matter content, but also in elemental composition. Major elements (Table 6.1) in the Khoot samples are Si (43-69 %), Ca (3-35 %), Al (6-9 %), Fe (7-11 %), K (2-6 %), and S (1-8 %) (Figure 6.1). The subsurface samples show an overall decreasing trend in Si content from the bottom (69%) of the drill hole to the top (43%) (Figure 6.1).

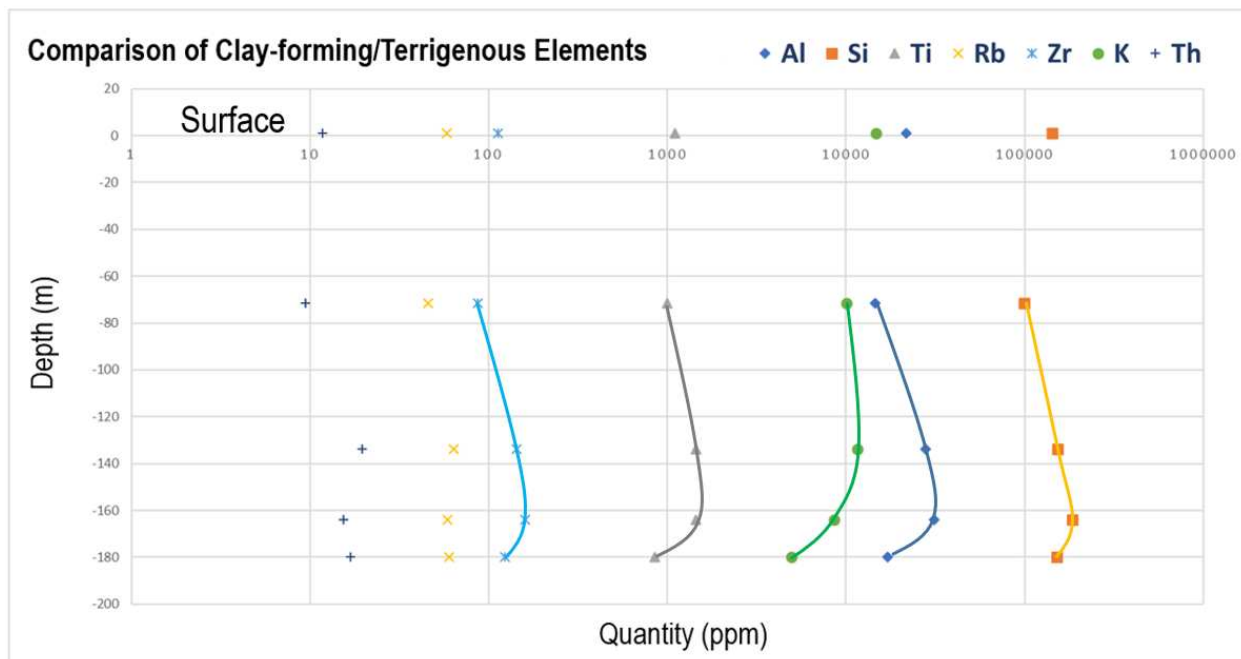


Figure 6. 2 Comparison of elements associated with terrigenous minerals, including clay minerals, feldspars and quartz.

Elements Al, Si, Ti, Rb, Zr, K and Th are associated with terrigenous environment and clay mineral deposits (ElGhonimy, 2015). Enrichment of these elements indicate higher terrestrial input and lack thereof means less terrestrial input. Figure 6.2 shows the quantity (ppm) of each of these elements in the five analyzed samples. It shows that the highest amount of these elements is present in Sample-2, although each element makes

up different percentage in the respective samples. As indicated above, Si is the highest in Sample-1 (Figure 6.3A). The Si in this sample is mostly from quartz (Figure 6.3A).

Contrary to the Si trend, the Ca content increases (Table 6.1) from 3% (Sample-1) to 35% (Sample-4) (Figure 6.1), indicating basin-ward facies change from the bottom of the drill hole towards the top, which agrees with the sequence stratigraphic interpretation from well log correlations in Chapter 3. Figure 6.3A is consistent with this result where Sample-4 has the highest Ca/K, a proxy for increasing carbonate minerals. Figure 6.3A also reflects the high amount of quartz in Sample-1. In the XRD reading presented in the next section, calcite peaks are most visible in Sample 3, followed by Sample-4 (Figure 6.7).

The amount of element K gradually increases from 2% in Sample-1 to 4% in Sample-4 (Figure 6.1). It is also very high in the outcrop sample, which is complimented by Figure 6.3B, in which the outcrop sample has the highest tendency to have K-feldspar as opposed to detrital clay.

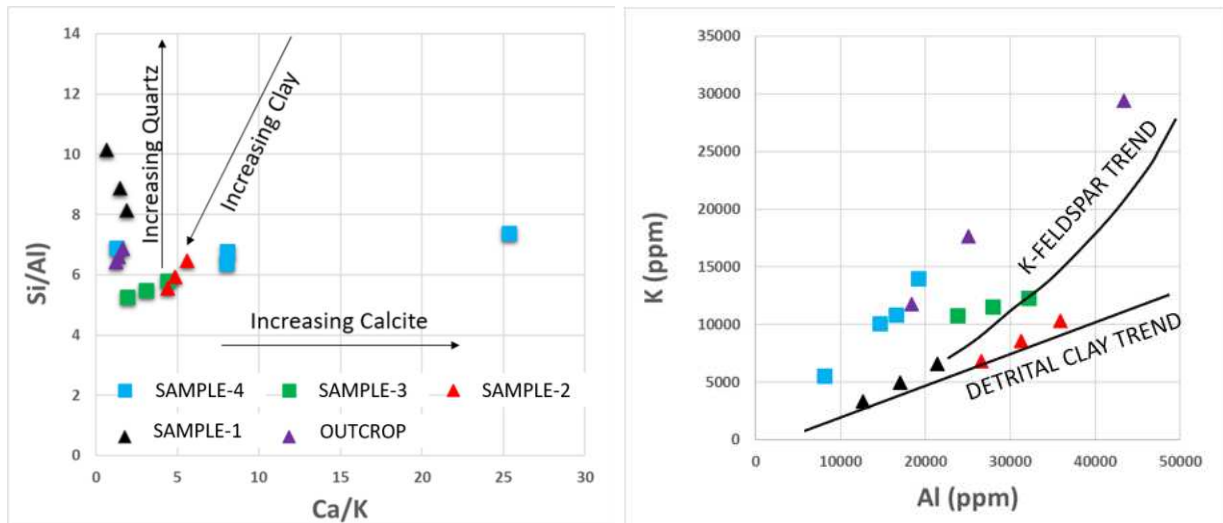


Figure 6. 3 A) Si/Al ratio vs. Ca/K ratio

B) Plot of element K vs. element Al

Ba/Sr and Rb/Sr ratios are indicators of detrital material enrichment (Akkoca and Sagioglu, 2005). On the contrary, low Ba/Sr and Rb/Sr are proxy for abundance of carbonate and smectite minerals (Akkoca and Sagioglu, 2005). Ba/Sr and Rb/Sr also

indicate deep lake facies, rather than basin margin deposits. Sample-1, which is enriched in both Ba/Sr and Rb/Sr (Figure 6.4), therefore has the highest input of terrestrial material. Sample-4, which is depleted in Ba/Sr and Rb/Sr has the least amount of terrestrial material. This is also in agreement with Figure 6.3A, where the Ca/K ratio is the highest in Sample-4.

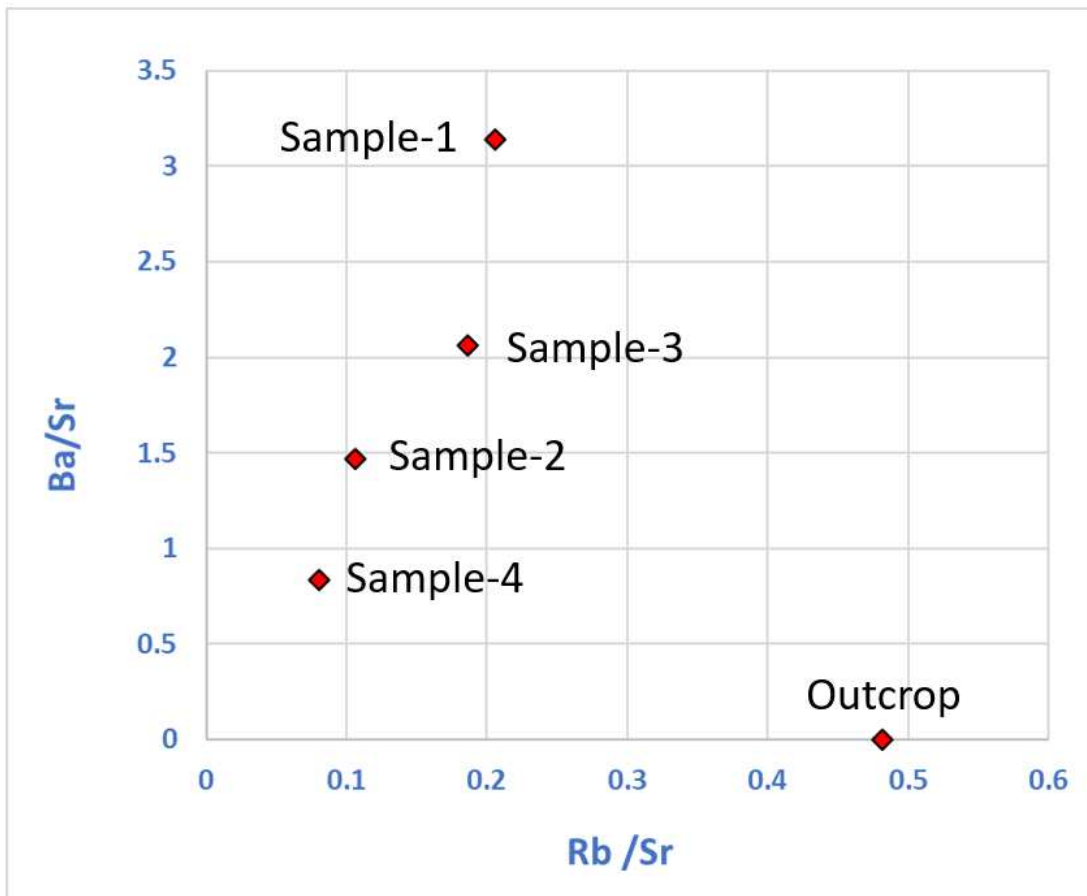


Figure 6. 4 Ba/Sr and Rb/Sr analysis indicates the presence of detrital materials vs carbonate minerals and smectite.

Sulfur is another element that shows similar trend to Si, where it gradually decreases from the bottom of the drill hole to the top. The bottom of the drill hole (Sample-1) has 6% S, which decreases to 2% in Sample-2, 1% in Sample-3, and 2% in Sample-4 (Figure 6.1). The amount of sulfur increases back to a high of 8% in the outcrop sample.

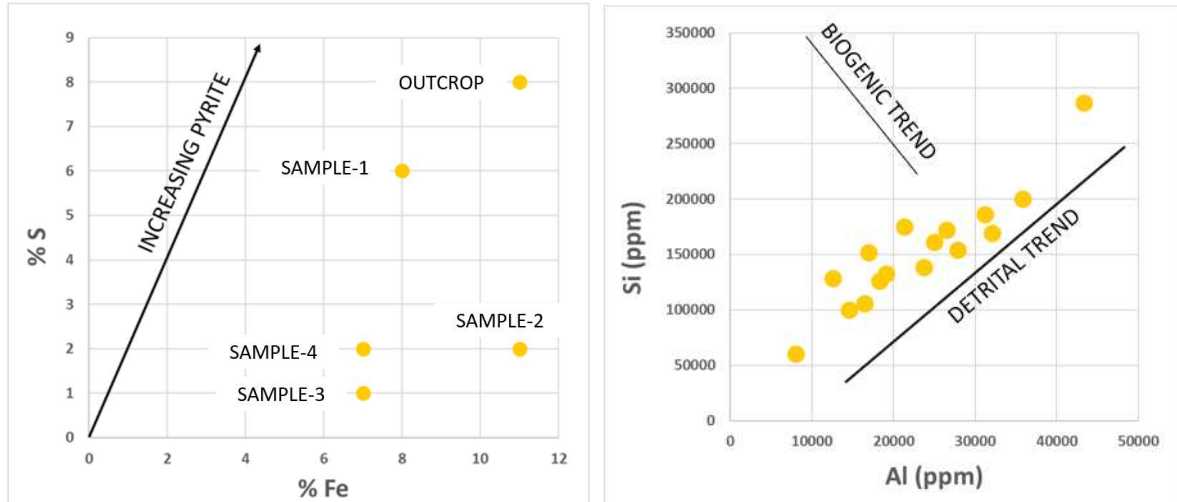


Figure 6. 5 A) Analysis of pyrite presence. B) Si vs. Al trends indicate origins of the silica present in studied samples.

Figure 6.5 A is displaying the five samples' preference to have pyrite. Pyrite is an indicator of anoxic environment (Bennington, 2018). The tendency to have pyrite is higher in Sample-1 and the outcrop sample.

The minor and trace elements in Khoot oil shale samples are shown in Table 6.1 and Table 6.2. Khoot oil shale samples showed no Au, Hg, Se, Re, Ta, and Hf, although there might be very small amounts present below the measuring device's detection limit.

As previously indicated, the Khoot outcrop sample is different from the subsurface samples in many ways. It has higher Arsenic (As), Bi (Table 6.2) and Sn (Table 6.1) than the subsurface samples, and depleted in Mg, Ba (Table 6.1), Cd, Cs, Te, Sb, Ag, Ni, Cu, Pd, and Co (Table 6.2). Mg can be an important element in the formation of chlorite. The level of As is 11.23-27.41 ppm in the subsurface samples, but it reaches 58.69 ppm in the outcrop sample. In a study of Green River oil shale, 30 ppm As was found in raw oil shale samples from the Mahogany zone and 20 ppm was present in the saline zone (Powers and Thoem, 1977). Based on observations from the Green River formation and Mongolian Khoot samples, increase in As is associated with higher TOC. The average concentration of Arsenic is 5 to 6 ppm in soil, although it may range from 0.1 ppm to 40 ppm (Lesikar et al., 2005).

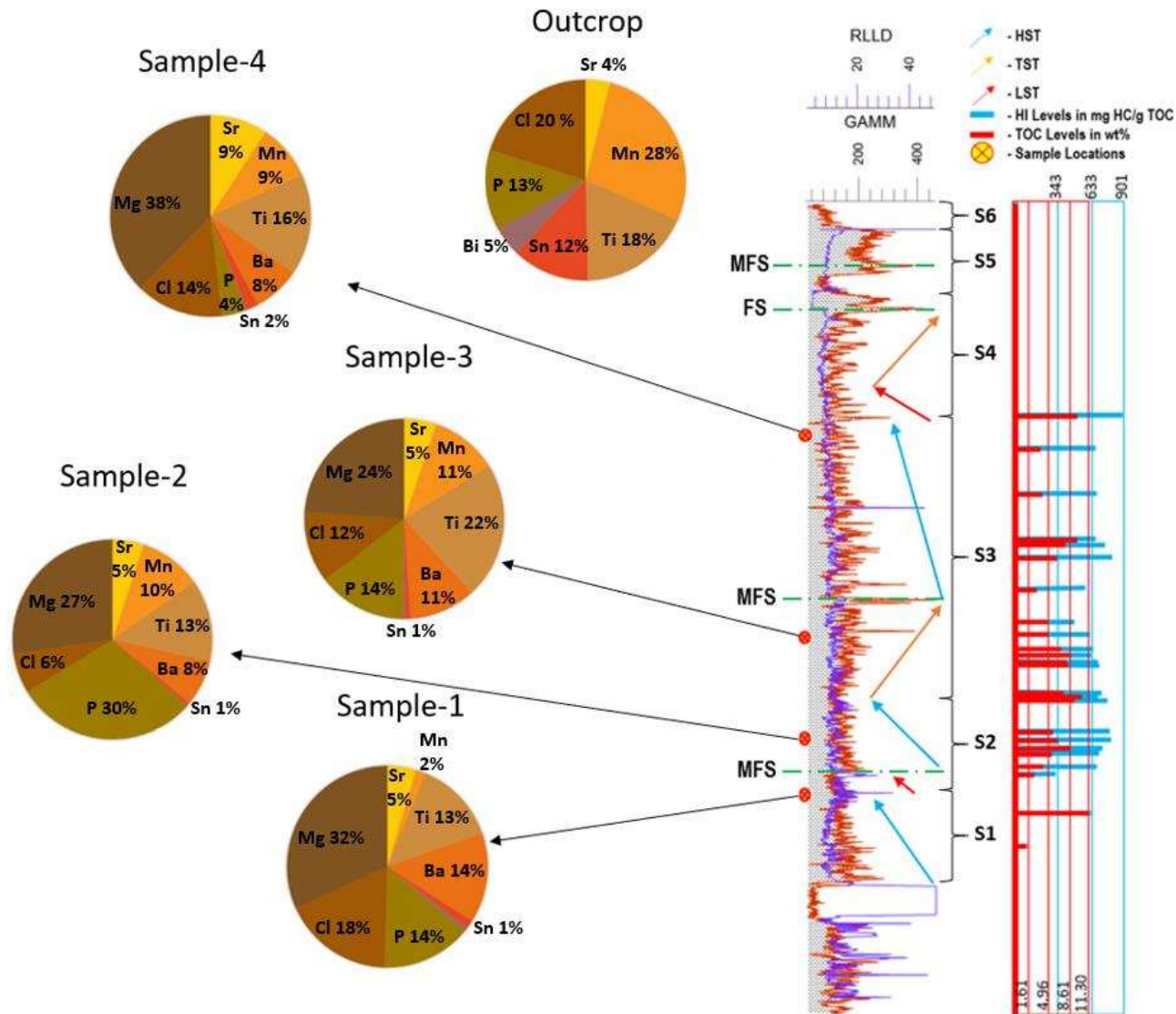


Figure 6. 6 Percentage of minor elements in the Khoot samples. Some of the elements present in the subsurface samples are absent in the outcrop sample.

The subsurface samples are enriched in heavy metals, such as Co, Cu, and Ni (Table 6.2). The element Cobalt is only present in Sample-1, which is the lowermost sequence in DH 1. These elements are indicators of groundwater invasion into the hydrocarbon containing units from a nearby aquifer. From this, it can be concluded that the oil shale deposited during Sequences 1, 2 and 3 may have been richer in organic content but might have gotten saturated with ground water. The original subsurface oil shale may have had higher level of organic matter but got depleted after aquifer water saturated the units.

Table 6. 1 Major and minor elements (ppm) detected in the Khoot subsurface and outcrop samples. The results displayed below are calculated average values of 2-3 scans from each sample.

	SAMPLE-1	SAMPLE-2	SAMPLE-3	SAMPLE-4	OUTCROP
Major Elements					
Si	151220	185486	153298	99092	143217
Ca	7298	41732	35368	81580	20508
Fe	17701	35348	18580	15590	28314
Al	17028	31256	27968	14600	21698
K	4942	8569	11508	10094	14721
S	14145	7627	3587	4743	19206
Minor Elements					
Mg	4001	2965	3104	3480	0
P	910	3219	933	724	796
Cl	1118	699	753	872	1227
Mn	100	1100	708	555	1682
Ti	846	1443	1440	996	1105

Table 6. 2 Trace elements (ppm) detected in the Khoot subsurface and outcrop samples. The results displayed below are calculated average values of 2-3 scans from each sample.

	SAMPLE-1	SAMPLE-2	SAMPLE-3	SAMPLE-4	OUTCROP
Ba	908	809	701	474	0
Sr	289	551	340	570	240
Sn	84	51	55	117	758
Zr	123.22	160.07	143.49	86.36	112.18
U	8.6	0	16.66	9.35	9.63
Rb	59.7	58.5	63.26	45.77	57.92
Th	16.87	15.37	19.52	9.34	11.66
Pb	32.27	32.02	31.43	19.33	30.7
As	27.41	25.47	13.56	11.23	58.69
Bi	40	14	26	10	290
Zn	71.97	109.39	78.98	90.6	106.82
Co	135.86	0	0	0	0
Ni	0	52.24	42.79	0	0
Cr	41.45	117.15	84.45	103.95	109.28
V	33.91	76.71	57.61	51.12	46.72
Sc	12.21	55.04	57.27	130.04	20.23
Cs	139.38	119.15	101.51	67.71	0
Te	237.61	190.52	184.24	144.11	0
Sb	91.19	64.34	68.82	60.57	0
Cd	39.11	34.49	27.79	27.97	0
Ag	25.53	13.06	13.12	18.35	0
Pd	18.14	15.17	0	0	0
Nb	6.92	10.04	9.17	5.13	10.03
Cu	31.02	16.71	13.79	13	0
Rb	59.7	58.5	63.26	45.77	57.92
Mo	11.94	10.99	11.16	95.49	22.38
Hf	0	0	0	0	0
Re	0	0	0	0	0
Au	0	0	0	0	0
W	0	0	0	0	0
Hg	0	0	0	0	0
Se	0	0	0	0	0

6.2 Mineralogical Analysis Results

XRD analysis of the oriented clay size (<3 μm) fraction of the samples shows that all five samples have similar results, in terms of clay mineral content (Figure 6.7). Peaks of some non-clay minerals, such as quartz, calcite, albite, and feldspar are also identified in Figure 6.7. The calcite peaks are the most obvious and sharp in Sample-3, which is generally in agreement with the elemental Calcium percentage in Figure 6.1.

Illite is the first clay mineral common in all five samples. Illite 001 and illite 002 peaks appear at 10.0 \AA and 5.0 \AA , respectively. Illite 003 (26.79°) peak appears a bit vague as the illite peak overlaps with the quartz and smectite peaks near 3.34-3.38 \AA (Figure 6.7). The remaining illite peaks are not as vivid and clear as the first two peaks. Illite shows a rather consistent result in all samples.

An important result from this study is regarding kaolinite. In Avid and Purevsuren (2002), it was reported that one of the distinctive features of Khoot oil shale is its absence in kaolinite. However, there are clearly possible kaolinite peaks showing in Figure 6.7. Kaolinite 001 (7.16 \AA) and Chlorite 002 (7.10 \AA) as well as Kaolinite 002 (3.58 \AA) and Chlorite 004 (3.54 \AA) are indistinguishable without any additional treatment (Moore and Reynolds, 1989). To distinguish these two clay minerals from one another, air-dried Sample-1, Sample-4 and the outcrop sample were heat treated to 550°C for an hour (Moore and Reynolds, 1989). At this temperature, kaolinite loses its crystalline structure and becomes amorphous (Moore and Reynolds, 1989). Also, as Smectite 001 collapses, Chlorite 001 becomes visible, if it is present (Moore and Reynolds, 1989).

The peaks around 12.3° (7.16 \AA) and 24.9° (3.58 \AA) in the studied samples completely disappeared after heat treatment. Further analysis has revealed that Sample-4 has both kaolinite and chlorite (Figure 6.8). The broad-breadth of the peaks near 7.16 \AA and 3.58 \AA as well as the new peak near 14.0 \AA (Chlorite 001) suggest presence of chlorite (Figure 6.8). Compared to that, Sample-1 and Sample-2 only have kaolinite (Figure 6.9 and Figure 6.10). The outcrop sample also shows indication of possible chlorite (Figure 6.11).

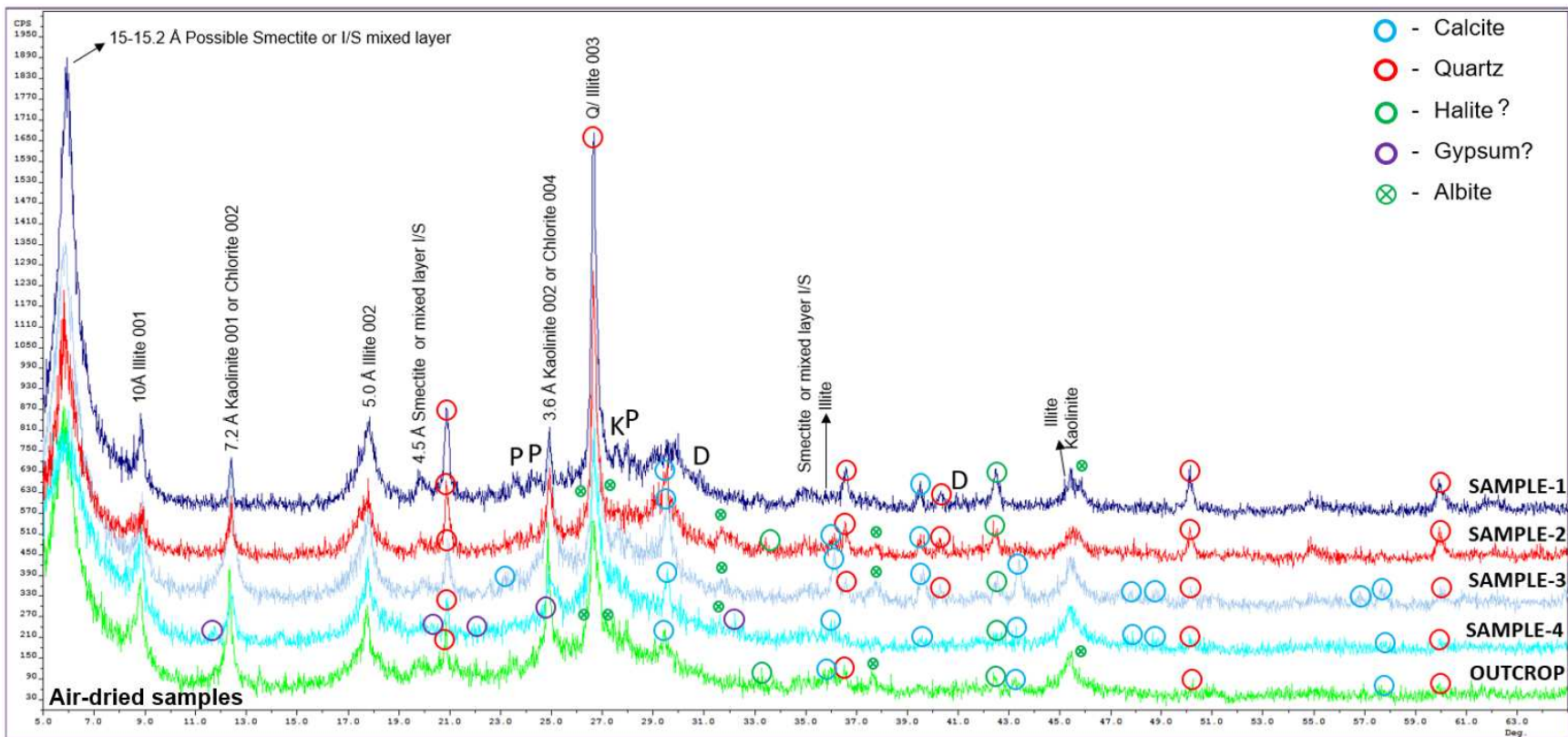


Figure 6. 7 X-Ray Diffraction patterns of Khoot samples. The samples were scanned under $\text{CuK}\alpha$ radiation from 5° to 65° 2θ at a continuous scan rate of $3^\circ/\text{minute}$.

A peak near 4.5 Å hints at halloysite, but this peak does not disappear after heat treatment, so halloysite was ruled out. However, Avid and Purevsuren (2002) did find halloysite in the Eedemt (Khoot) outcrop samples.

Smectite is the next common clay mineral in the five studied samples. However, the intensity of smectite peaks decrease from Sample-1 at the bottom of DH 1 to the top. In the centrifuged oriented air-dried samples, smectite peaks are difficult to identify except for the S 001 peak near 15.0 Å.

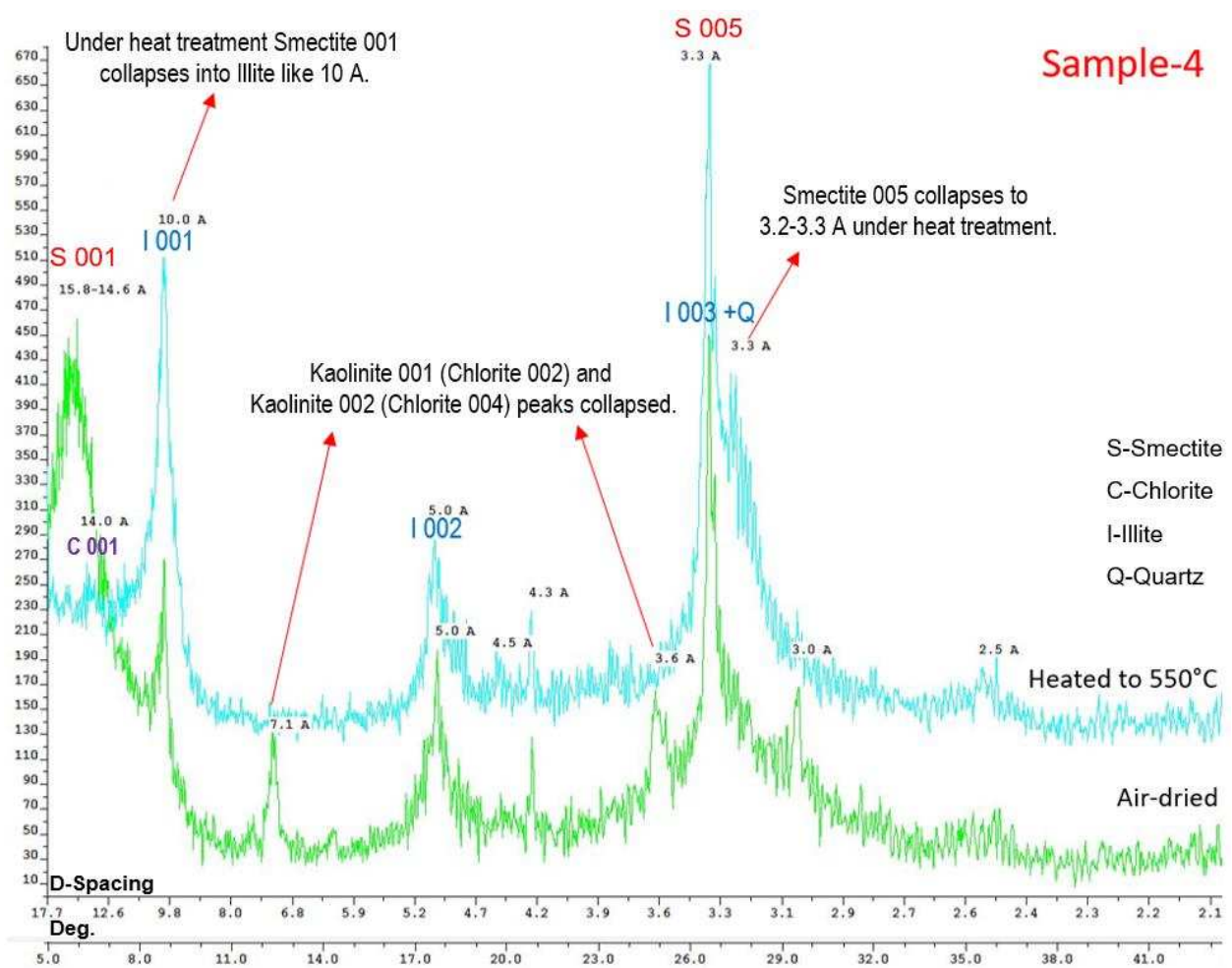


Figure 6. 8 Heat-treated Sample-4 compared against the untreated sample. The sample was heated for 1 hour at 550°C.

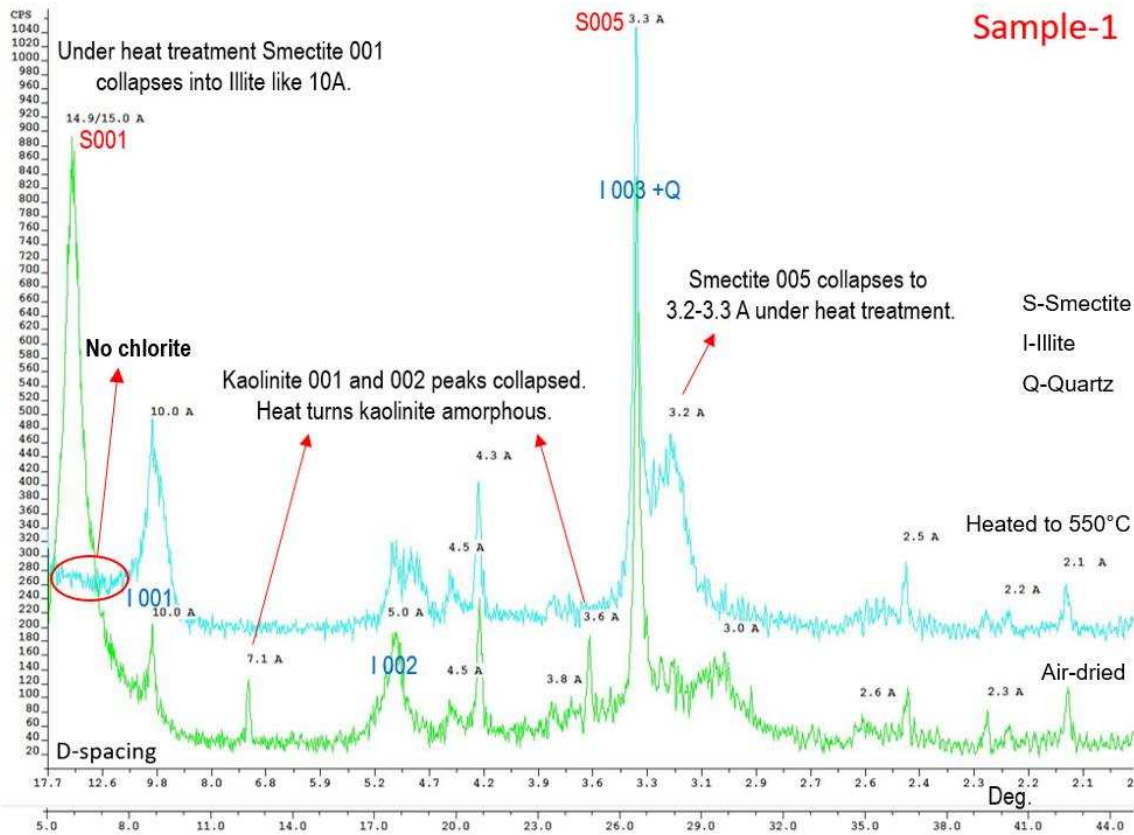


Figure 6. 9 Heat-treated Sample-1 compared against the untreated sample. The sample was heated for 1 hour at 550°C.

To prove that the peak is indeed smectite, it needs to be either heat-treated or Ethylene Glycol (EG)-treated (Moore and Reynolds, 1989). Both treatments were performed on the outcrop sample, which yielded satisfactory results. Figure 6.11 shows the result of the heat-treated outcrop sample and Figure 6.12 is the EG-treated outcrop sample result.

After heat-treatment, the 001 smectite peak collapses to illite-like 10 Å (Figure 6.11). Smectite 005 peak also collapses to 3.2 peak, which results in decrease of the Illite/Quartz peak near 3.34-3.4 Å (Figure 6.11). Smectite 003 and 004 peaks are better identified in the EG-treated sample, where the 003 and 004 peaks show up near 8.5 Å and 5.6 Å, respectively (Figure 6.12). Percentage of illite is 0 to 10% as indicated by the d_{20} ($<5.49^\circ$). EG-treatment also helps to identify smectite by shifting the S001 peak to 17.0-17.1 Å (Figure 6.12).

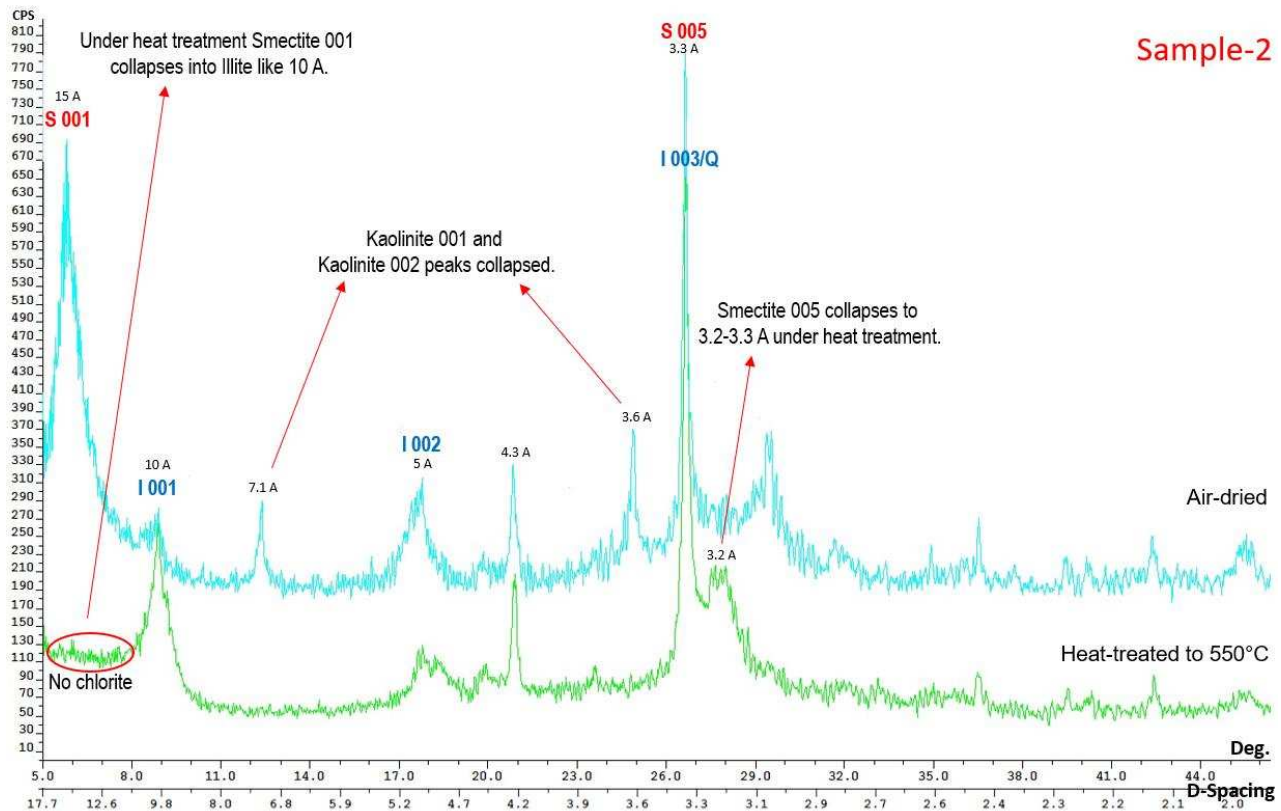


Figure 6. 10 Heat-treated Sample-2 compared against the untreated sample. The sample was heated for 1 hour at 550°C.

Similar results were obtained from the heat-treated Sample-1, Sample-2 and Sample-4 (Figures 6.8, 6.9, 6.10). The smectite peaks collapsed with heat treatment due to smectite dehydration (Hegab et al., 2015). Because of this, the Illite 001 peak at 10.0 Å is amplified, which happens due to the smectite collapsing into illite like 10.0 Å peak. The smectite peaks expand to 10 Å and 4.87 Å. The EG-treated Sample-1, Sample-2 and Sample-4 provided poor result as S001 did not shift from 15 Å to 17 Å. Moreover, S002 and S003 did not amplify after EG-treatment.

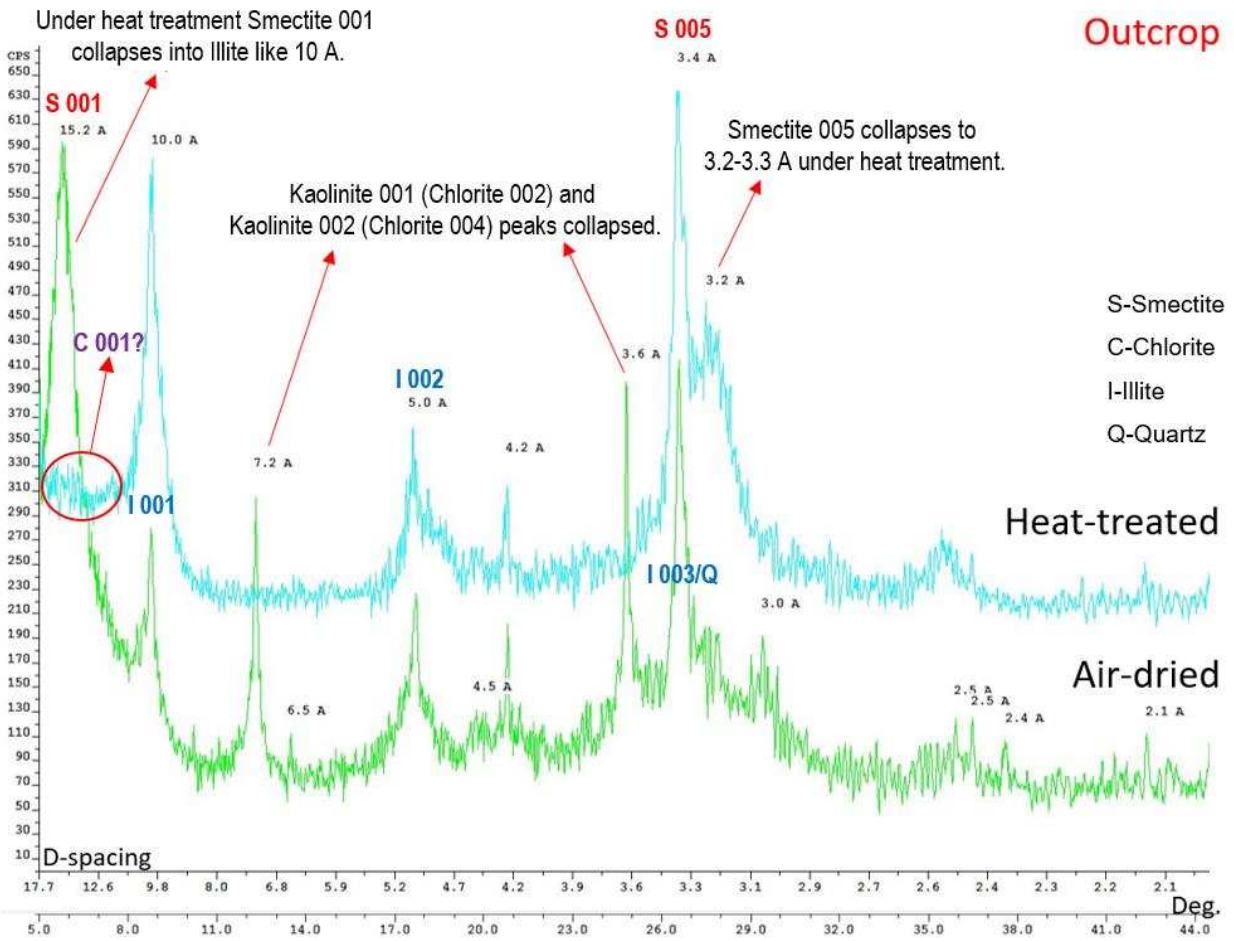


Figure 6. 11 Heat-treated outcrop sample compared against the untreated sample. The sample was heated for 1 hour at 550°C.

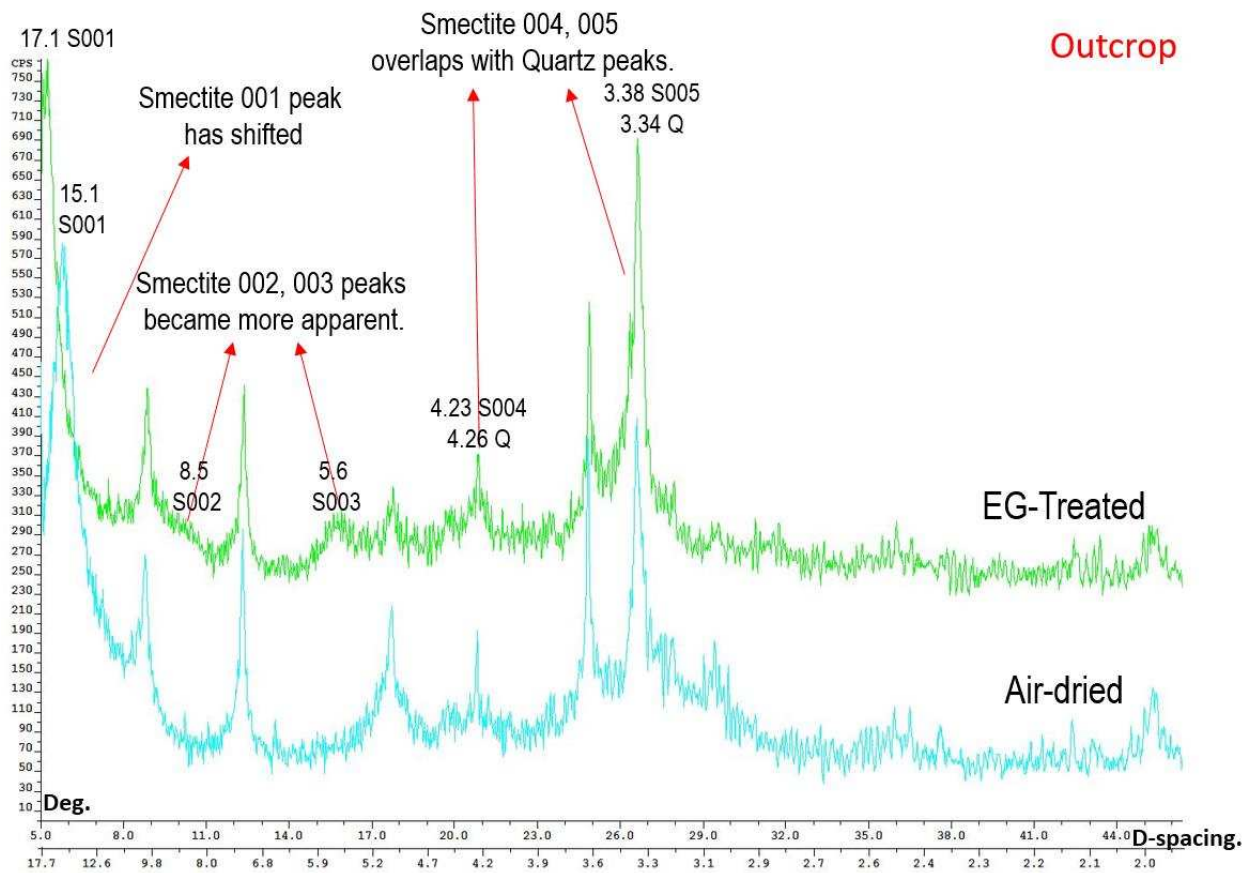


Figure 6. 12 X-ray diffraction analysis of the EG-treated outcrop sample compared to the non-treated sample. The sample was left under EG-treatment for 2 days.

6.3 Weathering and Depositional Environment

Study of clay minerals provide information on the depositional environment, climatic change, weathering and even hydrocarbon generation potentials. Figure 6.13 shows the calculated clay mineral ratios of the Khoot samples. The ratios were measured from Smectite 001, Kaolinite 001, and Illite 001 peaks. The ratios are Smectite 001/ Kaolinite 001 (S/K), Kaolinite 001 /Illite 001 (K/I), Smectite 001/Illite 001 (S/I), and Illite 001 /Smectite 001 (S/I).

Smectite is a proxy for minimal chemical weathering and proximity to aeolian, fluvial, lacustrine and turbidite sandstones or basin-margin settings (McKinley et al., 2009). However, the ratios were calculated from the air-dried samples' smectite peaks rather than EG-treated smectite peaks. Moreover, the kaolinite peaks in Sample-4 and the outcrop sample contain some chlorite.

The lake-bottom sequences (Sample-1, Sample-2) have much higher smectite with respect to kaolinite than the upper-lake sequences (Sample-3, Sample-4) and the outcrop sample. It is also evident that kaolinite is increasing with respect to smectite towards the top. The S/K ratio is ~8 in Sample-1, ~5 in Sample-2 and decreased to ~2.3 in Sample-3. The S/K ratio does not change significantly from Sample-3 to the outcrop sample, although it decreases as well.

The upward decrease in smectite with respect to kaolinite is indicating a paleoclimatic transformation from dry, arid environment to a warm and humid climate (Campo et al., 2007; Deconinck et al., 2003). Similar trends were observed from the Early Jurassic Blue Lias Formation in Southern England and Paleogene fluvial-lacustrine sequence in the Maiz Gordo Formation in northwestern Argentina, where the upward sequences had much higher kaolinite and the bottom sequences were abundant in smectite. Studies also suggest that kaolinite is a proxy for transgression as well as basin subsidence (Deconinck et al., 2013), which agrees with the Khoot well-log correlation in Figure 3.5.

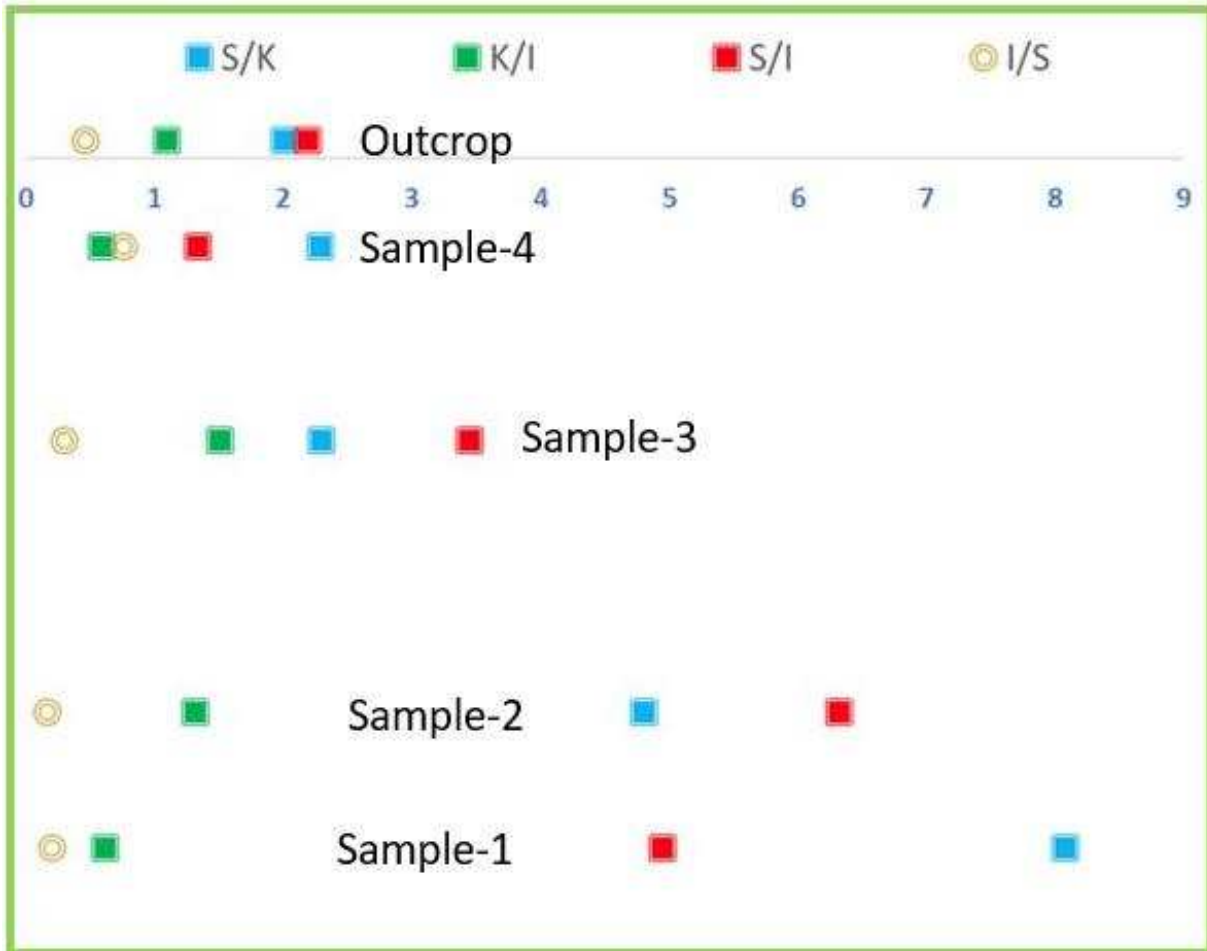


Figure 6. 13 Clay mineral ratios of the five studied samples. S/K stands for Smectite 001 /Kaolinite 001. K/I means Kaolinite 001/Illite 001. And S/I and I/S stand for Smectite 001 /Illite 001 and Illite 001/Smectite 001, respectively. The smectite peaks were measured from air-dried samples.

Overall, the greater abundance of smectite in the I/S mixed clay layer (illite 0% to 10%) from the outcrop sample supports the results obtained from Rock-Eval 6 data, where hydrocarbon expulsion was inhibited (Jiang, 2012). Higher percentage of illite in I/S mixed layer clays indicate hydrocarbon expulsion in unconventional plays (Jiang, 2012). Oil shales in the Khoot Basin formed during the deposition time of sequences 1 and 2 in an arid, dry environment (high smectite with respect to kaolinite) in a playa lake. The basin started to have more accommodation space during the deposition of Sequence 3 as indicated by the increasing kaolinite with respect to smectite. The greater abundance of carbonate minerals and calcium in the upper sections support the above-mentioned idea. Also, the thick TST and HST, and barely visible LST in the upper sequences are evidences for deepening lake. The outcrop sample, on the other hand, deposited after some time when the climate changed into warm, humid environment.

6.4 Whole Oil Gas Chromatograph (WOGC) Analysis Results

Extracts of the three studied samples share broad similarities. They all have a strong odd over even carbon preference observable in the *n*-alkanes (carbon preference index (CPI) > 3 for all samples). Strong odd over even carbon preference is an indicator of immaturity. Moreover, all extracts have immature signatures in the biomarker assemblages, including hopenes, dominance of the 22R hopanes over 22S, 17 β , 21 α hopanes, and 17 β , 21 β hopanes. These observations are consistent with lacustrine, sulfate-poor depositional environments.

The *n*-alkanes peak at *n*-C₂₃ for the outcrop sample (Figure 6.14) and Sample-4 (Figure 6.15) or at *n*-C₂₅ for Sample-2 (Figure 6.16). Hopane/sterane ratios are greater than 1 for all samples. Dibenzothiophene, an aromatic sulfur compound, was not detected in any of the samples. All samples had pristane/phytane (Pr/Ph) ratios well below 1.0, ranging from 0.2-0.6. To be specific, the Pr/ Ph ratio is 0.6 for Sample-2, 0.3 for Sample-4, and 0.2 for the outcrop sample, which is the lowest of all three. Phytane occurs in reducing type environment while pristane forms in oxidizing environment, such as peat swamps (Peters and Moldowan, 1993).

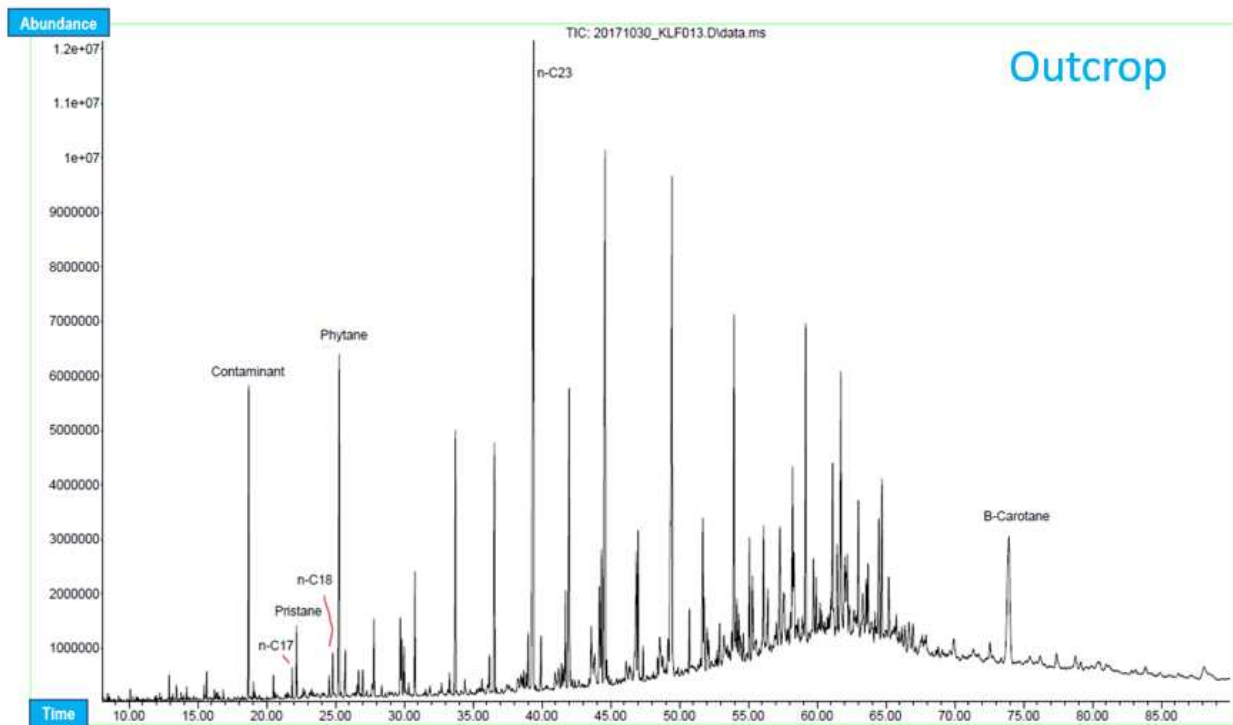


Figure 6. 14 The WOGC result of the outcrop sample. The *N*-alkanes peak at *n*-C₂₃.

Contrary to Mongolian source rocks and oil samples studied in Johnson et al. (2003), gammacerane, an indicator of stratified water columns or highly saline to hypersaline environment (Dembicki, 2016), was not detected in any of the samples. Many lacustrine deposits have gammacerane. The Eocene Green River oil shale, for example, has abundance of gammacerane (Dembicki, 2016). Extended hopanes and tricyclic terpanes were not particularly abundant in any of the samples. C₄₀ aromatic carotenoids and their diagenetic products, aryl isoprenoids, were not detected in any of the samples.

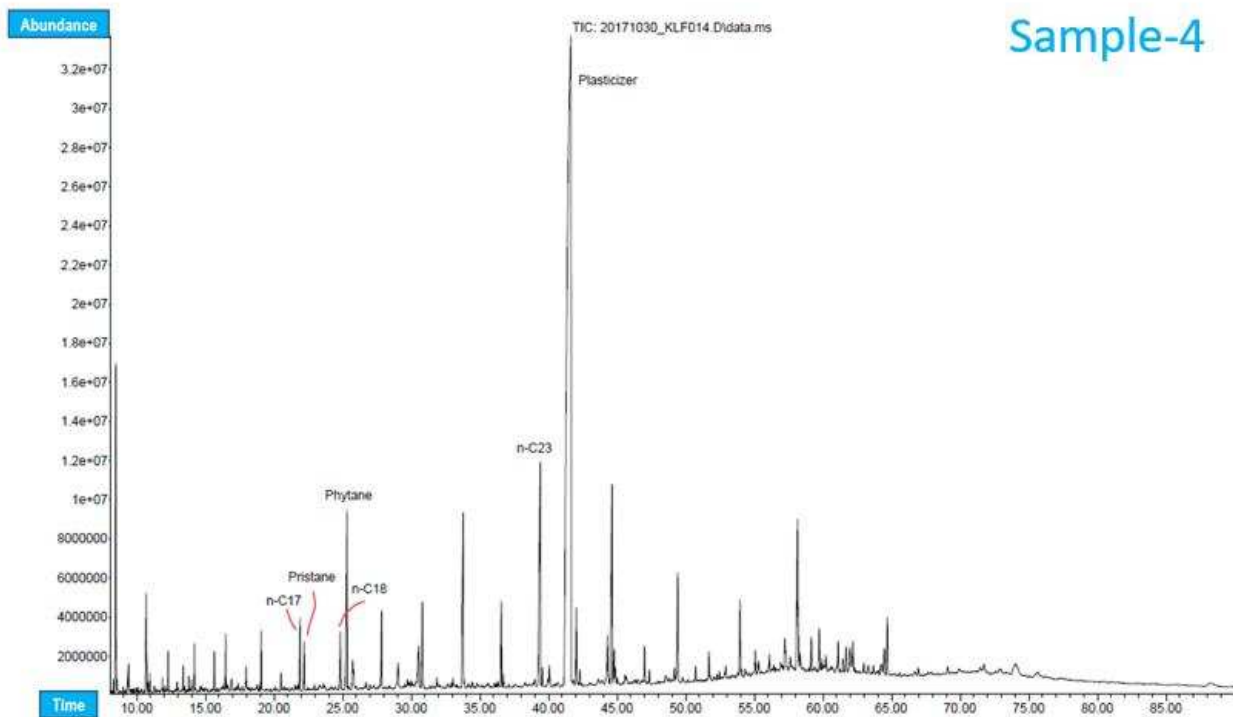


Figure 6. 15 The WOGC result of Sample-4. The *N*-alkanes peak at *n*-C₂₃.

However, there are some key differences between the extracts suggesting differences in the organic facies, possibly related to different phases of lacustrine deposition. Compared to the subsurface samples (Sample-4 and Sample-2), the outcrop sample (Figure 6.14) has a relatively high abundance of phytane and β -carotane. β -carotane and γ -carotane were present in the subsurface samples but at lower relative abundances than the outcrop sample.

The subsurface samples have a higher abundance of plant aromatic compounds, specifically cadalene and retene, than the outcrop sample. Cadalene, Simonelite and Retene are biomarkers for higher plants (Hauteville et al., 2006).

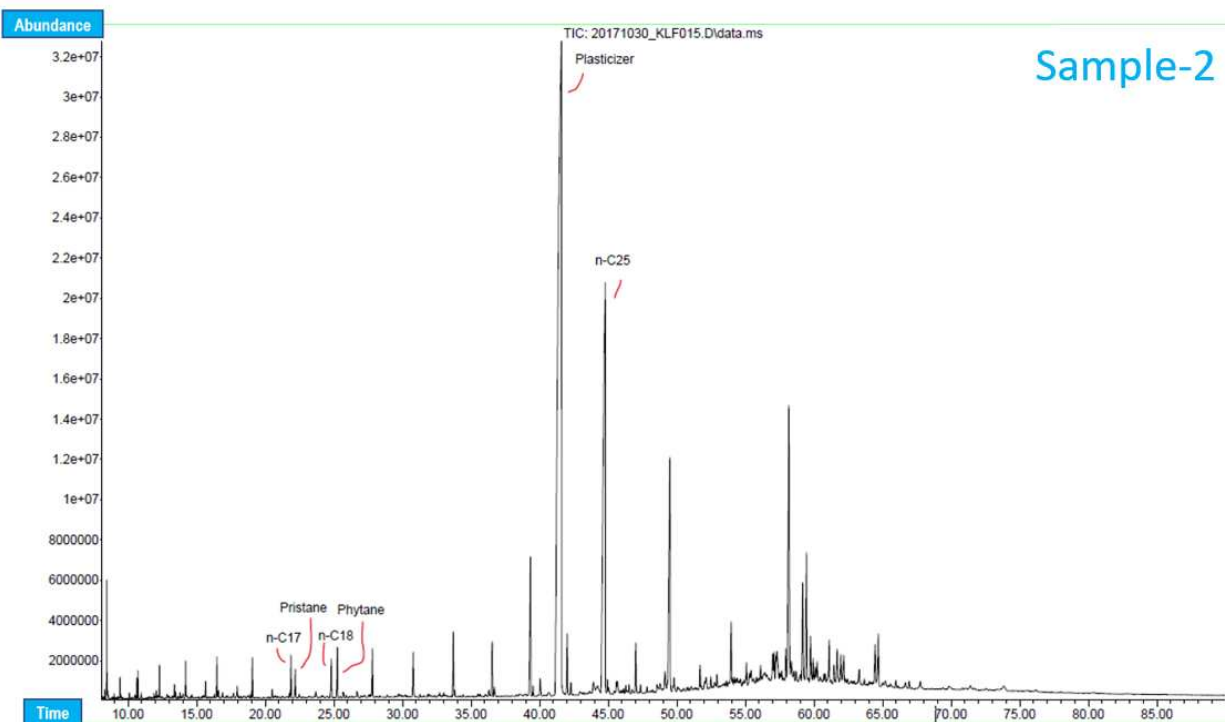


Figure 6. 16 The WOGC result of Sample-2. The *N*-alkanes peak at *n*-C₂₅.

Together, these differences may suggest that the surface sample was slightly more saline and stratified than the subsurface samples, which received more higher plant organic matter than the surface sample. The outcrop sample shows broad similarity to the Zuunbayan field oil in Mongolia (Figure 6.17). Although the Zuunbayan and Khoot oil shales are being plotted as estuarine and paralic environment, Johnson et al. (2003) stated that the Mongolian source rock samples are indeed lacustrine deposits with algal input (Figure 6.17). The surface sample (Figure 6.14) also appears to be more biodegraded (Figure 6.18) than the core samples (Figure 6.15 and Figure 6.16). Sample-2 shows more of mixed organic matter while Sample-4 and the outcrop sample plot in the algal reducing environment (Figure 6.18).

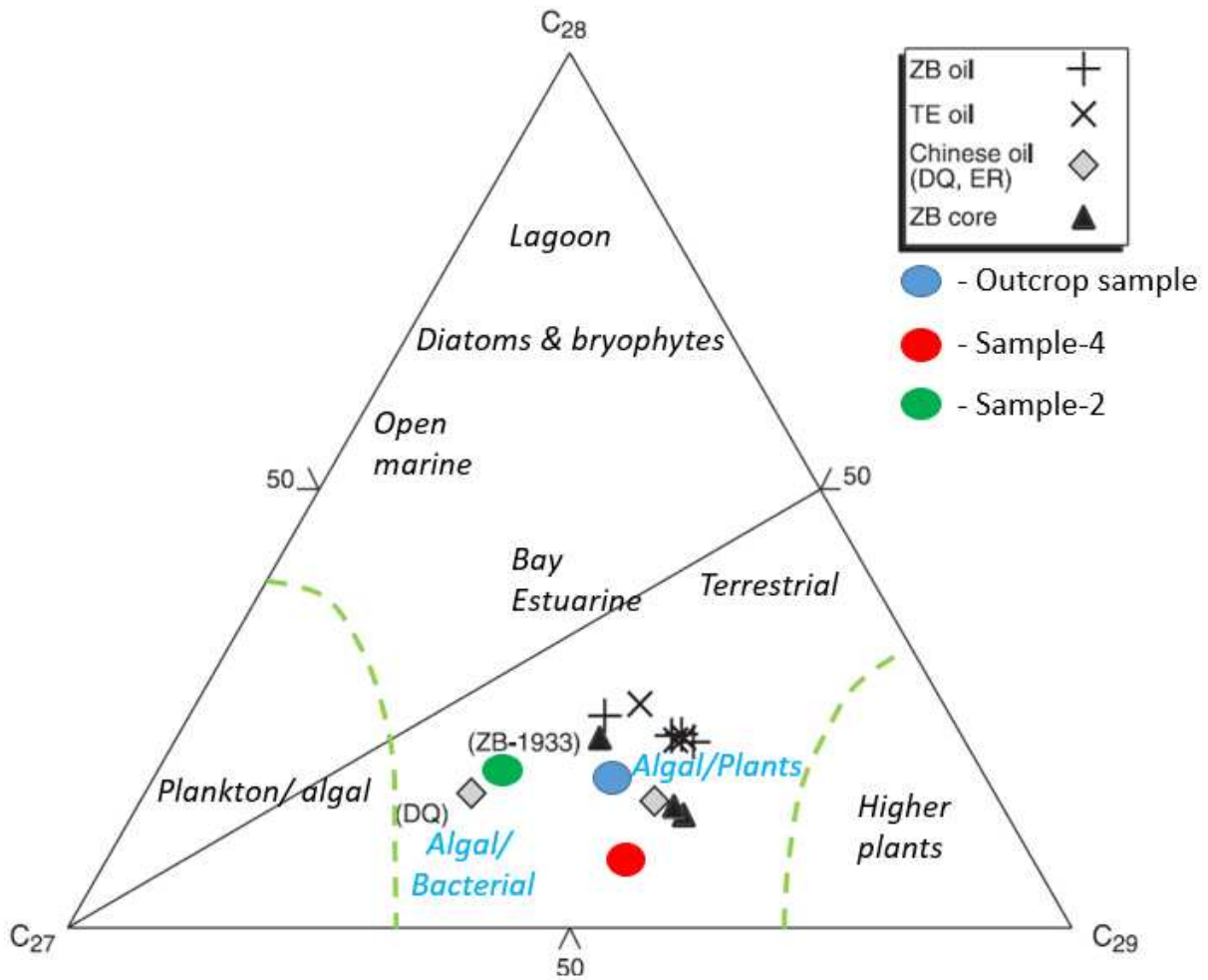


Figure 6. 17 Ternary plots of C₂₇, C₂₈ and C₂₉ steranes. The background image is modified from Johnson et al (2003). ZB stands for Zuunbayan and TE stands for Tsagan Els. Both oil samples and core sample were from the Zuunbayan sub-basin in the East Gobi Basin. In this diagram, the Khoot samples are showing broad similarities to the East Gobi Basin oil samples and core.

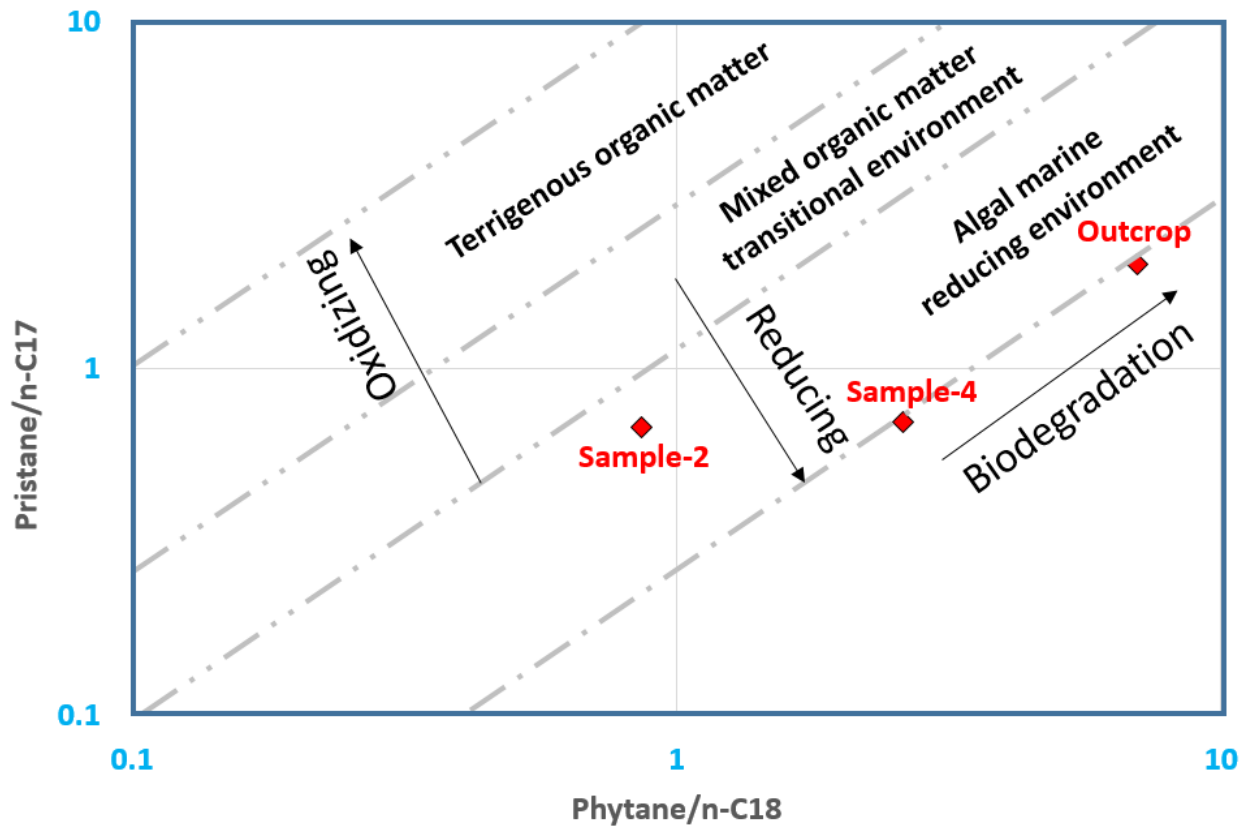


Figure 6. 18 Graph of pristane/ $n\text{-C}_{17}$ versus phytane/ $n\text{-C}_{18}$ for the Khoot samples.

Results of these studies indicate that the samples that were plotted as Type II on the Rock-Eval analysis plots are indeed mixed Type I/II kerogen. Sequence 1 followed by Sequence-2 received the greatest amount of terrestrial material input and therefore shows a mixed Type II kerogen. Similar algal/allochthonous terrestrial mixed Type II kerogen was found from the black shales from the Hartford and Newark basins in eastern United States (Spiker et al., 1988).

CHAPTER 7
THE ULTIMATE EXPELLABLE POTENTIAL OF THE
KHOOT SOURCE ROCKS

7.1 KinEx Basics

The Ultimate Expellable Potential (UEP) is the calculated volumetric expression of a source rock's hydrocarbon expelling potential (Roller and Pepper, 2017). It is calculated within KinEx (Zetaware) software platform using HI, transformation ratio (TI) and Gas/Oil Generation Index (GOGI). The TI is calculated as $S1/TOC$ and the GOGI values are defined by KinEx.

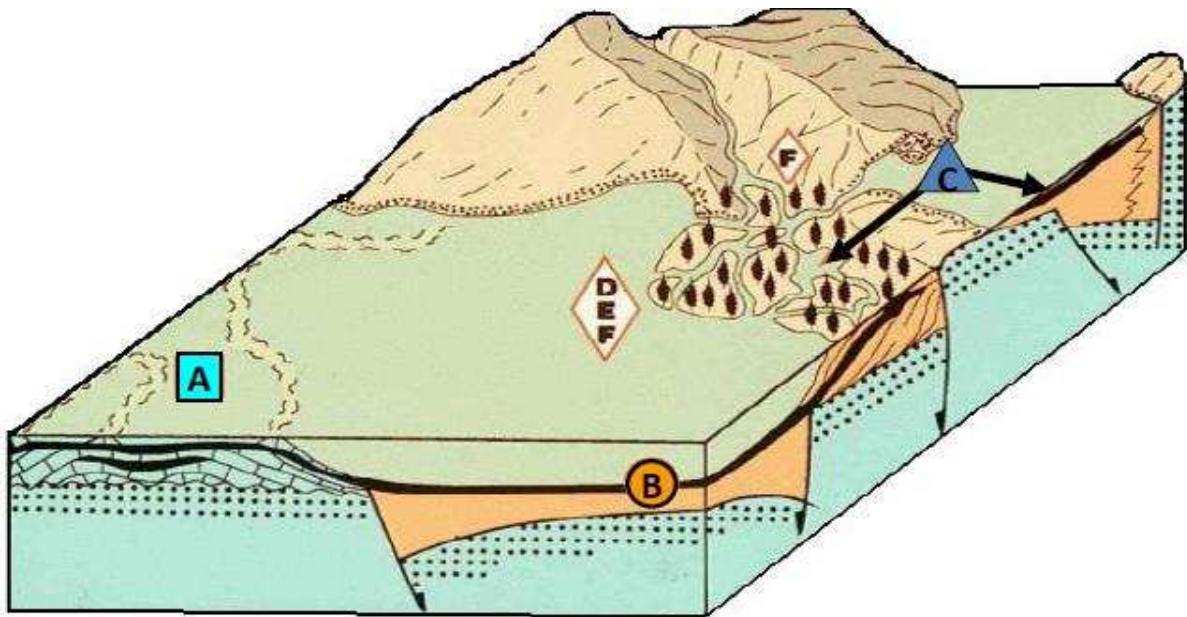


Figure 7. 1 Illustrated depositional environments of the five types of organofacies KinEx recognizes (from Roller and Pepper, 2018).

Figure 7.1 shows the depositional environments of the five types of organofacies KinEx recognizes. The highest UEP variability is observed from lacustrine (C) and terrestrial plays (D/E, F), whereas marine (A, B) plays show a relatively homogenous

UEP (Roller and Pepper, 2018). The description of each organofacies is outlined in Table 7.1.

Table 7. 1 Description of the depositional environments and basic characteristics of the organofacies types (from Roller and Pepper, 2018).

Organofacies	Sub-facies	Organofacies Descriptor	Principle Biomasses	Sulfur incorporation	Environmental Association	Kinetic model	Immature HI	Immature OI	Immature GOI	Possible Tissot Scheme Equiv.
A	A _c	aquatic, marine, clay-poor, carbonate-rich	algae / bacteria	high	marine; carbonate shelves, upwelling zones on slopes, deep basins; clastic-starved; any age	A	high to low depending on preservation/oxidation	high to low depending on preservation/oxidation	high to low depending on preservation/oxidation	I-IV
	A _s	aquatic, marine, clay-poor, silica-rich	algae / bacteria	high	marine; shelves, upwelling zones on slopes, deep basins; clastic-starved; any age					
B		aquatic, marine, clay-rich	algae / bacteria	moderate	marine; shelves, upwelling zones on slopes, anoxic deep basins; clastic; any age	B	high to low depending on preservation/oxidation	high to low depending on preservation/oxidation	high to low depending on preservation/oxidation	I-IV
C	C _f	aquatic, non-marine, lacustrine, fresh water	waxy algae / bacteria	low	"tectonic" non-marine ever-wet deep basins and paludal delta plains	C	high to low depending on preservation/oxidation	high to low depending on preservation/oxidation	high to low depending on preservation/oxidation	I-IV
	C _s	aquatic, non-marine, lacustrine, saline (SO ₄)	waxy algae / bacteria	moderate	"tectonic" non-marine evaporative basins with SO ₄ -rich run-off					
D/E	D	terrigenous, non-marine, significant wax and resin	significant higher plant resin and cuticle / bacteria / lignin	low	ever-wet delta plains; Mesozoic esp. angiosperm-rich Barremian and younger	D/E	moderate to low	moderate to high	moderate to high	II-III ^H
	E	terrigenous, non-marine, significant wax	significant higher plant cuticle / bacteria / lignin	low						II-III ^H
F		terrigenous, non-marine, wax / resin-poor	lignin	low	delta plains; Late Devonian and younger	F	low	high	high	III-IV

The next image (Figure 7.2) shows the expelled liquid and gas content of the most common types of organofacies for a 100 m thick section (Zetaware website). Organofacies A through C expels dominantly HC6+, which are a liquid hydrocarbon, organofacies D/E releases dominantly HC1-5 (gas), and organofacies F only expels HC1-5.

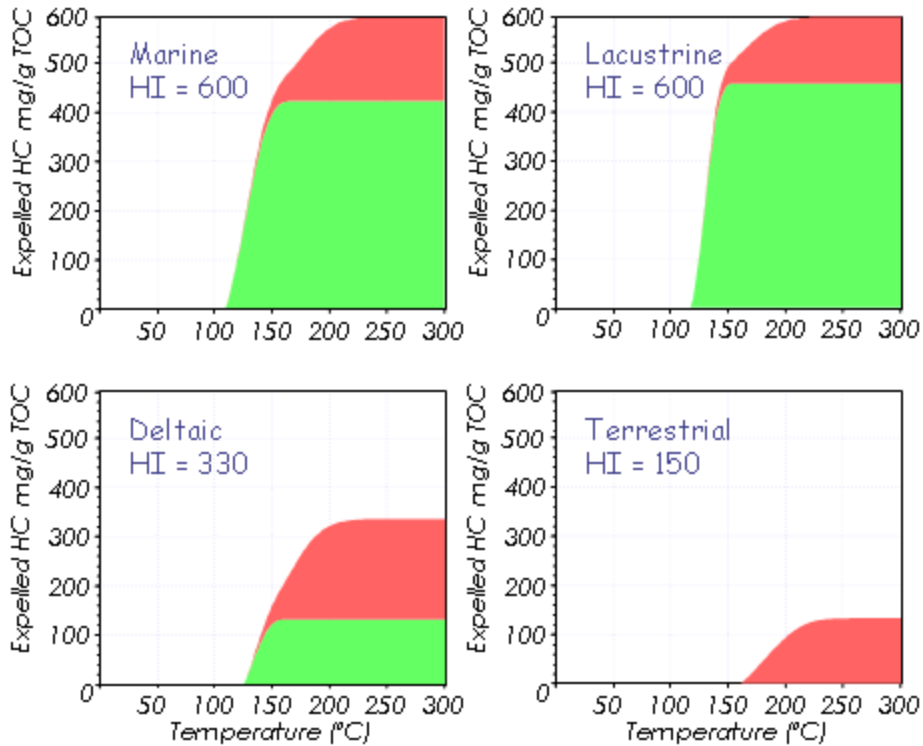


Figure 7. 2 Calculated UEP from the most common depositional environments (from Zetaware software).

7.2 Modeling the Khoot Basin

The Khoot basin is a small-scale basin situated between two larger Early Cretaceous sedimentary basins: Middle Gobi to the south and Choir-Nyalga to the north (Figure 7.3). The Khoot basin depo-center is even smaller (Figure 7.4). At the surface, however, organic-rich oil shale deposits outcrop in the area, which led to exploring this basin. The oil shale outcrops in this area are the best quality in the country (Avid and Purevsuren, 2001). However, these excellent quality oil shales are absent in the subsurface of Khoot basin. Moreover, the subsurface lacustrine deposits show high lateral variability, which led to classifying Khoot source rocks into three different classes:

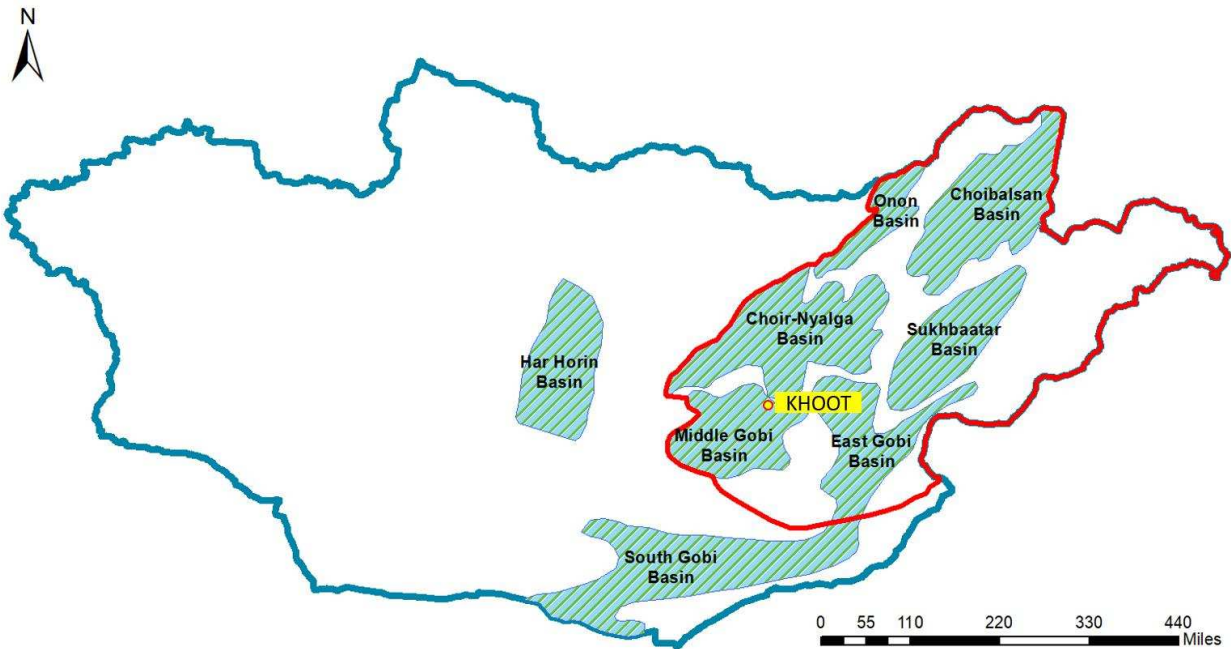


Figure 7. 3 Location of the Khoot Basin in the Eastern Mongolian Basinal Province. This small basin is located between two large sedimentary basins: Middle Gobi and Choir-Nyalga.

- Khoot-C: The Khoot-C source rock is the basinally restricted strata deposited in the wedged thick basin depo-center. The area in which these rocks are deposited is shown in Figure 7.4. The extent of the depo-center was identified from the subsurface seismic and well-log data (see previous section) and gravity data. Data from DH 1 was assumed to be representative of these source rocks.
- Khoot-M: The Khoot-M source rock is the organic-lean basin-margin source rock. Based on the subsurface data, this source rock facies is likely the most abundant type of source rock in the basin. The extent of Khoot-M source rock's deposition is the green area in Figure 7.4, although the real distribution might vary from one part of the basin to the next. Data from DH 4 was used for the UEP calculations.
- Khoot-O: The Khoot-O source rock is the highly organic-rich outcrop source rock. Samples from Campaign 2, which were collected from a vertically continuous outcrop, was modeled as a pseudo-well. As previously mentioned, this source rock is absent in the subsurface.

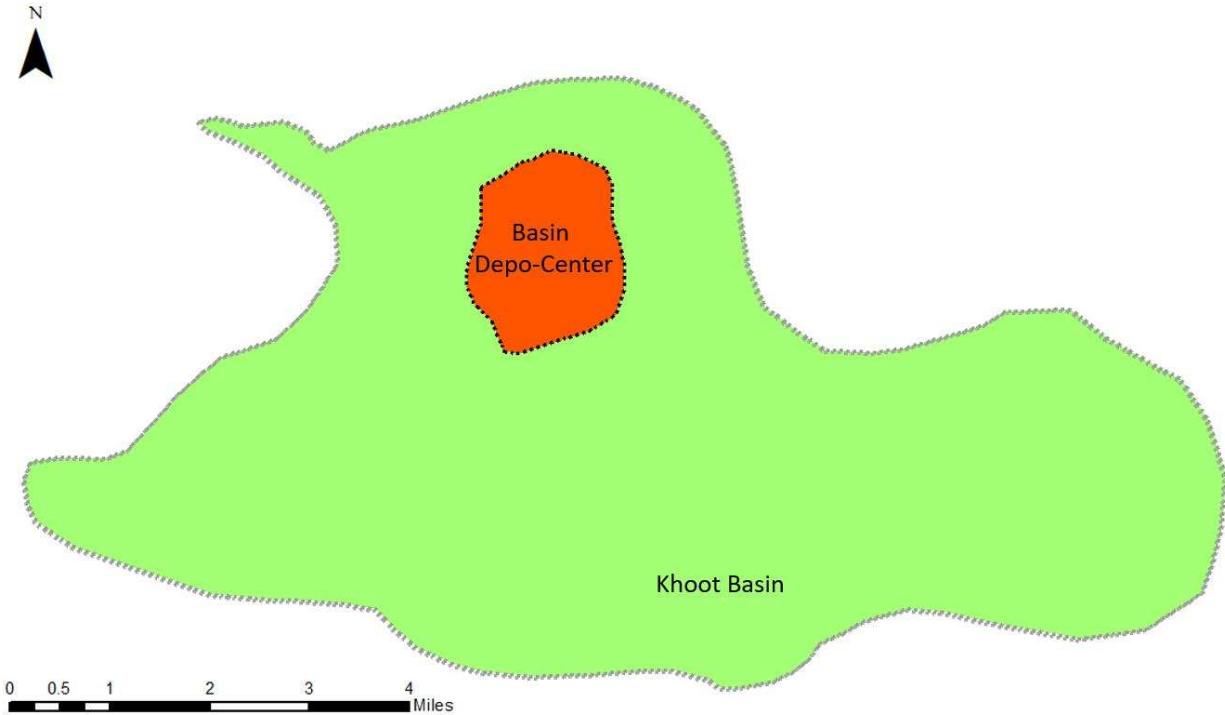


Figure 7. 4 Map of the Khoot basin. The basin depo-center is relatively low. The remaining parts of the basin is relatively flat.

In order to calculate the UEP, the original TOC and HI need to be restored first. These values are calculated from the present-day TOC, HI and the transformation ratio (TR). The transformation ratio (%TR) is calculated as $\%TR = (S1 / (S1 + S2)) * 100\%$. Tables 5.2 and 5.3 outline the results of this calculation. Because the S1 values are relatively low for all Khoot samples, the present-day HI and TOC values do not differ much from the original values. It is especially true for the outcrop samples, which have noticeably higher S2 values than the subsurface samples. The outcrop samples have much higher potential (102.44-223.7 mg HC/g rock) to create new hydrocarbon compared to the subsurface samples (10.02-85.82 mg HC/g rock) (Table 5.2 and 5.3). On the other hand, the S1 (0.05-2.25 mg HC/g rock) values do not differ much for all Khoot source rocks (Table 5.1 and Table 5.2).

Table 7. 2 Calculated original TOC and HI values from the present-day Rock-Eval measurements of DH 1 samples.

S1	S2	Present TOC	Present HI	% TR	TOC _o	HI _o
0.18	32.64	4.92	663	0.55	5.2	665
0.66	62.57	8.61	727	1.04	9.1	730
0.51	53.87	7.48	720	0.94	7.9	723
0.41	51.38	8.03	640	0.79	8.4	642
0.14	45.65	5.78	790	0.30	6.2	791
0.31	71.69	9.19	780	0.43	9.8	781
2.25	71.56	11.3	633	3.05	11.7	642
0.07	27	3.97	680	0.26	4.2	681
0.57	53.12	6.54	812	1.06	7.0	815
0.22	45.51	6.75	674	0.48	7.1	675
0.66	85.82	9.53	901	0.76	10.4	903
0.07	19.45	3.34	582	0.36	3.5	583
0.21	44.38	7.1	625	0.47	7.5	626
0.06	10.02	2.92	343	0.59	3.0	344
0.35	53.56	6.72	797	0.65	7.2	797
0.12	24.81	3.72	667	0.48	3.9	668
0.09	28.94	4.28	676	0.31	4.5	677
0.37	40.32	5.67	711	0.91	6.0	714
0.39	58.79	7.79	755	0.66	8.3	757
0.4	60.59	8.67	699	0.65	9.2	701
1.08	71.45	10.39	688	1.49	10.1	693
0.05	0.38	1.61	24	11.63	1.6	27
0.38	58.21	8.22	708	0.65	8.7	710
0.16	24.34	4.96	491	0.65	5.2	493

Table 7. 3 Calculated original TOC and HI values from the present-day Rock-Eval readings of DH 4 and Campaign 2 outcrop samples.

S1	S2	Present TOC	Present HI	% TR	TOC _o	HI _o
Parameters of Drill Hole 4 Samples						
0.14	12.54	2.47	508	1.10	2.6	511
0.37	53.82	6.54	823	0.68	7.0	825
0.18	23.76	3.9	609	0.75	4.0	611
1.11	58.16	7.22	806	1.87	7.6	811
0.05	4.94	1.47	336	1.00	1.5	338
2.01	77.7	11.11	699	2.52	11.6	706
0.74	40.86	5.83	701	1.78	6.1	706
Parameters of Campaign 2 Outcrop Samples						
2.12	223.7	24.75	904	0.94	26.9	906
0.86	102.44	12.67	809	0.83	13.6	811
0.93	130.84	15.22	860	0.71	16.5	862
1.21	130.84	16.79	779	0.92	17.9	781
1.66	120.89	14.35	842	1.35	15.3	845
0.64	100.77	12	840	0.63	13.0	841

Table 7.4 shows the input variables used for Khoot-C source rocks. The heating rate is set at 2°C/my. The estimated GOGI for the non-marine lacustrine rocks ranges between 0.12 and 0.15. The GOGI for the few aquatic marine clay-rich source rocks is 0.22-0.23. The calculated TI for these samples is 0.019-0.098.

The difference in the expulsion temperatures for non-marine (lacustrine) deposits and marine (clay-rich) deposits is shown in Figure 7.5a. The expulsion temperature is slightly higher for the lacustrine source rocks. The combined expulsion temperature for the oil portion and the gas portion is also shown in Figure 7.5b. The oil starts to expel around 120 °C and the gas starts to expel around 140 °C.

Table 7. 4 Input values used for the DH 1 UEP calculations.

My Kerogens

- A-Aquatic marine clay-poor
- B-Aquatic marine clay-rich
- C-Aquatic non-marine (lacustrine)
- D/E-Terrigenous terrestrial wax/resin
- F-Terrigenous terrestrial lignin-rich
- Bohai (lacustrine)
- Bowen Permian

Linear
 Isothermal
 Imported

Initial Temperature (C)

Final Temperature (C)

Heating Rate (C/my)

name	HI mg/g	TOC %	GOGI	TI mg/g	Thickness (m)
<input type="checkbox"/> C-Aquatic non-marine (lacustrine)	902.72	10.41	0.12	0.063...	1
<input type="checkbox"/> C-Aquatic non-marine (lacustrine)	668.43	3.93	0.14	0.030...	1
<input type="checkbox"/> C-Aquatic non-marine (lacustrine)	680	3.97	0.14	0.016...	1
<input type="checkbox"/> C-Aquatic non-marine (lacustrine)	675.43	7.13	0.14	0.030...	1
<input type="checkbox"/> C-Aquatic non-marine (lacustrine)	756.85	8.3	0.13	0.046...	1
<input type="checkbox"/> C-Aquatic non-marine (lacustrine)	814	6.98	0.13	0.081...	1
<input type="checkbox"/> B-Aquatic marine clay-rich	582	3.5	0.22	0.02	1
<input type="checkbox"/> B-Aquatic marine clay-rich	492.9	5.17	0.23	0.030...	1
<input type="checkbox"/> C-Aquatic non-marine (lacustrine)	626	7.47	0.15	0.028...	1
<input type="checkbox"/> C-Aquatic non-marine (lacustrine)	701	9.17	0.14	0.043...	1
<input type="checkbox"/> C-Aquatic non-marine (lacustrine)	710	8.71	0.14	0.043...	1
<input type="checkbox"/> C-Aquatic non-marine (lacustrine)	723	7.91	0.13	0.064...	1
<input type="checkbox"/> C-Aquatic non-marine (lacustrine)	692	10.91	0.14	0.098...	1
<input type="checkbox"/> C-Aquatic non-marine (lacustrine)	781	9.85	0.13	0.031...	1
<input type="checkbox"/> C-Aquatic non-marine (lacustrine)	791	6.21	0.13	0.022...	1
<input type="checkbox"/> C-Aquatic non-marine (lacustrine)	797	6.72	0.13	0.048...	1
<input type="checkbox"/> C-Aquatic non-marine (lacustrine)	730	9.11	0.13	0.072...	1
<input type="checkbox"/> C-Aquatic non-marine (lacustrine)	711	5.99	0.14	0.061...	1
<input type="checkbox"/> C-Aquatic non-marine (lacustrine)	677	4.53	0.14	0.019...	1

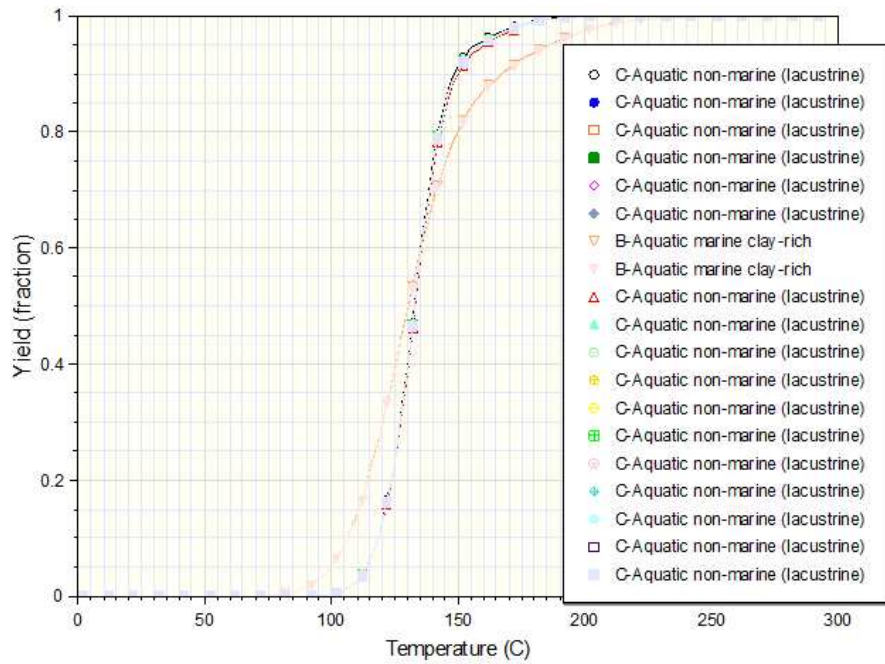


Figure 7. 5 A) HC yield fractions of aquatic non-marine (lacustrine) deposits and aquatic marine clay-rich samples.

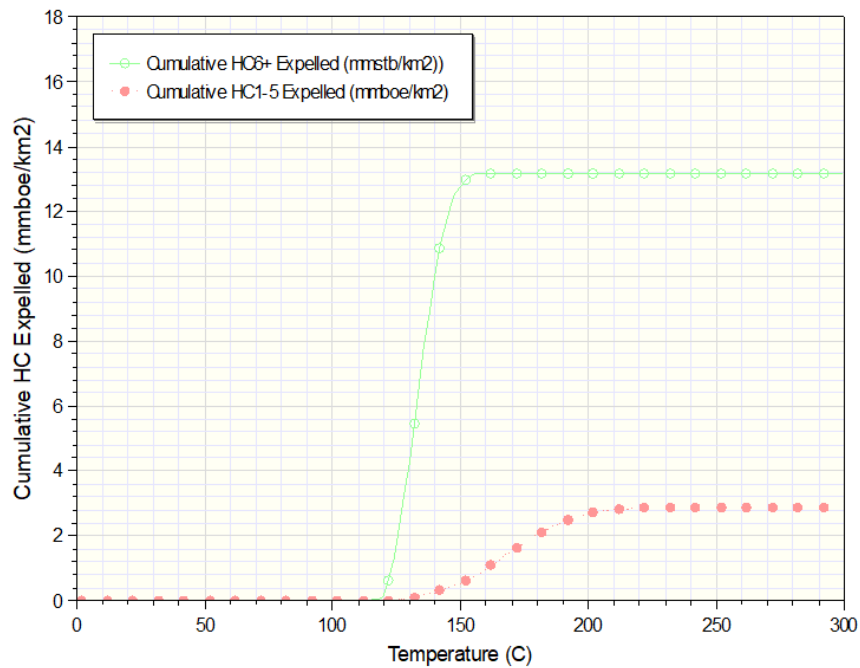


Figure 7. 5 B) Kinetic curves of the cumulative hydrocarbons expelled from DH 1 source rock interval. The red curve shows the HC1-5 expelled. The green curve shows the HC6+ expelled.

7.2 The Khoot Basin's Potential for Hydrocarbon Exploration

Result of DH 1 modeling is displayed in Figure 7.6. It shows that each interval's calculated UEP closely aligns with the levels of HI in the bed. The total UEP of the Khoot basin-center source rocks is 16.05 mmboe/km². The section thickness is 19 m. The total average calculated UEP is 0.84 (mmboe/km²)/m. On a closer look, the UEP for the oil portion is 0.69 (mmboe/km²)/m and the gas portion is 0.15 (mmboe/km²)/m.

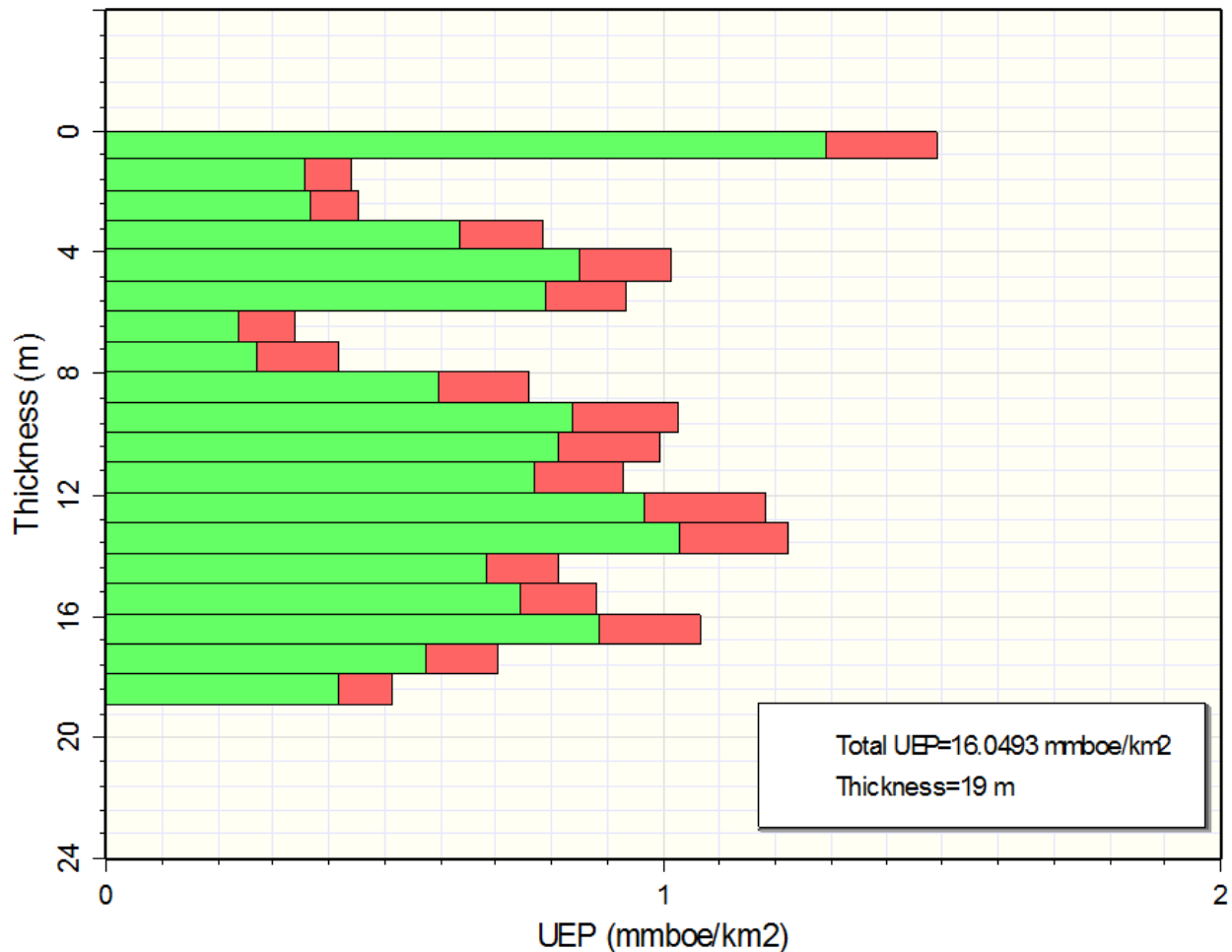


Figure 7. 6 The calculated UEP from each source rock interval in DH 1.

The UEP associated with the basin-margin (Khoot-M) section and the pseudo-well (Khoot-O) section were also calculated. An average Khoot-M source rock will expel 0.54 (mmboe/km²)/m oil and 0.12 (mmboe/km²)/m gas, which leads to a total UEP of 0.66 (mmboe/km²)/m (Table 7.5). Khoot-O source rock, on the other hand, has much

higher UEP (2.11 (mmboe/km²)/m) than all the studied sections in the subsurface (Table 7.5). The UEO is 1.83 (mmboe/km²)/m and the gas portion is 0.28 (mmboe/km²)/m.

Table 7. 5 Calculated UEP of the three different types of Khoot basin.

Ultimate Expellable Potential (UEP) of the Khoot Source Rocks					
	Thickness	Oil	Gas	Total	Unit
Basin Depo-center Khoot- C Source Rock Characterization					
Total	19 m	13.2	2.85	16.05	mmboe/km ²
Normalized to 1 m	1 m	0.69	0.15	0.84	(mmboe/km ²)/m
Basin-margin Khoot-M Source Rock Characterization					
Total	7 m	3.8	0.84	4.64	mmboe/km ²
Average	1 m	0.54	0.12	0.66	(mmboe/km ²)/m
Khoot-O Outcrop Source Rock Characterization					
Total	6	11	1.7	12.77	mmboe/km ²
Average	1	1.83	0.28	2.11	(mmboe/km ²)/m

In Table 7.6, the Khoot samples are compared to world level source rocks studied in Roller and Pepper (2018). The outcrop source rock UEP is much higher than the compared world-level source rocks. The Khoot basin depo-center source rocks have higher UEP than the Arabian Basin Tuwaiq formation source rocks, West Siberian Basin Bazhenov formation (Russia) and the Shahejie source rocks of the Bohai Basin (China). It also has more potential to create oil than gas compared to the above-mentioned world-class source rocks. The basin-margin source rocks have similar UEP to the Tuwaiq formation UEP.

Although the quality of an average subsurface Khoot source rock is equal or better than some world-class source rocks like the Bazhenov and Tuwaiq, it is not as big as the world-class plays like the Bazhenov and Tuwaiq, which were chosen by Roller and Pepper (2018). The Khoot Basin is approximately 78 km² and the basin

depo-center pay-zone is 4.5 km². Basin areas were measured in ArcMap. The source rock thickness is approximately 160 m in the basin depo-center, which decreases down to 70 m in the rest of the basin. Thus, the approximate GRV of the basin depo-center is 0.72 km³, which yielded a total UEP of 0.6 bnboe (UEO: 0.5 bnboe). On the other hand, the entire Khoot basin GRV is 5.865 km³. The resulting basin-wide UEP is 4.94 bnboe and the UEO is 4.073.4 bnboe. The higher quality outcrop source rock is absent in the subsurface of the Khoot Basin, as previously mentioned.

Table 7. 6 Volumetric qualities and expulsion potentials of the Khoot basin and compared world-class basins.

Comparison of Khoot Basin with World-class Basins							
Source Bed Formation	Eedemt	Eedemt	Tuwaiq	Bazhenov	Bakken	Shahejie	Units
Basin	Khoot Basin-center	Khoot Basin-margin	Arabian	W. Siberian	Williston	Bohai	
Organofacies	C	C	A	A/B	B	C	
Depositional Area	4.5	78	340,000	1,750,000	206,000	61,000	km ²
Thickness (max)	160 m	70 (160)	45 (150)	24 (60)	4 (23)	102 (709)	m
Source Bed GRV	0.72*	5.865*	14,320**	49,145**	1,029**	5,240**	km ³
Basinwide UEP	0.6	4.94	9,400	31,500	1056	568	bnboe
Basinwide UEO	0.5	4.07	7,600	24,200	814	429	bnboe
Basinwide UEG	0.1	0.87	1,800	7,300	242	139	bnboe

7.3 Potentials of the Middle Gobi Basin and the Choir-Nyalga Basin

The small Khoot basin is obviously not suited for development as the UEP is very low. However, this small basin is situated between two larger Early-Cretaceous sedimentary basins with abundant oil shale, organic-rich mudstone, and coal deposits (Erdenetsogt et al., 2009).

The larger Central Gobi basin and the Choir-Nyalga basins have an approximate area of 34,202 km² (25,000 km² according to Erdenetsogt et al., 2009) and 59,435 km² (50,000 km² according to Erdenetsogt et al., 2009), respectively. The new basin areas were measured in ArcMap. Each of these basins has several sub-basins bounded by faults (Erdenetsogt et al., 2009). These basins have thick oil shale layers and have the highest petroliferous potential, but the exact thickness and quality of the source rocks are unknown (Erdenetsogt et al., 2009). If each basin has a minimum of 70 m and a maximum of 250 m Khoot-C type source rock, the Middle Gobi basin would yield a minimum of 2,023 bnboe (max: 7,225.2 bnboe) and the Choir-Nyalga basin would yield a minimum of 3,515.6 bnboe (max: 12,555.6 bnboe) (Table 7.7). If the quality of the source rocks in these basins is the same as Khoot-O source rock, then these values are doubled from the above values. If this condition is met, the basins would yield a maximum of 18,041 bnboe (Middle Gobi basin) and 31,351 (Choir-Nyalga basin) bnboe. The minimum yield is 5,051 bnboe for the Middle Gobi basin and 8,778.5 bnboe for the Choir-Nyalga basin. These values were also calculated for the basin areas that were provided in Erdenetsogt et al (2009) (Table 7.7).

The hydrocarbon potential of the eastern Mongolian Middle-Gobi and Choir-Nyalga basins are not as great as the Russian giant West Siberian basin but are much better than the Williston basin and the Bohai basin (Table 7.7). These two basins in Mongolia are a close match to the Arabian Basin. The rest of the eastern Mongolian basins, which were not studied in this chapter probably have similar potential. Some of these basins are already producing basins.

Table 7. 7 Hydrocarbon potentials of the Middle Gobi and Choir-Nyalga basins.

UEP Estimates from Measured Basin Areas						
Source Rock	Khoot-C			Khoot-O		
Basin	Middle Gobi	Choir-Nyalga	Unit	Middle Gobi	Choir-Nyalga	Unit
Area	34,202	59,435	km ²	34,202	59,435	km ²
Max Thickness	0.25	0.25	km	0.25	0.25	km
GRV	8,550.5	14,858.75	km ³	8,550.5	14,858.7	km ³
UEP	7,225.2	12,555.6	bnboe	18,041.5	31,351.9	bnboe
UEO	5,942.6	10,326.8	bnboe	15,647.4	27,191.5	bnboe
UEG	1,282.6	2,228.8	bnboe	2,394.1	4,160.4	bnboe
Source Rock	Khoot-C			Khoot-O		
Basin	Middle Gobi	Choir-Nyalga	Unit	Middle Gobi	Choir-Nyalga	Unit
Area	34,202	59,435	km ²	34,202	59,435	km ²
Min Thickness	0.07	0.07	km	0.07	0.07	km
GRV	2,394.1	4,160.4	km ³	2,394.1	4,160.4	km ³
UEP	2,023.0	3,515.6	bnboe	5,051.6	8,778.5	bnboe
UEO	1663.9	2891.5	bnboe	4381.3	7613.6	bnboe
UEG	359.1	624.1	bnboe	670.4	1164.9	bnboe
UEP Estimates from Basin Areas in Published Papers						
Source Rock	Khoot-C			Khoot-O		
Basin	Middle Gobi	Choir-Nyalga	Unit	Middle Gobi	Choir-Nyalga	Unit
Area	25,000	50,000	km ²	25,000	50,000	km ²
Max Thickness	0.25	0.25	km	0.25	0.25	km
GRV	6,250	12,500	km ³	6,250	12,500	km ³
UEP	5281.2	10562.5	bnboe	13187.5	26375	bnboe
UEO	4,343.7	8,687.5	bnboe	11,437.5	22,875	bnboe
UEG	937.5	1,875	bnboe	1,750	3,500	bnboe
Source Rock	Khoot-C			Khoot-O		
Basin	Middle Gobi	Choir-Nyalga	Unit	Middle Gobi	Choir-Nyalga	Unit
Area	25,000	50,000	km ²	25,000	50,000	km ²
Min Thickness	0.07	0.07	km	0.07	0.07	km
GRV	1,750	3,500	km ³	1,750	3,500	km ³
UEP	1,478.7	2,957.5	bnboe	3,692.5	7,385	bnboe
UEO	1,216.25	2,432.5	bnboe	3,202.5	6,405	bnboe
UEG	262.5	525	bnboe	490	980	bnboe

CHAPTER 8

DISCUSSION AND CONCLUSION

This study has provided new insights into the geochemical and depositional history of the Khoot basin. Also, this is the first time a comprehensive geologic study was undertaken on the Khoot basin. As there was no previous research available on the Khoot basin, the current research was limited to the available data from Genie Oil and Gas. The initial analysis of the Khoot samples from Rock-Eval results indicated that the Khoot samples shared broad similarities. However, detailed study has shown some key areas, which define the differences between the Khoot outcrop and subsurface samples.

8.1 Integration of Rock-Eval Data and Sequence Stratigraphic Interpretation

Out of the six stratigraphic sequences, Sequence 1 has the lowest average HI (400 mg HC/TOC) and the lowest average TOC (3-4%) (Figure 8.1). However, the Tmax is greater for Sequence 1 deposits. In a Green River study by Feng (2011), it was demonstrated that sequence boundaries are associated with the lowest TOC and usually low HI. However, in the Khoot basin, sequence boundaries are associated with the highest TOC (up to 11 wt%) and HI levels (over 900 mg HC/g TOC). On the other hand, near the maximum flooding surfaces organic matter type becomes Type II (HI becomes less than 600) and the organic richness decreases down to 4-5 wt% TOC. Between these surfaces, the Rock-Eval parameters decrease or increase gradually. From a maximum flooding surface to a sequence boundary (HST), the Rock-Eval parameters gradually increase (Figure 8.1). This trend is most obvious in the HST of sequences 2 and 3 (Figure 8.1). On the other hand, from a sequence boundary to the next flooding surface (TST), Rock-Eval parameters decrease (Figure 8.1). A number of things may have caused this. Flooding may have interrupted preservation of the organic material, but also may be bringing in terrestrial higher plant materials. Organic geochemical analysis in Chapter 6 has demonstrated that the Type II kerogen in the

Khoot subsurface samples was a mixed (algal/higher plant) Type II kerogen rather than a marine Type II kerogen.

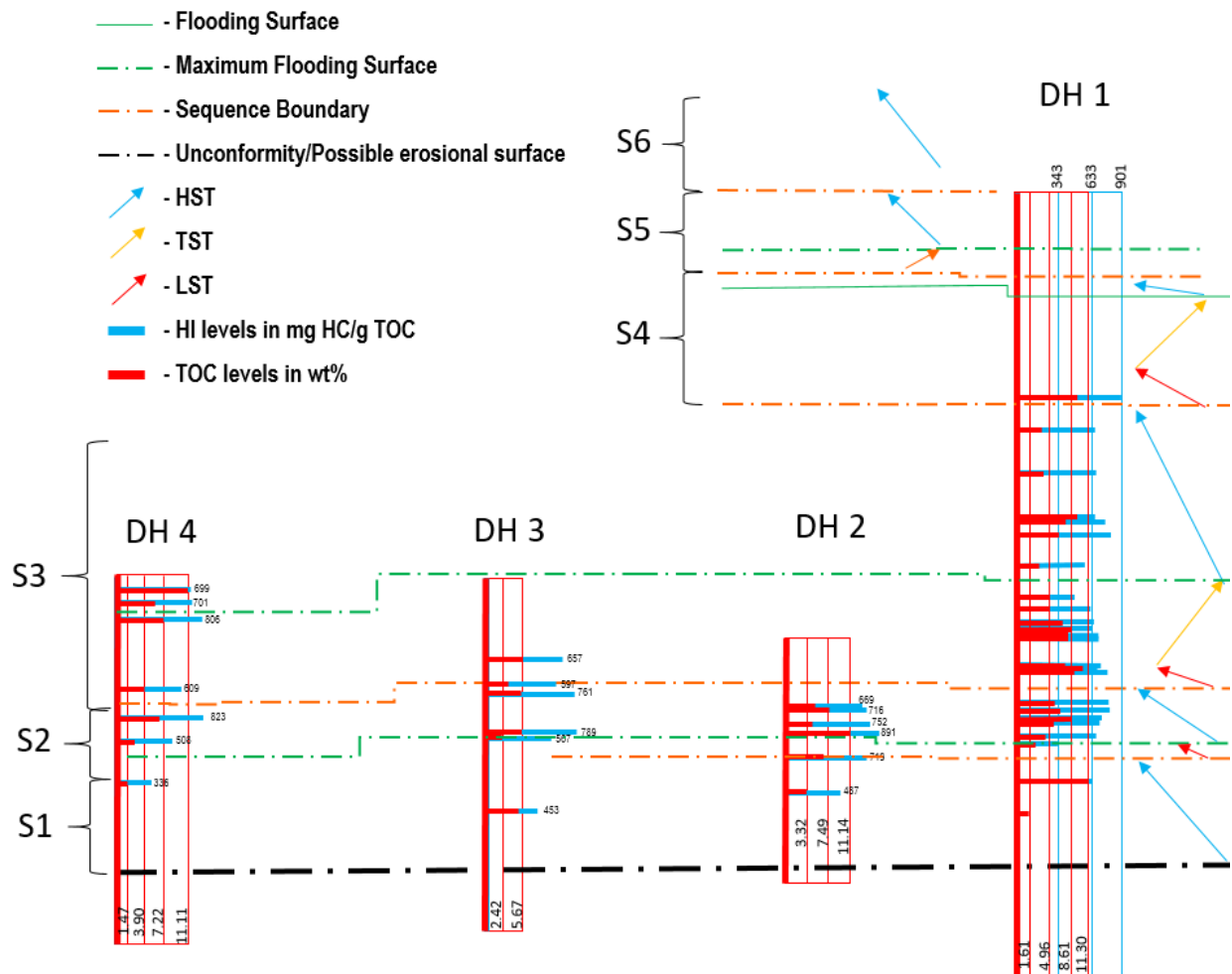


Figure 8. 1 TOC and HI correlation across DH 1, DH 2, DH 3 and DH 4. For the log correlation, see Chapter 3.

Zones with higher HI and TOC levels also correspond with higher Tmax values, showing that Tmax values are not only dependent on burial temperature and pressure, but also dependent on the organic matter type (Figure 8.2). Figure 8.2 is an enlarged well-log and Rock-Eval bar plot for DH 1. It shows that the calibrated samples have similar trends in all parameters. In addition, it shows better correlation with the well log patterns, as opposed to the non-calibrated samples, which showed no association with the well log patterns.

DH 1

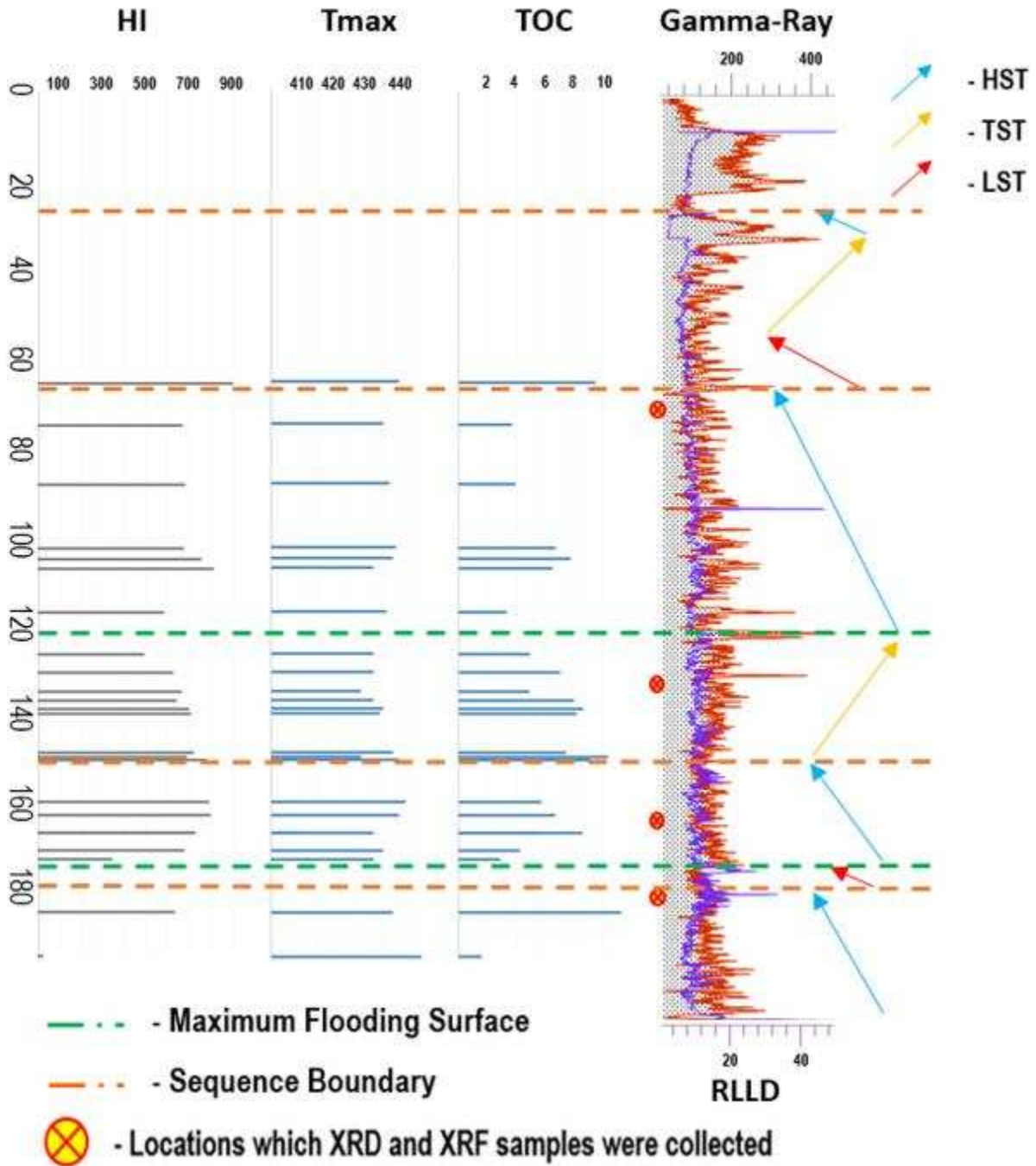


Figure 8. 2 Interpreted well-log and selected Rock-Eval parameter trends from DH 1.

Descriptions of these sequences is consistent with the balanced-fill lacustrine basin type described in Bohacs et al (2000). The other two types being over-filled basin and under-filled basin (Figure 8.3). Each fining upward cycle is evident in the gamma ray logs. It is less distinguishable in the resistivity log, but the overall fining up trend is evident as previously mentioned. The overall kerogen is Type I, but it is Type II in Sequence 1. Kerogen type also changes to Type II near the flooding surface in sequences 2 and 3. The organofacies type is laterally continuous, especially in the basinally restricted zone where DH 1 and DH 2 were drilled. Fluvial input is minimum, and the dominant facies association is deep lacustrine mudstone and playa lake oil shale, which indicates fluctuating profundal lacustrine environment.

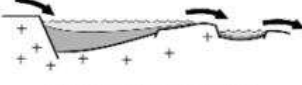
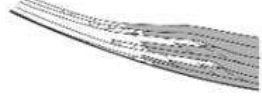
Lake Type & Lacustrine Facies Association	Stratigraphy	Source Potential	Hydrocarbon Characteristics
OVERFILLED  <i>Fluvial-Lacustrine Facies Association</i>	Maximum progradation:  <ul style="list-style-type: none"> Parasequences related to lateral progradation (relatively subtle) Maximum fluvial input 	<ul style="list-style-type: none"> Low to moderate TOC Mixed type I-III kerogen Marked organic facies contrasts Distinct lateral changes in organic facies 	<ul style="list-style-type: none"> Generate both oil and gas Very waxy, low-sulfur oils Terrigenous biomarker assemblage dominant
BALANCED-FILL  <i>Fluctuating-Profundal Facies Association</i>	Mixed progradation and desiccation:  <ul style="list-style-type: none"> Distinct shoaling cycles common Fluvial input variable 	<ul style="list-style-type: none"> Moderate to high TOC Predominantly type I kerogen, with type I-III mixtures near flooding surfaces Relatively homogeneous and laterally consistent organic facies 	<ul style="list-style-type: none"> Mostly oil generative Paraffinic but relatively nonwaxy oils; low sulfur Algal biomarker assemblage dominant
UNDERFILLED  <i>Evaporative Facies Association</i>	Maximum desiccation:  <ul style="list-style-type: none"> High-frequency wet-dry cycles Minimum fluvial input 	<ul style="list-style-type: none"> Low overall TOC (w/ some high TOC intervals) Type I kerogen Minimum organic facies contrasts Laterally consistent organic facies 	<ul style="list-style-type: none"> Mostly oil generative Paraffinic oils; moderate to high sulfur Distinctive "hypersaline" biomarker assemblage

Figure 8. 3 Three different basin types: Overfilled, Balanced-fill and Underfilled (Bohacs et al., 2000).

A key question of the research was in regards to the organic richness difference between the outcrop and subsurface samples. Analysis of the calibrated outcrop samples suggest that the area right near where DH 3 was drilled corresponds to low HI (<600 mg HC/g TOC), TOC (<10 wt%) and low Tmax (<435°C) (Figure 8.4). These rocks, although exposed at the surface as an outcrop, are stratigraphically lower than the outcrops exposed near DH 1 and DH 2 (Figure 3.5). Moreover, the outcrop in this area is stratigraphically slightly younger than the maximum flooding surface in Sequence 3. And as previously stated, maximum flooding zones are associated with lower TOC, HI and Tmax in the subsurface as well.

DH 3 was drilled in a graben. If the graben was not there, the outcrop near DH 3 would have been Sequence 1 deposits. The outcrop near DH 4 has higher Rock-Eval parameters because this area corresponds to another depo-center. Outcrops near DH 1 and DH 2 are of exceptional quality: TOC > 17 wt%, HI > 800 mg HC/g TOC, and Tmax >435°C. These outcrops have higher Rock-Eval parameter values because 1) They are deposited in the basin depo-center. 2) It was observed from the subsurface data that source rock quality was becoming better from the bottom of the basin to the top. The outcrop samples were probably deposited in the TST or HST of younger sequences than the subsurface, which are exposed due to uplift. 4) The subsurface oil shale deposits and the outcrop near DH 1 and DH 2 are younger deposits.

Although there are some good quality source rocks and oil shale in the basin depo-center both in the subsurface and in the outcrop, the basin is too small for further hydrocarbon exploration.

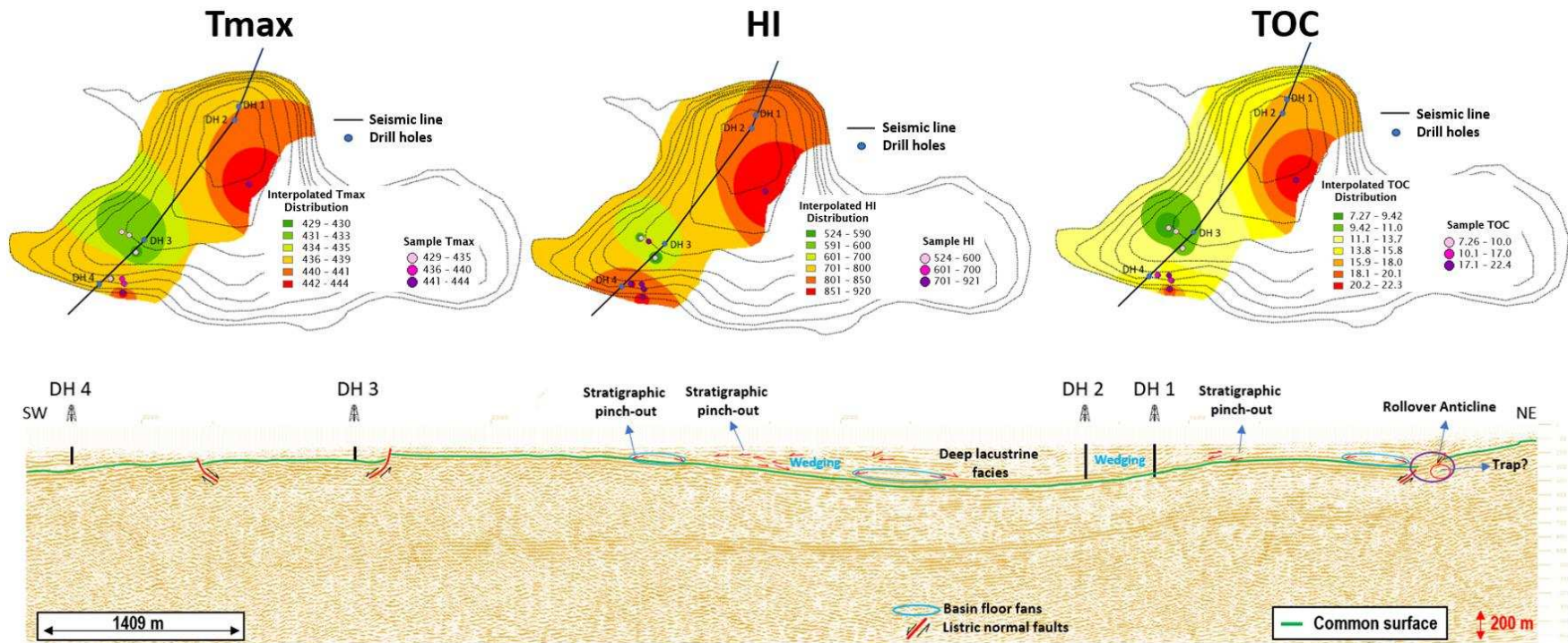


Figure 8. 4 Interpolated (IDW) maps of the Khoot basin that were created from calibrated Rock-Eval data. Each map was created using different parameters. Black line on maps is the seismic line.

8.2 Depositional Environment Inferred from Geochemical Data

X-Ray Diffraction analysis and XRF analysis revealed that the Khoot outcrop samples were deposited in a warm humid environment while the subsurface samples were deposited in a dry, arid environment, likely resembling a playa lake. The upper sections, therefore, are enriched in kaolinite in respect to smectite, which is the dominant type of clay mineral in Sequences 1-3 of the subsurface deposits. Moreover, the Khoot subsurface samples have higher abundance of plant aromatic compounds (e.g. cadalene, retene); hence, it has a mixed Type II kerogen, especially at the flooding surfaces and at the lake bottom sequence (Sequence I). On the other hand, the outcrop sample received greater abundance of algal material and was deposited and preserved in a reducing environment. Sequences 1 and 2 were likely deposited in a playa lake, where the oil shale formed and accumulated. Sequences 3 and 4 are deposited in a climatically fluctuating rapidly rising lake. Especially in sequences 3 and 4, the lake level continuously increased, but the basin was deprived of fluvial sediment influx as indicated by the thick transgressive systems tracts and the thick high-stand systems tract in Sequence 3. Presence of kaolinite and low relief shoreline architecture indicates that the paleolake in the Khoot basin was a shallow lake.

The mineral content of the subsurface samples, which are older, is much greater (S3' up to 70 mg CO₂/g rock) than the mineral content present in the outcrop samples, which are younger (S3' is below 24 mg CO₂/g rock). The organic-rich (17-25%) outcrop samples were deposited during a time of high lake in the basin depo-center, which had low dilution and greater preservation capacity. Within the subsurface, the mineral content increases in the Khoot-M samples located in the basin margin section (DH 3, DH 4 and DH 5), indicating higher dilution. The mineral content of the basin-center Khoot-C samples is below 35 mg CO₂/g rock. The organic richness of DH 3 – DH 5 is low (<11%) because these wells are located near the basin margin, where the condition was not met for preservation of organic matter. Moreover, the subsurface samples received mixed terrestrial/algal organic input while the outcrop samples received higher algal component. Detailed summary of each group of samples is given in Table 8.1.

Table 8. 1 Summary of geochemical, geological and organic matter characteristics of the source rocks distributed across the Khoot basin.

	Seq. Tract	Lithology	TOC	Kerogen Type	Thermal Maturity	Organic Input	S3'	Clay	Pyrite	Si	Ca
Sequence 1, DH 1	HST	Oil shale, mudstone	3-4%	Type II	Mature	Higher Plant/Algal	1-10	K; I; S	Has Pyrite	69%	3%
Sequence 2, DH 1	HST	Oil shale, mudstone	4-11%	Type I	Immature-Early Mature	Higher Plant/Algal	15-33	K; I; S	Less or no Pyrite	58%	13%
Sequence 3, DH 1	TST	Oil shale, mudstone, mud shale	4-9%	Shifts from Type I to Type II	Immature-Early Mature	Higher Plant/Algal	15-27		Less or no Pyrite	59%	14%
Sequence 3, DH 1	HST	Mudstone, mud shale	3-8.6%	Shifts from Type II to Type I	Immature-Early Mature	Higher Plant/Algal	12-34	K; I; S; Cl	Less or no Pyrite	43%	35%
Sequence Boundary, DH 1	N/A	N/A	9%	Type I	Early Mature	N/A	N/A	N/A	N/A	N/A	N/A
Maximum Fl. Surface, DH 1	N/A	N/A	2%	Type I/II	Immature	N/A	N/A	N/A	N/A	N/A	N/A
Sequence 1, DH 3 and 4	HST	Oil shale, mud shale	1.5-5.5%	Type II	Immature	N/A	20-70	N/A	N/A	N/A	N/A
Sequence 2, DH 3 and 4	HST	Mud shale	1.8-7%	Type II/I	Immature-Early Mature	N/A	20-70	N/A	N/A	N/A	N/A
Sequence 3, DH 3 and 4	TST	Oil shale, mudstone	3.9-11%	Type I	Immature	N/A	20-70	N/A	N/A	N/A	N/A
Outcrop	N/A	Oil shale	17-25%	Type I	Mature	Algal	10-22	K; I; S; Cl	Has Pyrite	56%	8%
Outcrop (DH 3 region)	N/A	N/A	7-11%	Type I/II	Immature-Early Mature	N/A	6-12	N/A	N/A	N/A	N/A
Shallow Depth	N/A	N/A	2-10%	Type II	Immature-Early Mature	N/A	20-36	N/A	N/A	N/A	N/A

8.3 Conclusion

Analysis of the Khoot basin samples indicate that Khoot oil shale samples have more internal variation than oil shale samples collected from different basins across Mongolia. The Khoot subsurface samples differ from the outcrop samples on many different levels, such as depositional environment and time, mineral content, kerogen type, organic richness, and thermal maturation.

The organic richness of the subsurface Khoot samples (Khoot-M and Khoot-C) resemble the Shinekhudag-type source rocks (Shawart Obo, Bayan-Erkhit and Shinekhudag). However, the thermal maturation of the Shinekhudag-type samples outpace the Khoot-C and Khoot-M samples. The Khoot outcrop samples are unique compared to all other studied samples in Mongolia. There are no other samples comparable to the Khoot outcrop oil shales in the studied basins in Mongolia, except for the Eedemt samples studied in Yamamoto et al. (1993). The Eedemt and Khoot are two names for the same locality.

Based on all of the above studies and analysis, the Khoot-O samples have exceptional hydrocarbon potential, but they are absent in the subsurface. Moreover, Mongolian oil shale and shale have excellent hydrocarbon generating potential, but no oil and gas was expelled thus far in the studied region. In addition to that, the Khoot-O samples have a greater abundance of toxic trace elements, such as arsenic. The Khoot outcrop sample has more arsenic (As=50 ppm) than the Green River Mahogany zone samples (As=30 ppm). The outcrop sample also has more Bi than any of the subsurface samples.

However, the Khoot-O samples mimic ZB oil from the neighboring East Gobi basin, in sterane diagrams. Therefore, it is possible that a more mature version of the Khoot-O sample is present in the neighboring larger Early Cretaceous basins. Based on this assumption the ultimate expellable potential was calculated for two large sedimentary basins that are near the Khoot basin, which are the Middle Gobi (Choir-Nyalga). They each have a potential to expel 2,023 (3,515) bnboe to a high of 18,041

(31,352) bnboe. The studied Khoot basin, however, is a small basin and therefore expels only 4.94 bnboe hydrocarbon.

Additionally, the Khoot basin is not suited for oil shale exploration because majority of the subsurface samples are of low-grade (TOC: 2-10 wt%). To be viable for oil shale development, the TOC has to be at least 10 wt% and the thickness has to be 100 m. The Khoot basin subsurface oil shale deposits do not meet any of these requirements. However, the Khoot oil shales can be very good to excellent source rock, if matured under ideal temperature and pressure conditions.

REFERENCES

- Akkoca, D.B., Sagioglu, A., "The authigenic dolomite and smectite formations in the Neogene lacustrine-fluvial Caybagi Basin (Elazig, Eastern Turkey)." *Geologic Carpathica* Vol.56. No. 6. 2005: 531-543.
- Ando, H., Hasegawa, H., Hasegawa, T., Ohta, T., Yamamoto, M., Hasebe, N., Ichinnorov, N. "Jurassic–Cretaceous lacustrine deposits in the East Gobi Basin, southeast Mongolia." *Journal of Geological Society of Japan*, Vol. 117, 2011: 11-12.
- Avid, B., Purevsuren, B., Dugarjav, J. "Investigation of pyrolysis analysis of Mongolian Khoot oil shale." *Oil Shale* Vol.17. No. 3. 2000: 241-251.
- Avid, B., Purevsuren, B. "Chemical composition of organic matter of the Mongolian Khoot oil shale." *Oil Shale* Vol.18. No. 1. 2001: 15-23.
- Bartov, Y. "Geology of Block 25." *Work in Progress*. 2014.
- Bohacs, K.M., Carroll, A.R., Neal, J.E., Mankiewicz, P.J., "Lake-basin type, source potential, and hydrocarbon character: an integrated-sequence-stratigraphic-geochemical framework." In: Gierlowski-Kordesch, E.H., Kelts, K.R. (Eds.), *Lake Basins Through Space and Time*. AAPG Studies in Geology, 46. Tulsa, OK, 2000: pp. 3–34.
- Dembicki, H.J., "Practical Petroleum Geochemistry for Exploration and Production." Elsevier Science & Technology Books, Amsterdam, 2016: 331.
- Erdenetsogt, B., Lee, I., Bat-Erdene, D, Jargal., L. "Mongolian coal-bearing basins: Geological settings, coal characteristics, distribution and resources." *International Journal of Coal Geology* Vol. 80. 2009: 87-104.
- Feng, J. "Source rock characterization of the Green River oil shale, Piceance Creek Basin, Colorado." M.Sc. thesis., Colorado School of Mines, 2011.
- Fritzell EH, Bull A.L, Shephard G.E. "Closure of the Mongol– Okhotsk Ocean: Insights from seismic tomography and numerical modelling." *Earth Planet Sci Lett* 2016: 1–12. doi:10.1016/j. epsl.2016.03.042
- Genyao, W., Yuan, W., Min, L. "Palinspastic reconstruction and geological evolution of Jurassic basins in Mongolia and neighboring China." *J. Paleogeography* Vol. 2 2013: 306–317.
- Graham, S. A., Hendrix, M. S., Johnson, C. L., Badamgarav, D., Badarch, G., Amory, J., Porter, M., Barsbold. R., Webb, L. E., and Hacker, B. R. "Sedimentary record and tectonic implications of late Mesozoic rifting, southeast Mongolia." *Geological Society of America Bulletin*, Vol. 113. 2001: 1560–1579.

- Hautevelle, Y., Michels, R., Malartre, F., Trouiller, A., "Vascular plant biomarkers as proxies for palaeoflora and palaeoclimatic changes at the Dogger/Malm transition of the Paris Basin (France)." *Organic Geochemistry* V. 37. 2006: 610 – 625.
- Ichinnorov, N., Purevsuren, S., Buyantegsh, B. "Preliminary result of palynological study of the Khootiin Khotgor locality." *MUST, Geology Journal* 19, 2008: 81–86. (in Mongolian)
- Johnson, C. L., Greene, T. J., Zinniker, D. A., Moldowan, J. M., Hendrix, M. S., Carroll, A. R. "Geochemical characteristics and correlation of oil and nonmarine source rocks from Mongolia." *AAPG Bulletin*, Vol. 87. No. 5. 2003: 817-846.
- Johnson, C. L., Graham, S. A., "Sedimentology and reservoir architecture of a synrift lacustrine delta, southeastern Mongolia." *Journal of Sedimentary Research*, Vol.74. 2004: 770–785.
- Li, G., Ando, H., Hasegawa, H., Yamamoto, M., Hasegawa, T., Ohta, T., Hasebe, N., Ichinnorov, N. "Confirmation of a Middle Jurassic age for the Eedemt Formation in Dundgobi Province, southeast Mongolia: constraints from the discovery of new spinicaudatans (clam shrimps)." *Alcheringa* Vol. 38 No.3. 2014: 305-316.
- Li, Y., Xu, W.L., Wang, F., Tang, J., Zhao, S., Guo, P. "Geochronology and geochemistry of late Paleozoic–early Mesozoic igneous rocks of the Erguna Massif, NE China: Implications for the early evolution of the Mongol–Okhotsk tectonic regime." *Journal of Asian Earth Sciences*. Vol.144. 2016: 205-224. 10.1016/j.jseaes.2016.12.005.
- Moore, D. M., Reynolds, R. C., "X-ray Diffraction and the Identification and Analysis of Clay Minerals" Oxford University Press, Inc. 1989: 1-378.
- Peters, K. E., "Guidelines for evaluating petroleum source rock using programmed pyrolysis: American Association of Petroleum Geologists Bulletin," Vol. 70. 1986: 11.
- Peters K. E., Moldowan J.M., "The biomarker guide: interpreting molecular fossils in petroleum and ancient sediments." PrenticeHall, Inc, Englewood Cliffs, New Jersey 1993.
- Purevsuren, B., Ochirbat, P. "Comparative study of pyrolysis and thermal dissolution of Estonian and Mongolian Khoot oil shales." *Oil Shale* Vol.33. No. 4. 2016: 329-339.
- Roller, E., Pepper, A. "Estimating the Ultimate Expellable Potential of Source Rocks: Defining "World Class" for Aquatic Organofacies with Examples from the Arabian, West Siberian, Bohai, and Williston Basins." *Search and Discovery Article*. No. 11055. 2018.

- Sladen, C., and Traynor, J. J., "Lakes during the evolution of Mongolia," in E. H. Gierlowski-Kordesch and K. R. Kelts, eds., *Lake basins through space and time: AAPG Studies in Geology* Vol.46. 2000: 35-57.
- Spiker, E.C., Kurt, R.K., Hatcher, P., Gottfried, R.M., Horan, M.F., Olsen, P.E., "Source of kerogen in black shales from the Hartford and Newark basins, eastern U.S. In: Froelich, A.J., Robinson Jr., G.R. (Eds.), *Studies of the Early Mesozoic Basins of the Eastern United States.*" U.S. Geological Survey Bulletin, V. 1776. 1988: 63–68.
- Thul, D. J., "Niobrara Source Rock Maturity in the Denver Basin: A Study of Differential Heating and Tectonics on Petroleum Prospectively Using Programmed Pyrolysis." M.Sc. thesis., Colorado School of Mines, 2000.
- Traynor, J. J., Sladen C., "Tectonic and stratigraphic evolution of the Mongolian People's Republic and its influence on hydrocarbon geology and potential," *Marine and Petroleum Geology*, Vol.12. 1995: 35–52.
- Yamamoto, M., Bat-Erdene, D., Ulziikhishig, P., Enomoto, M., Kajiwara, Y., Takeda, N., Suzuki, Y., Watanabe, Y., Nakajima, T., "Preliminary report on geochemistry of Lower Cretaceous Dsunbayan oil shales, eastern Mongolia," *Geological Survey Bulletin, Japan*, Vol. 44. 1993: 685– 691.
- Yang, J. H., Wu, F. Y., Shao, J. A., Wile, S. A., Xie, L. W., Liu, X. M., "Constraints on the timing of uplift of the Yanshan Fold and Thrust Belt, North China." *Earth and Planetary Science Letters*, Vol. 246. No.3-4. 2006: 336-352.
- Yang, Y.T., Guo, Z.X., Song, C.C., Li, X.B., He, S., "A short-lived but significant Mongol-Okhotsk collisional orogeny in latest Jurassic–earliest Cretaceous." *Gondwana Research*. Vol. 28. No. 3. 2015: 1096–1116.